INERTIAL DEPOSITION OF PARTICLES IN MODELS OF HUMAN AIRWAYS

by

JOHN R. JOHNSTON

Thesis for the Degree of Doctor of Philosophy

UNIVERSITY OF EDINBURGH

1974

I hereby declare that
this thesis embodies the
results of my own special
work, and that it has been
composed by myself.

ABSTRACT

This thesis is concerned with the inertial deposition of aerosol particles in models of human branching airways.

Homogeneous, monodisperse particles of known characteristics were generated using a spinning disk aerosol generator of the Research Engineers - May type: These were passed through simple bend systems of differing geometries, and the fractional deposition measured by a fluorimetric technique. The parameter characterising 50 per cent deposition in the bend was found to agree with that predicted theoretically.

Five inter-related models of branching airways were used, having geometries generally compatible with existing anatomical data.

A quantitative study was performed, adopting essentially the same experimental procedure as for the bends. The magnitude of the inertial deposit was measured, and the overall effect of fluid flow rate, particle size, branching angle and size of model determined.

Confirmation of the existing theoretical efficiency was obtained for an average branching angle of $\pi/6$ radians: The 50 per cent impaction parameter was shown however, to be dependent on the adopted bifurcation geometry.

CONTENTS

LIST OF ILLUSTRATIONS AND TABLES

CHAPTER ONE

INTRODUCTION AND HISTORICAL REVIEW

The role of inhaled particles in the causation of ill-health in the community needs no amplification.

In the highly complex anatomy of the lung, the overall effect of these particles will depend on their deposition, rate of clearance and cytotoxicity. Much information is available concerning many aspects of these problems.

This thesis concerns one field, that of deposition; in particular, the phenomenon of inertial precipitation.

The purpose of the following chapter is to describe, in general, the role played by the lung in handling inhaled particles, and serves as an introduction to the later experimental work.

1.1 DESCRIPTION OF THE LUNG

The human respiratory tract can be divided conveniently into two distinct anatomical compartments. The trachea to the terminal bronchioles is termed the pre-acinar or conducting airways and consists of a network of tubes branching in a roughly dichotomous manner. If the trachea is classified as the zeroth generation, the successive generations (assuming perfect dichotomy) will contain members 2^n in number. A typical member of the nth generation however will be of smaller diameter than one belonging to the (n-1)th. This increase in number and corresponding diminution in diameter has the overall effect of reducing the average velocity of any gas inspired to a value decreasing with increasing depth into the lung.

If any lung generation is considered as consisting of perfect tubes of known diameter, with the trachea (n = o) of diameter D, then for a given volume flow of $\dot{V}$ $m^3 s^{-1}$ through the trachea

$\bar{V} = \frac{4\dot{V}}{\pi D^2}$ where $\bar{V}$ = average velocity in trachea

At any given depth n in the conducting airways, this volume flow will be shared between each (identical) member of the nth generation.

$\dot{V}_n = \left\{\frac{1}{2^n}\right\}\dot{V}$, $\dot{V}_n$ = flow in one member of nth generation

If $D_n = k_n D$ where D_n = diameter of member of nth generation

and k_n = constant $\leqslant 1$

Then $\bar{V}_n = \frac{4\dot{V}_n}{\pi D_n^2}$ = average velocity in any member of nth generation

$$= \frac{4}{\pi}\left\{\frac{1}{2^n}\dot{V}\right\}\cdot\frac{1}{k_n^2 D^2}$$

$$= \frac{1}{2^n k_n^2}\cdot\left\{\frac{4\dot{V}}{\pi D^2}\right\}$$

$$= a\,\bar{V} \quad \text{where } a = \frac{1}{2^n k_n^2} \qquad \ldots\ldots\ldots\ldots\ldots\ldots\ldots\ldots\ldots 1.1.1$$

Thus, the velocity of a gas at any particular level in the conducting portion of the respiratory tract is a function of its average velocity in the trachea. In turn, this depends on the volume of gas inspired per unit time through the mouth or nose. In any given calibre of airway, this volumetric flow rate determines the degree of turbulence, a phenomenon which can be described by the REYNOLDS number, a parameter which gives the ratio of the inertial to the viscous forces acting in the fluid (REYNOLDS, 1883).

Mathematically, this Reynolds number is given as

$$Re = \frac{\sigma \bar{V} L}{\eta} \quad \text{.....1.1.2}$$

where σ = fluid density (kg m^{-3})

$\bar{V}$ = average velocity of fluid (ms^{-1})

η = dynamic viscosity of fluid (Nsm^{-2})

L = characteristic dimension of the airway (m)

For a circular tube, L is usually the diameter. The Reynolds number is dimensionless, its value for any particular flow system being indicative of the rectilinearity of the fluid motion. Thus for a value of $Re \lesssim 2800$ the fluid motion would be considered as laminar or streamline, viscosity being the dominant mechanism characterising the flow. This value is dependent on the entry conditions to the tube and can drop to around 2320 if the inflow is very irregular (SCHILLER, 1922). Beyond this "critical" value of Re, the fluid would be considered to be in a transition phase with eddy components present. These instabilities increase with increasing Re until at high values the fluid motion is completely turbulent or sinuous.

In the laminar flow region in narrow tubes the HAGEN-POISEUILLE equation (HAGEN, 1839; POISEUILLE, 1840) is used to describe the rate of fluid flow.

$$V = \frac{\pi R^4 dp}{8 \eta \, dl} \quad \text{.....1.1.3}$$

where V = volumetric flow rate ($m^3 s^{-1}$)

R = tube radius (m)

η = coefficient of viscosity (Nsm^{-2})

dp/dl = pressure drop per unit length of tube ($kgm^{-2}s^{-2}$)

An important characteristic of a motion of this type is that the velocity profile in the tube is a paraboloid of revolution mathematically described by

$$V = 2\bar{V}\left(1 - \frac{r^2}{R^2}\right) \quad \text{.....1.1.4}$$

where $\bar{V}$ = average velocity of fluid (ms^{-1})

and V = velocity of fluid at distance r from the tube axis (ms^{-1})

In turbulent flow, this profile is much flatter, the velocity distribution across the tube being more uniform (PRANDTL, 1952).

As previously stated, the flow rates, and consequently the Reynolds numbers in any given lung generation are dependent on the inspiration rate. In the conducting airways, the Re for moderate rates of breathing are of the order of 1500-2000 (JAEGER and MATTHYS, 1970) in the trachea, with increased streamlining of fluid motion as depth into the lung increases.

Beyond the terminal bronchioles exists the second of the important compartments - the alveolar region. This is the functional part of the lung as regards gas exchange. The oxygen from inspired air is transferred to the blood across a delicate membrane of about 1μm thickness (AVERY et al, 1973). Simultaneously, carbon dioxide is transferred in the opposite direction to be carried from the lung during exhalation.

The alveoli in the normal adult number approximately 296 x 10^6 (WEIBEL and GOMEZ, 1962; WEIBEL, 1963). DUNNILL (1962) has shown that at 8 years of age the number of alveoli has increased to 280 x 10^6 from approximately 24 x 10^6 at birth. Recent confirmation of these results (although with slight numerical differences) has been obtained by DAVIES and REID (1970).

One consequence of this vast number of terminal air spaces is that the blood/gas interface covers an area of approximately $70m^2$, although the exact value depends on the age and surface area of the body. (WEIBEL, 1963).

Consequently, the Reynolds number of any inspired gas within the alveolar depths can be assumed to be vanishingly small, with volume flow having little meaning.

The anatomical description of the lung adopted here conveniently pinpoints the important regions where certain deposition mechanisms have their maximum efficiency.

Deposition of aerosols in the lung is effected by inertial precipitation, sedimentation and diffusion. In passing, interception should be mentioned as a mechanism dependent on the ratio of the aerosol particle size to that of the airway. It is of no great importance for particles (HATCH and GROSS, 1964) being swamped by the other mechanisms, but is very relevant in problems concerning the deposition of fibrous materials e.g. asbestos. As such particulates have played no part in this study, no further mention will be made of interception.

1.2 INERTIAL PRECIPITATION (IMPACTION)

When an air stream laden with particles suddenly changes direction, these particles, by virtue of their inertia, will tend to travel on their original trajectory. The probability of deposition will depend on their mass and speed of travel and on the site of any potential impediments to their motion.

Consider a particle projected into still air. The equation of motion can be expressed as

$$m\ddot{s} = -b\dot{s} \quad \text{.....1.2.1}$$

where m = particle mass (kg)

$\ddot{s}$ = acceleration of particle (ms^{-2})

$-b\dot{s}$ = drag acting against particle motion (hence the negative sign). ($kgms^{-2}$).

Thus $m\dot{v} = -bv$ where v = velocity (ms^{-1})

$\therefore\ m\frac{dv}{dt} = -b\frac{ds}{dt}$ where s = distance (m).

$\therefore\ m\frac{dv}{ds}\cdot\frac{ds}{dt} = -b\frac{ds}{dt}$

Integrating, $m\int dv = -b\int ds$

$\therefore\ s = -\frac{mv}{b} + \text{Constant} \quad \text{.....1.2.2}$

If the particle was travelling at velocity Vo when entering the still air

$s = o$ when $v = Vo$

$\therefore\ \text{Constant} = \frac{mVo}{b}$

i.e. $s = \frac{m}{b}(Vo - v) \quad \text{.....1.2.3}$

The maximum projection distance can be calculated. When the particle is brought to rest, $v = o$.

$\therefore\ s_{maximum} = \frac{m}{b}Vo \quad \text{.....1.2.4}$

For a spherical particle of diameter d (greater than the mean free path of the air molecules) travelling at a speed where inertia effects can be ignored (GREEN and LANE, 1964)

$$s_{max} = \frac{\pi d^3}{6}\rho\frac{1}{3\pi d\eta}\cdot Vo \quad \text{.....1.2.5}$$

where ρ = particle density (kgm^{-3})

η = viscosity of air (Nsm^{-2})

$3\pi d\eta$ = Stokes drag (Nsm^{-1})

Hence $s_{max} = \frac{d^2\rho}{18\eta} \cdot Vo$ 1.2.6

This, by definition, is the STOP DISTANCE of any particle travelling in the nominal Stokes regime (STOKES, 1850).

Since $\frac{d^2\rho}{18\eta}$ has the dimensions of time this quantity is often referred to as the RELAXATION TIME of the particle.

Equation 1.2.6 shows that in a given medium the stop distance is proportional to the square of the particle diameter and the speed of travel. Accordingly, in the upper respiratory tract from the trachea to a few generations beyond, where the flow rates are fast, the branching points of the airways will be most effective in arresting any invading particle. Obviously, the larger particles of a polydisperse aerosol flux entrained in the carrier gas, will have a far greater probability of impaction, since their inertia will be higher.

It has been shown previously that as depth into the lung increases, the velocity of the carrier fluid decreases. This implies that any particles in the polydisperse cloud which have escaped deposition by inertial forces in the upper airways will suffer a progressive decrease in impactibility.

Inertial precipitation accordingly loses efficiency as a deposition mechanism, and is superseded in importance by sedimentation.

1.3 SEDIMENTATION

Gravity settlement of particles is the predominant mechanism of deposition in the lung regions where the motion of the inspired air is quiet i.e. the transit time of a particle through the generations is relatively long.

Any particle influenced by gravity in this region will fall freely and rapidly reach a terminal velocity, when the effective weight of the particle is balanced by the aerodynamic drag force acting on it.

Thus, in an infinite medium of density σ, the motion of a spherical particle of diameter d (greater than the mean free path of the medium molecules) can be described by the STOKES equation

$$3\pi d\eta v_t = \frac{\pi d^3}{6}(\rho-\sigma)g \quad \text{.....1.3.1}$$

where v_t = terminal velocity attained by the sphere (ms^{-1})

ρ = sphere density (kgm^{-3})

η = medium viscosity (Nsm^{-2})

g = acceleration due to gravity (ms^{-2})

Rearranging, $$v_t = \frac{d^2(\rho-\sigma)g}{18\eta} \quad \text{.....1.3.2}$$

If the medium is air, σ can usually be neglected since $\rho \gg \sigma$

Thus, $$v_t = \frac{d^2\rho g}{18\eta} \quad \text{.....1.3.3}$$

This equation can be used conveniently to introduce the concept of aerodynamic diameter of a particle. By definition, this is the diameter of a hypothetical particle of unit density which has a falling speed identical to that of the particle of density ρ in question.

Thus if d_o is the aerodynamic diameter

then, $$v_t = \frac{d_o^2 . 1 . g}{18\eta}$$

i.e. $$d_o = d\sqrt{\rho'} \quad \text{.....1.3.4}$$

The aerodynamic diameter is of particular use when comparing the sedimentation and impaction probabilities of species of aerosols of differing densities. A correction is necessary to the terminal velocity when the sedimenting particle is of size comparable to the mean free path of the air molecules (0.0653μm at 293°K and one atmosphere - GREEN and LANE, 1964). The medium in this instance can no longer be considered as continuous from the view point of the particle. The resistance to motion therefore decreases with the particle "slipping" between the molecules. Accordingly, the terminal velocity of the

aerosol particle must be multiplied by a term known as the CUNNINGHAM correction factor (CUNNINGHAM, 1910).

i.e. v_t (corrected) = v_t (calculated) $(1 + \frac{2A\lambda}{d})$ 1.3.5

where $A = 1.26 + 0.4 \exp(\frac{-1.1d}{2\lambda})$ according to DAVIES (1945)

λ = mean free path of gas molecules (m)

Since gravity acts in the downward direction, any analysis of sedimentation, in the airways where this mechanism predominates, must take into account the random orientation of these airways with respect to the horizontal. In a horizontal tube a particle of terminal velocity v_t acted on by gravity for time t, will fall a distance $v_t.t$ vertically downwards: If the particle starts (at t = o) on the tube axis, and $v_t.t$ = R (the tube radius) it will deposit. When the tube is inclined at angle θ to the horizontal, the vertical fall must equal $R/\cos\theta$ if the particle starting on the axis is to be deposited.

Residence time and orientation of the given airway are thus important parameters as regards gravity settlement. This should be compared with the probability of impaction which does not depend on these entities.

In the case of regular tubes, the probability of deposition by sedimentation has been investigated theoretically by several workers (NATANSON (FUCHS,1964); PICH, 1972) and criteria established for either total penetration or total deposition.

The polydisperse flux of aerosol which has been considered to pass through the trachea in this analysis, has been acted upon by inertial precipitation and sedimentation mechanisms in its passage through the conducting airways. Consequently, on entering the alveolar region, the air stream has been denuded of the larger size particles.

The smaller particulates which have penetrated to this depth are normally of size comparable to the mean free path of the gas molecules, and accordingly subjected to the influence of the third deposition mechanism - Diffusion.

1.4 DIFFUSION

Owing to the continuous random motion of gas molecules, (BROWNIAN MOTION), any aerosol particles in the acinus will be subjected to an unceasing bombardment (in a 4π solid angle).

EINSTEIN'S equation (1905) mathematically describes the phenomenon.

i.e. $\overline{\Delta x}^2 = \frac{2kT}{3\pi\eta d} tC$ 1.4.1

where $\overline{\Delta x}^2$ = mean square displacement (m)

k = BOLTZMANN constant (JK^{-1})

T = Temperature (^oK)

t = time (s)

η = gas viscosity (Nsm^{-2})

d = particle diameter (m)

C = Cunningham correction factor

It can be seen that the probability of deposition by the diffusion mechanism increases with decrease in particle size. A size does exist however which has a minimum probability of deposition. This value, found experimentally to be about $0.5\mu m$ diameter exists because of the "balancing-out" of sedimentation and diffusion forces (DAVIES, 1961). Recent evidence however (HEYDER et al, 1973) has shown that the minimum may, in fact, cover a range of sizes where the effects are possibly dominated by intrapulmonary mixing of air during breathing. Particles of about $0.5\mu m$ have been used as tracers of gas flow in the lung by several investigators (ALTSHULER et al, 1959; PALMES and KAMINER, 1960; MUIR, 1966).

Although the deposition mechanisms have been "isolated" in this analysis, it should be noted that they act simultaneously.

A normal cycle of breathing, at rest, consists of inhalation, pause and exhalation with a frequency of about 15 breaths per minute. This present analysis of particle deposition is concerned with inhalation. The pause time at end-inspiration influences the magnitude of deposition due to sedimentation and diffusion in the inhaled aerosol. Since the air-flow in the lung is considered to act in a "first-in - last-out" principle (FOWLER, 1949; WEST et al, 1957) any particles which have escaped deposition will traverse the lung in reverse i.e. alveolar regions to trachea with increasing velocity of motion. The predominant deposition mechanisms previously described will thus act, but in reverse order.

Since sedimentation and diffusion have been amply treated, both theoretically and experimentally by numerous investigators (PICH, 1972; DAVIES, 1973), the magnitude of deposition by these mechanisms in a rigorously defined geometrical system can be predicted with relative confidence.

In the human, the complexity of the anatomical arrangement of the lung airways precludes an exact description of the geometrical boundaries of this system. Analysis of the regional deposition of aerosols therefore becomes an exercise in the intelligent application of the physics of the particulates to a system whose dimensional array and geometry can only be approximated.

Analysis of sedimentation and diffusion deposition fractions in the human lung is also complicated by the following criterion: Namely, any aerosol particles presented to the "regions" where these mechanisms act must have passed through the "region" of impaction. Consequently,

a knowledge of the fraction deposited by inertial forces helps to define the complementary fractions which tend to be deposited by the other mechanisms (dependent on time).

Survey of the literature has shown that the information readily available for assessing impaction probability is sparse. Accordingly, it is the purpose of this study to try and add further information to that available in the hope that calculations of total deposition of aerosols will be improved.

1.5 HISTORICAL REVIEW

The inhalation and retention of particulates in the human respiratory tract have been studied theoretically and experimentally in the past by various investigators.

Historically, FINDEISEN (1935) was the first to attempt to characterise the problems in physico-mathematical terms. Although his adopted anatomical model was relatively unsophisticated, the analysis served to define the general regions where the various physical factors were important.

LANDAHL (1950) modified the anatomical model of FINDEISEN, and extended his calculations to account for the simultaneous action of the primary deposition mechanisms. The results obtained for total deposition generally agreed with the experimental results of LANDAHL and HERRMANN (1948).

Overall improvements in the characterisation of the important anatomical features (WEIBEL, 1963), the reproducible generation of accurately known-sized particles (SINCLAIR and LA MER, 1949; WALTON and PREWETT, 1949) and in the measuring and computational techniques of experiment (ALTSHULER et al, 1957; ALTSHULER, 1959; BEECKMANS, 1965; DAVIES, 1972; HEYDER et al, 1973) have enabled the compilation of

literature relevant to the physiological mechanisms affecting particulate removal in the human lung, both in health and disease (MUIR and DAVIES, 1967; LOVE, 1973).

In general, the agreement between theory and experiment is good.

Existing inertial impaction theory, with respect to bronchial bifurcations, is normally based on the experimental results of LANDAHL and HERRMANN (1949) pertaining to simple right-angle bends. The resultant mathematical parameters derived from this work have been utilised (LIPPMANN and ALBERT, 1969) or referred to (ALTSHULER, 1959; TASK GROUP ON LUNG DYNAMICS, 1966; SCHLESINGER and LIPPMANN, 1972) whenever assessment of the inertial impactibility of particles is of interest.

Recognition of the complexity of fluid motion at a bifurcation has led, in recent years, to more fundamental research on the impaction problem. BELL (1970) and BELL and FRIEDLANDER (1973) have used large scale idealised models of a typical branching airway, in an attempt to relate, in particular, the site of deposition of the particles to the fluid mechanical variables.

CHAPTER TWO

EXPERIMENTAL

(i) PARTICLES

2.1 THE AEROSOL GENERATOR

Homogeneous, monodisperse aerosols in sufficient concentration for experimental purposes may be produced conveniently by the technique of disrupting a film of liquid by centrifugal atomisation, an effect first noted by JOHNSON and WALTON (1947).

An apparatus incorporating an adaptation of the high-speed air-driven top of BEAMS (1937) was developed by WALTON and PREWETT (1949), thereby enabling an investigation of the important parameters pertaining to the phenomenon. Their apparatus was considerably improved by MAY (1949) and further improvements by the same investigator (1966) allowed enhanced stability, reliability, ease of operation and improved performance.

Basically, when a liquid is fed on to the centre of an air (or electrically) driven rotor capable of high speeds, the liquid flows over the rotor surface in the form of a very thin film, to be centrifuged from the edge as a spray of droplets. These droplets are characterised by their monodispersity (within very close limits). For a given size of an air-driven rotor and a given liquid, variation of the rotor speed by alteration of the compressed air input causes a variation in the size of the resultant droplets.

The equation governing the production of the spray by this atomisation technique was derived by WALTON and PREWETT (1949) using the analogy of drop formation at a stationary tip (RAYLEIGH; 1879).

$$d = \frac{k}{w}\left[\frac{\gamma}{\rho D}\right]^{1/2} \quad \text{.....2.1.1}$$

where d = droplet size (m)

w = angular velocity of rotor (rad s^{-1})

γ = surface tension of solution (Nm^{-1})

ρ = density of solution (kgm^{-3})

D = rotor diameter (m)

k = dimensionless parameter

The parameter k has been found experimentally to have a mean value of 4.5 for an air-driven top (WALTON and PREWETT, 1949; MAY, 1949).

Several points should be noted about equation 2.1.1. Firstly, there is no mention of liquid viscosity, liquid feed rate or rotor edge profile (sharpness). In operation, the spinning top (disk) aerosol generator produces, in addition to the monodisperse primary droplets, a population of satellite droplets which are about one quarter of the size of the main droplets and about four times as numerous (MAY, 1949); a few spuriously occurring droplets of size greater than the primaries may also be present. Experimentally, it has been found that over the range from about 0.001 to 1.5 Nsm^{-2} viscosity appears to have little effect of the drop formation process, although at higher viscosities, the proportion of satellites tends to increase, and a limit exists in the liquid feed rate above which monodisperse drops are not formed. This limiting feed rate value is higher in the 0.001 to 1.5 Nsm^{-2} range (WALTON and PREWETT, 1949).

Disk edge profile is of no great importance for large droplets, but when spraying fine droplets, of size comparable to the disk edge roughness, it is recommended that the more perfect the finish, the better the instrument performance (MAY, 1949).

Facing Page 16

Fig. 2.1 The R.E. - MAY Spinning Top Aerosol Generator.

Normally, the liquid feed rate on to the centre of the disk is about 0.17×10^{-4} ls^{-1}, although ELLISON (1967) is in agreement with WHITBY et al (1965) who state that liquid feeds up to about 0.015 times the disk diameter in metres can be used without noticeable impairment of the resultant aerosol quality.

The larger droplets previously mentioned have an obscure origin, but since they comprise between about 1 and 2 per cent of the main droplets by number (MAY; 1949), their presence poses no major set-backs to the efficient operation of the apparatus.

On the other hand, the satellite droplets are much more numerous. The apparatus of MAY (1966) was designed to eliminate, amongst other problems, the presence of these satellites. In this device, use is made of ejector and Coanda effects at the disk head, which ensure the automatic entrainment and subsequent removal of the satellite particles from the system.

Commercially available (RESEARCH ENGINEERS LTD., LONDON), the spinning top apparatus (fig. 2.1) will produce, satisfactorily, droplets down to about 10μm diameter (MAY, 1966).

To obtain solid particles the technique used is that of spraying a solution (of known concentration) of a suitable involatile in a given solvent; on evaporation of the solvent, spherical particles of a given size remain.

The required concentration of solution which will yield particles of pre-determined size from a given droplet flux may be determined in the following manner. The solution will be sprayed (ideally) as n identical droplets each of volume $\pi d^3/6$ where d is the diameter. On evaporation of the solvent, n dry particles each of mass $\pi d_p^3/6 \cdot \rho_p$ obtain where d_p is the particle diameter and ρ_p is its density.

The concentration of the solute in one droplet was therefore

$$(\pi d_p^3/6 \cdot \rho_p) \;/\; (\pi d^3/6)$$

Since the particles were identical, this was also the concentration of the original solution.

i.e. $c = d_p^3 \rho_p / d^3$

$$\therefore \quad c = (d_p/d)^3 \cdot \rho_p \qquad \text{.....2.1.2}$$

or/ $$d_p = d(c/\rho_p)^{1/3} \qquad \text{.....2.1.3}$$

Substituting for d from equation 2.1.1 yields

$$d_p = \frac{k}{w} (\gamma/\rho D)^{1/2} \cdot (c/\rho_p)^{1/3} \qquad \text{.....2.1.4}$$

This technique for producing particles of predetermined size has been used satisfactorily by numerous investigators (PHILIPSON, 1973; ALDRICH and JOHNSTON, 1974*).

Since the production of a spray by the spinning disk method necessitates the disruption of a liquid film into discrete units (droplets), a high probability exists that a sizeable fraction of the spray will be electrostatically charged (WHITBY and PETERSON, 1965; CHOW and MERCER, 1971) although the total charge of the spray as a whole will be zero. On spraying solutions, this "imbalance" of charge will be conserved as the solvent evaporates, resulting in dry particles which may have a high charge to mass ratio. The surface forces involved may tend to impair the production of spherical particles (WHITBY and PETERSON, 1965).

Many investigators have examined the charge distributions on droplets and the resultant particles, with a view to establishing the reduction of this electrification phenomenon to an equilibrium value (WHITBY and PETERSON, 1965; WHITBY et al, 1965; WHITBY and LIU, 1968; FRY, 1969; CHOW and MERCER, 1971).

* IN APPENDIX

Passage of charged droplets or particles through a bipolar atmosphere produced by a radioactive source (WHITBY and LIU, 1968; FRY, 1969) or a corona discharger (WHITBY and PETERSON, 1965) have been accepted as the most convenient methods for charge neutralisation. Indeed, the former technique is used in commercially available aerosol generators (ENVIRONMENTAL RESEARCH CORPORATION, MINNESOTA). WHITBY and PETERSON (1965) and WHITBY et al (1965) state that passage of a droplet cloud through a bipolar atmosphere prior to completion of evaporation reduces the tendency for surface forces to distort the droplet shape; a post-evaporation atmosphere will reduce the final charge on the resultant dry particles to a low equilibrium value.

The aerosol generator employed in this study was used to generate homogeneous monodisperse aerosols of uranine/methylene blue mixtures. Uranine (fluorescein sodium) is a very common pigment which, when excited with spectral energy in the range 0.42 to 0.45μm will fluoresce, emitting visible energy of longer wavelength (0.47 - 0.56μm). The ease of detection of this fluorescence ($\gtrsim 10^{-10} kgl^{-1}$) and the pigment's ready solubility in the common organic and inorganic solvents makes it a very convenient aerosol for experimental purposes (STEIN et al, 1966). Compounds of uranine have also been used successfully as aerosols in the laboratory (STÖBER and FLACHSBART, 1973).

Great difficulty was encountered when attempting to produce aerosols of pure uranine alone. The particles obtained tended to be crystalline and had impaired sphericity (SEHMEL, 1967). This made satisfactory reproduction extremely difficult. Mixing the uranine with known proportions of methylene blue pigment greatly enhanced the sphericity, reduced the tendency for crystallising out and allowed for much easier

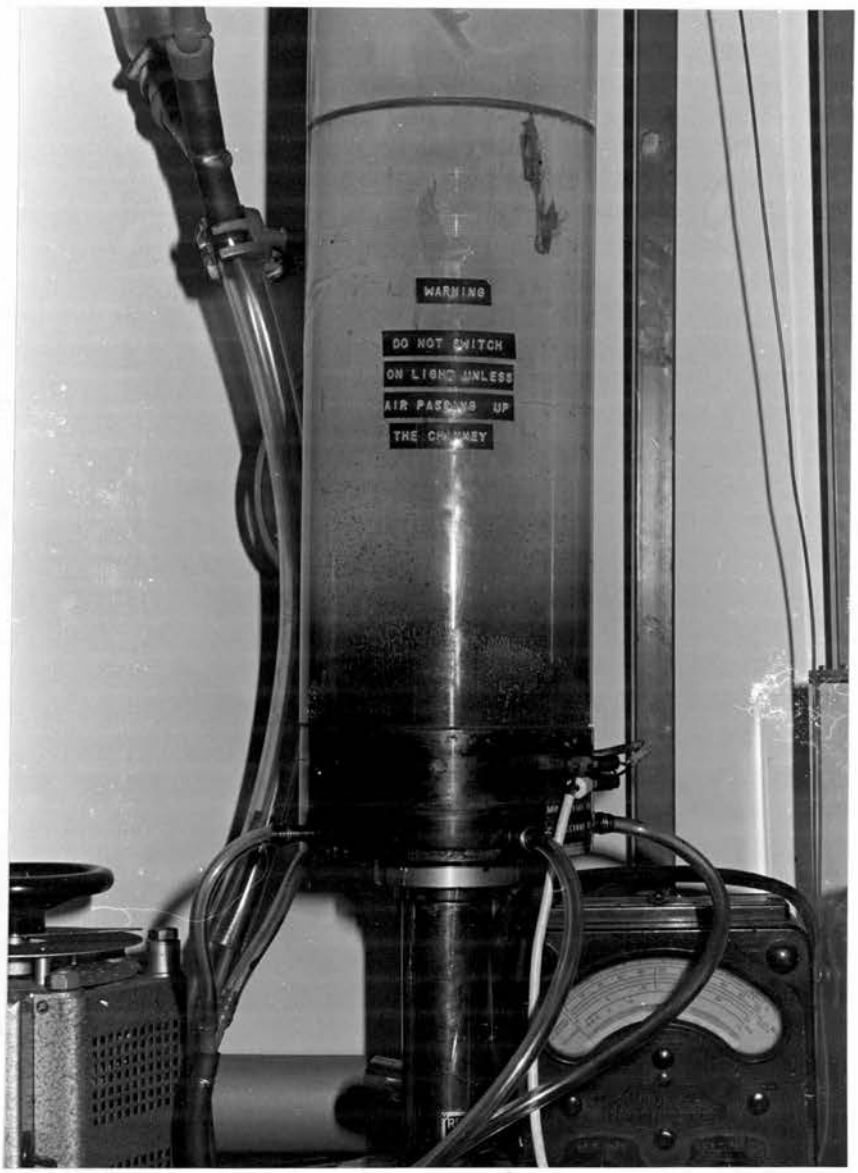

Fig. 2.2 Method "A" Assembly

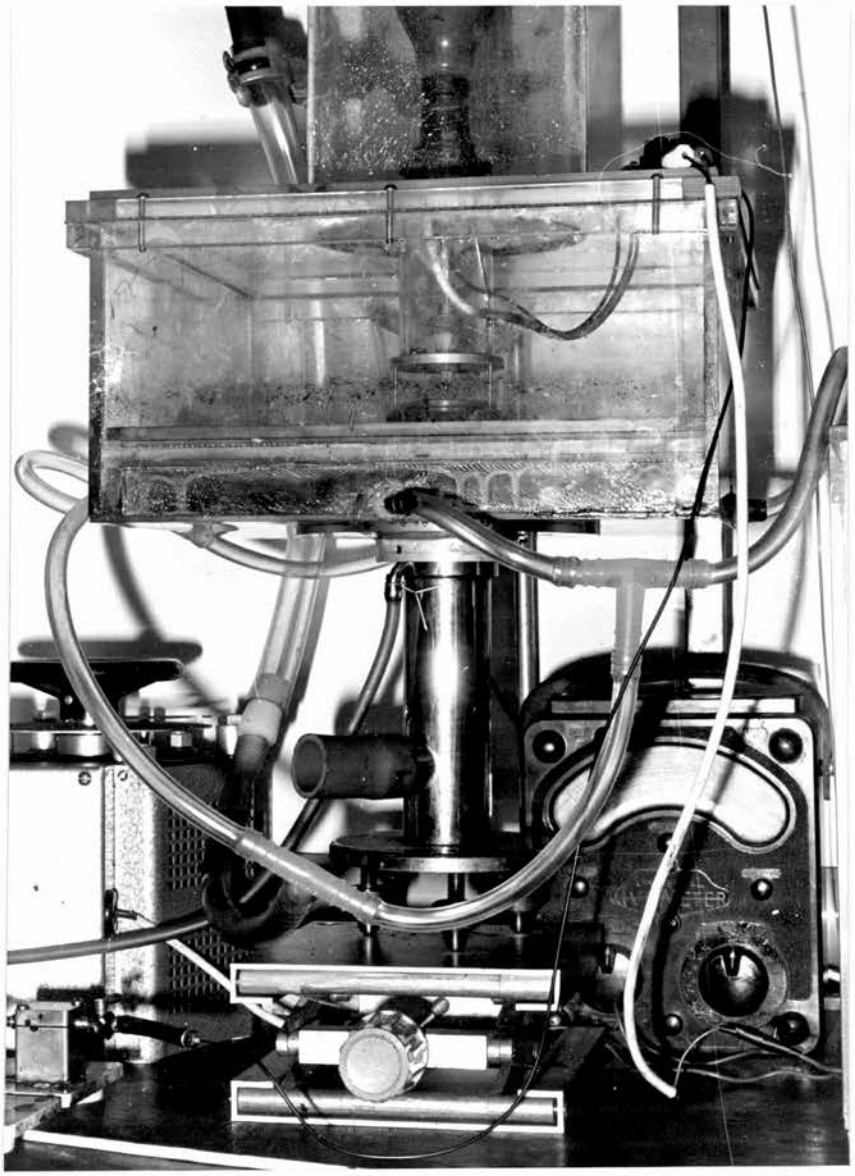

Fig. 2.3 Method "B" Assembly

Fig. 2.4 Acrylic Tube and Light Attachment

microscopic examination of any particulate sample (SEHMEL, 1967; WHITBY et al, 1965).

The spinning disk aerosol generator could be mounted in either of two distinct assemblies, the choice being dependent on the particular operating conditions required. The simpler of the two mountings (Method A, fig.2.2) obtained when the generator was connected by a length of perspex tubing abutting one leg of an inverted 0.15m diameter U-tube arrangement (fig. 2.6). The other leg was directly connected into a perspex aerosol holding-chamber with an outlet to atmosphere. The generator could be separated from the U-tube system (to allow access to the top for regular maintenance e.g. cleaning) simply by lowering the levelling screws at the generator base. Method A assembly was used for the majority of experiments utilising a fixed size of particle.

Method B differed from Method A in that the effective "diameter" of the tube surrounding the disk was increased severalfold by a box arrangement of greater width than the 0.15m diameter tubing used in Method A. Connection to the inverted U-tube was accomplished by a smaller length of perspex tubing than in A, but of similar design (fig. 2.3). Access to the disk etc. was facilitated by the use of a "Labjack" (A. GALLENKAMP & CO. LTD., GLASGOW) placed under the feet of the aerosol generator.

Methods A and B differed only in the design of the mounting.

Surmounting the hypodermic needle unit connected to a Palmer Injector Apparatus (C.F. PALMER LTD., LONDON) used to feed solution to the disk surface, was an acrylic tube attachment which supported an electric bulb in a suitable fitting along the tube axis (fig. 2.4). This bulb was connected to the mains supply via a switch and Variac.

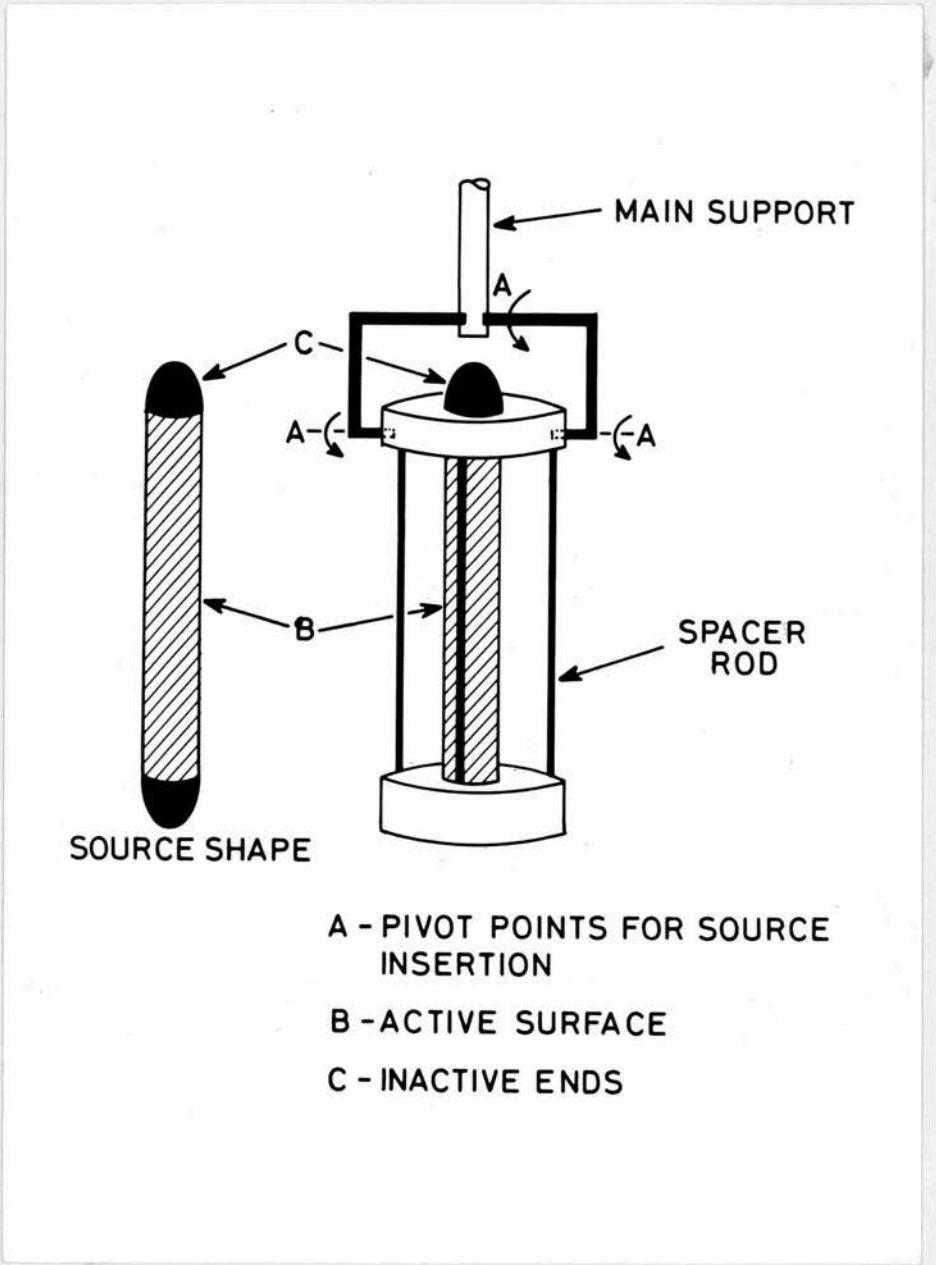

Fig. 2.5 Support for Radioactive Sources

Evaporation of any liquid requires a source of energy which will supply the latent heat necessary for the phase change. For a given liquid, the energy required is a function of the mass to be evaporated. The Variac enabled the power supply to the bulb to be varied, thereby allowing for different liquid feed rates to the spinning disk (if necessary).

A specially designed support rod (fig. 2.5) holding an earthed Nickel tube containing 10mCi of Krypton-85 radioactive gas was placed in position above the "heater" to neutralise the droplet spray (WHITBY and LIU, 1968; FRY, 1969).

In operation of the aerosol generator, the flux of droplets produced was blown upwards through the U-tube assembly by a dry air supply monitored by Rotameters (GEC-ELLIOTT PROCESS INSTRUMENTS LTD., CROYDON) and entering at the base of the leg. The turbulence of the air was damped out before encountering the droplets, by passage through a perspex or fine mesh grid acting as a flow straightener. Passage of the aerosol over the heater and through the bipolar atmosphere produced by the source resulted in evaporation and the prevention of distortion to the droplets.

In transit through the upward conduit of the assembly the solvent was completely evaporated from the droplets, being taken up by the dry carrier air (ELLISON, 1967). The resultant dry particles were then carried through the downward leg of the system, again passing through the field of another 10mCi Krypton-85 source. An earthed support rod held this nickel tube containing the radioactive gas concentric within the leg. Any remaining static electrification was therefore minimised (WHITBY and LIU, 1968).

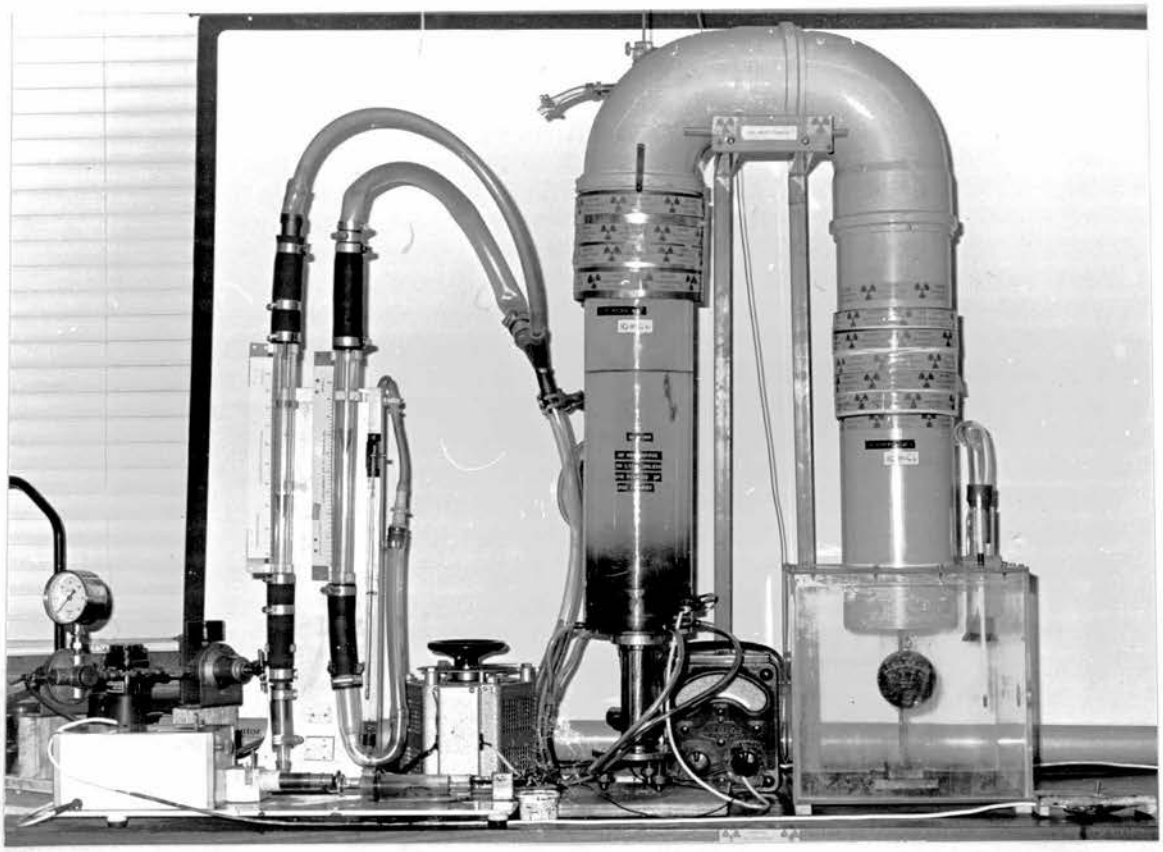

(i) Method "A" Assembly

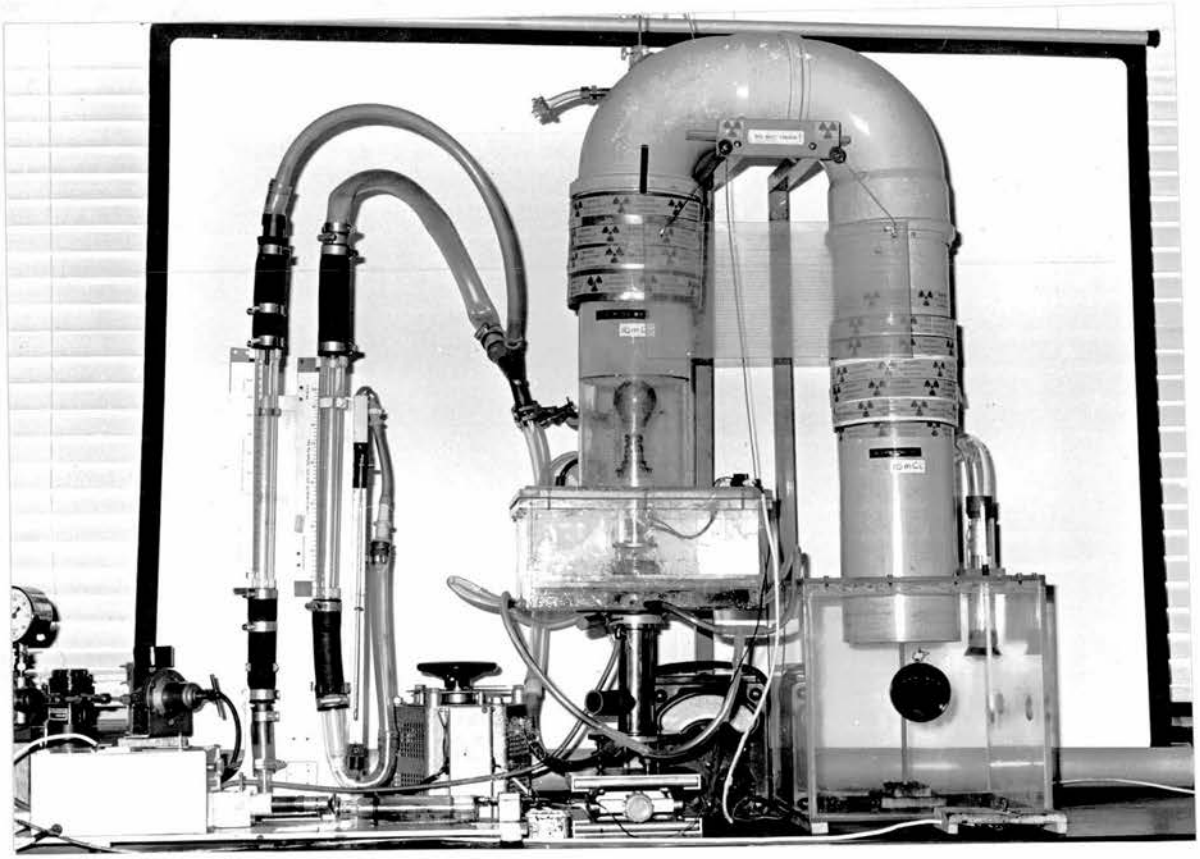

(ii) Method "B" Assembly

Fig. 2.6 The Aerosol Generators

The aerosol flux finally entered the "holding" chamber and could be drawn off for experimental purposes or allowed to pass to atmosphere.

To generate dry particles in a range of sizes with the spinning disk aerosol generator, one method was to hold the disk at a fixed number of revolutions (simply by holding the compressed air input pressure constant) and vary the concentration of the feed solution (in accord with equation 2.1.3). The other technique was to fix the solution concentration and vary the disk speed.

From equation 2.1.1, it can be seen that the drop size is inversely proportional to the disk speed. By virtue of mass, large drops have a greater projection distance (tangentially) from the disk edge than small ones. Consequently, as the speed of the disk was reduced (droplet diameter increasing) a speed was reached where the projection distance equalled the disk edge to conduit wall distance (approximately the radius). These drops impacted on the walls and were lost from the system. This automatically set a limit to the lowest speeds usable in the apparatus, particularly method A. Method B was in fact designed to complement A and to extend the working range of the generator. Fig.2.6 shows the complete aerosol generator for both methods of assembly.

MAY (1949) points out that for water, drop ring radius in inches is one tenth of the drop diameter in microns. Accordingly in Method A, it was obviously impossible to generate water droplets greater than about 30 μm. Method B assembly did not have this limitation. (It should be noted that the proportionality between drop mass and projection distance can be used to advantage to eliminate the spurious large drops previously mentioned, since they will tend to impact on the leg walls).

Because of the high surface tension of water and aqueous solutions, the disk surface was not readily wetted. It was extremely important for correct operation of the apparatus that a thin even film of liquid spread over the disk. By grinding the surface and edge of the disk with carborundum (Grade 100) and adding a few ml of sodium di-octyl sulpho-succinate (AEROSOL-OT) solution - a wetting agent - prior to spraying any aqueous solution, the process proceeded satisfactorily. Solutions made up in this experimental investigation were in the ratio of 2:1 Uranine: Methylene Blue, in distilled water as solvent.

Because of the automatic satellite removal of the R.E. - MAY spinning disk apparatus there was a tendency for solute to build up on the rim of the stator. Eventually, this affected the performance of the apparatus. It was found necessary that the system be stripped down regularly for cleaning purposes and routine grinding of the rotor. In agreement with MAY (1949), it was found that running time was not indefinite, but inversely dependent, as a function of time, on the concentration of solution used.

2.2 THE RADIOACTIVE SOURCES & ASSOCIATED SHIELDING

The Kr-85 beta sources (RADIOCHEMICAL CENTRE, AMERSHAM) used in this study for neutralising aerosol static electrification effects were Class 1V Radionuclides (Low Toxicity)—(CODE OF PRACTICE, 1968).

The relatively long half life of these isotopes (10.6 years) ensured a constant supply of ions throughout the duration of the project.

Since the author was classed as "non-designated" with respect to the use of radioactive isotopes, the total dose rate from the Kr-85 sources should not have exceeded 0.75 mrem/hour averaged over any one minute outside the shielding (CODE OF PRACTICE, 1968).

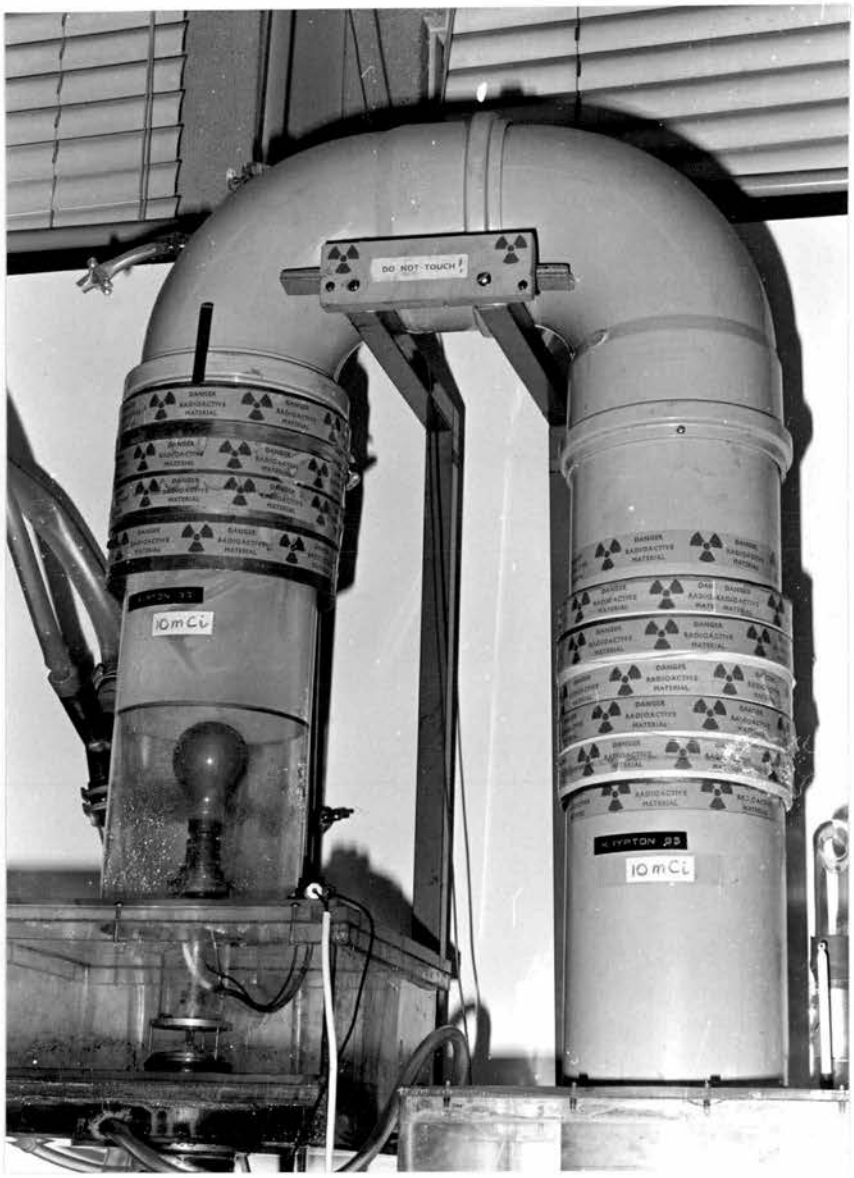

Fig. 2.7 Radioactive Sources and Shielding

The type of shielding required was decided by consideration of the types and energies of the radiations from the sources, which are principally β^- but have a γ-component, although of fairly low energy (0.51MeV) and abundance (0.7%). The thicknesses of the materials were calculated using BS4094 Part 1 (1966) i.e. recommendation for Data on Shielding from Ionising Radiation - Part 1. Shielding from γ-radiation.

Since both sources were mounted coaxially within the U-legs of the generator and were permanent fixtures to the apparatus, the shielding materials were themselves permanently located by being wrapped round the outsides of the legs and held in position by suitably large Jubilee Clips (fig. 2.7).

As the conduit legs were made of plastic of about 4×10^{-3}m thickness the β^- particles would be easily absorbed. H.M.S.O. Handbook of Radiological Protection (1971) states however that the Bremsstrahlung may be comparable to the γ-emission, so several layers of Aluminium were superimposed on the plastic cylinder for complete attenuation of the β^- emission. Further layers of lead sheeting on top of the aluminium completed the shielding precautions.

Monitoring was performed using a calibrated Mini-Instruments Radiation and Contamination Monitor (MINI-INSTRUMENTS, LONDON) and was found to be well below the maximum permissible level.

When routine maintenance to the apparatus was needed it was necessary for the spinning disk unit to be separated from the assembly as a whole. This left the source in the "upward" conduit exposed without adequate shielding. To remedy this defect, a large sheet of 3×10^{-3}m thick perspex was placed between the source and the operator, thereby reducing the dose of radiation to the hands etc., during the short time required for disk cleaning.

As a check on the system, the shielding precautions as a whole were examined by the National Radiological Protection Board (Scottish Centre) and the apparatus approved as adequately shielded within the meaning of the Code of Practice for the Protection of Persons against Ionising Radiations in Research and Teaching (1968).

Regular monitoring was undertaken to comply with the Local Rules for the use of Radiation within the premises.

2.3 CHARACTERISATION OF THE AEROSOLS

MORROW (1970) states that particles in the size range 1-10μm are of most interest "since they will not so successfully delineate within the respiratory tract and because these particles are ordinarily the most significant in controlling the mass of aerosols". The particulates used in this study lay within this range.

Acceptance of the spinning disk apparatus as the most suitable generator necessitated the satisfaction of the following criteria. Firstly, the size characteristics of the produced aerosols must be readily calculable. Equation 2.1.4 allowed this to be done within the limits of experimental error. Secondly, the production of the particles must be reproducible. Since there are only two methods of varying the resultant particle size with a generator of this type i.e. fix speed and vary concentration of solution or vice versa, careful monitoring of these entities ensures faithful reproducibility. Thirdly, the resultant aerosol should be monodisperse. It is not impossible to work with polydisperse aerosols (CUDDIHY et al, 1973) but it is obviously more convenient to work with particles which can be treated as identical, with relatively little error involved.

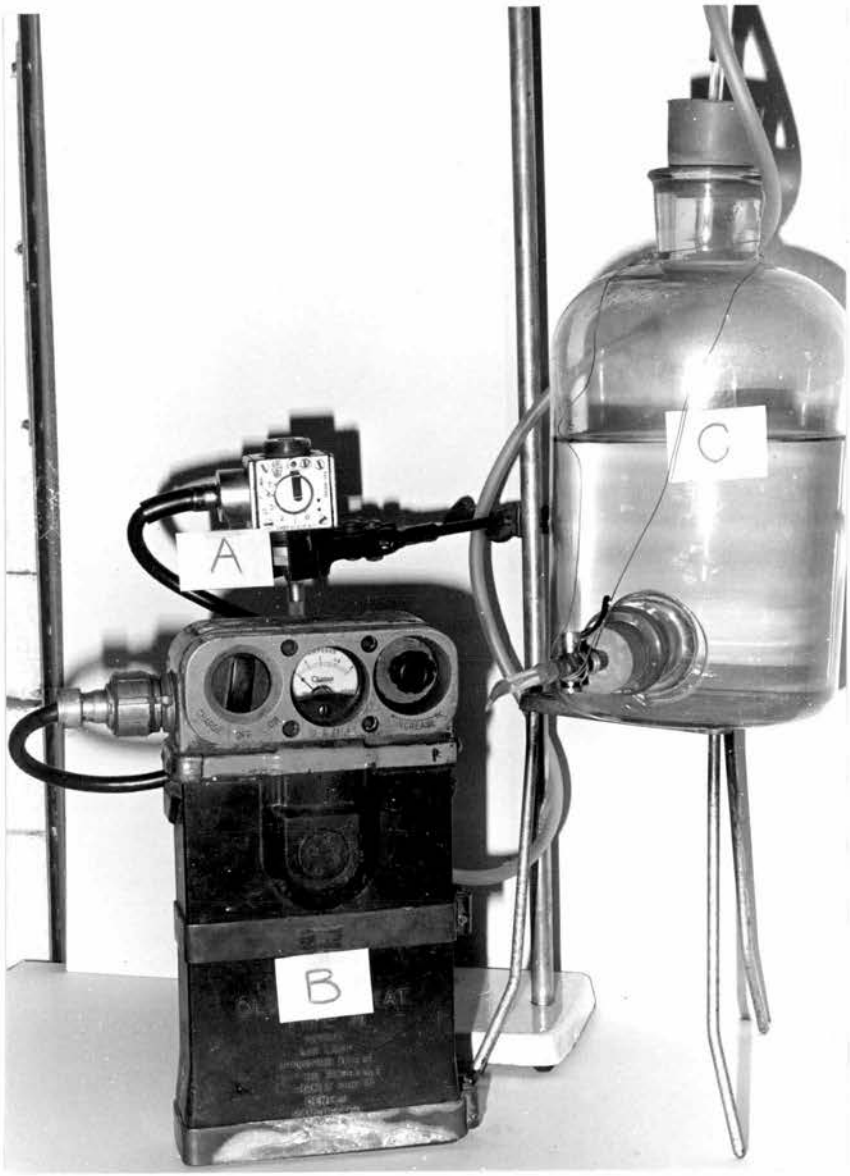

Fig. 2.8 The Thermal Precipitator

A. Sampling Head

B. Battery

C. Aspirator Bottle

Facing Page 25

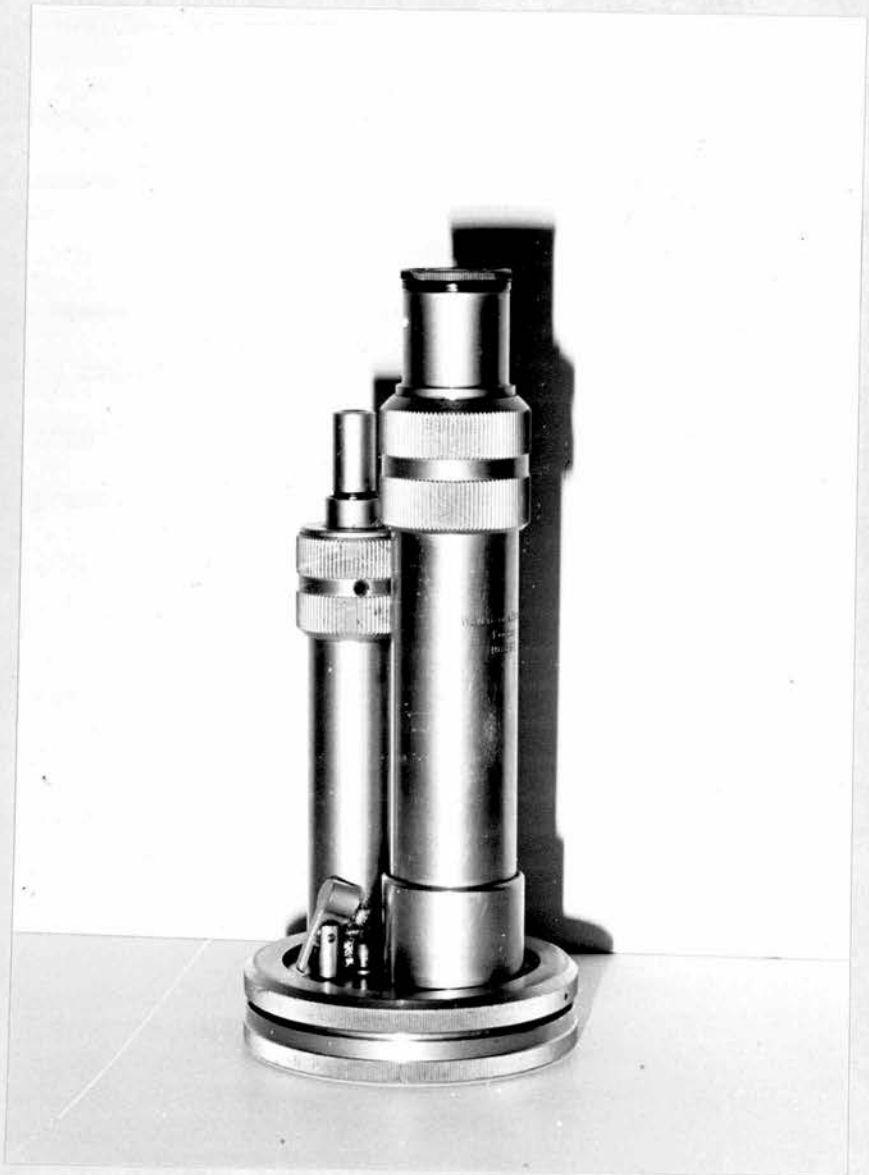

Fig. 2.9 The Konimeter

With Method A generator set-up, the disk speed was fixed at a constant number of revolutions per second, by holding the input air pressure constant. The feed rate of solution was kept at $0.17 \times 10^{-4} ls^{-1}$ for all concentrations of solutions.

Samples were taken for analysis either with a Standard Thermal Precipitator (S.T.P.) (fig.2.8) aspirating at a known flow rate, or with a WATSON Konimeter. (W. WATSON & SONS, BARNET) incorporating a built-in microscope and graticule (fig.2.9). These instruments were also used when Method B set-up was in operation.

The S.T.P. utilises the phenomenon of the dust-free space surrounding a hot body in its operation (WATSON, 1936). Air laden with particles is drawn through a sampling head containing a thin wire attached to a battery. The wire is heated by the electric current and consequently produces a dust free space surrounding it. Within the boundaries of this zone lie two glass coverslips on either side of the wire. Particles approaching the dust free space have no alternative but to deposit on these slides since they are forbidden entry to the dust-repellant zone itself. The coverslips are then removed for microscope examination. Because of the operating procedure i.e. fixed low aspiration rate and constant battery current, the S.T.P. was not found to be a convenient piece of apparatus for rapid assay of any of the particulate clouds used in this study.

On the other hand, for rapid examination of any aerosols with the minimum of inconvenience to the operator, the Konimeter was very convenient. Basically, this instrument works by impaction. A plunger of known stroke delivers, through a thin orifice, a fixed volume (5ml) of

air, laden with particles. These particles, owing to their inertia deposit on a glass plate smeared with a thin layer of adhesive. The particular model of Konimeter used, allowed the collection of 30 samples before cleaning of the plate became necessary. The most convenient feature of the model, however, was a built-in microscope and graticule. This optical system comprised a x12 objective and x18 eyepiece, with an overall magnification of 216 diameters. By rotating the dust deposition plate in situ any of the 30 samples could be placed in the field of view of the objective. A focussing knob allowed for correct viewing of the specimen.

The graticule in the eyepiece consisted of two intersecting lines forming two vertically opposite angles of 18^{o}. Parallel to one of these lines ran another separated from it by $5\mu m$. Aerosol clouds of particles $5\mu m$ in diameter were used in many of the experiments (to be explained in later chapters) because of the easy monitoring of their size using this feature of the graticule.

Any sample taken with the S.T.P. was analysed by light microscopy in order that a size distribution with its attendant parameters be drawn to characterise the specimen. The glass plate of the Konimeter could also be removed for similar scrutiny. A given aerosol may be characterised by defining a representative particle diameter in the sample and giving a measure of the spread of the distribution of sizes. This procedure is necessary since no aerosol is perfectly monodisperse (RAABE, 1970).

Most naturally occurring aerosols are distributed log - normally e.g. a plot of number of particles per size range against logarithm of particle size can be described by the statistical parameters characterising a normal distribution. Plotting fraction per size range against

particle size itself would yield a curve skewed slightly to the right.

Representative parameters of such distributions are the mean, the mode and the median, with the spread defined by the geometric standard deviation (σg). These parameters are easily assessed when the distribution is plotted on logarithmic probability paper, since a straight line obtains (GREEN and LANE, 1964).

Another technique, used when dealing with aerosols exhibiting near monodispersity, is to measure the diameters of a portion of the given population of particulates, derive a mean size and calculate a coefficient of variation from the standard deviation of the sample (FUCHS and SUTUGIN, 1966).

$$\text{i.e. Coefficient of Variation } (\alpha) = \frac{\text{Standard Deviation}}{\text{Mean Size}}$$

These authors state that a coefficient of variation less than about 20% is acceptable for defining a monodisperse aerosol with as low a value as possible being ideal. The value of σ_g corresponding to this value of the coefficient of variation is about 1.2, a perfect aerosol having $\sigma_g = 1.0$.

In this study, unless otherwise specified, all particles are defined by their count mean diameter with distribution spread characterised by σ_g. For small values of α, FUCHS and SUTUGIN (1966) show that

$$\ln \sigma_g \simeq \text{Coefficient of Variation}$$

The samples of particles obtained at the various settings of the aerosol generator were normally analysed by comparison with the circles of a PATTERSON - CAWOOD graticule (1936), previously calibrated with a stage micrometer. This allowed computation of a cumulative size distribution and the definition of the relevant important parameters.

As will be seen in later chapters, a sizeable fraction of the experiments did not require an absolute value for the diameter of the

Disk Speed* (r.p.s.)	Solution Concentration (kgl^{-1})	Mean Diameter (μm)	Geometric Standard Deviation (σ_g)
1500	0.01	4.2	1.13
1500	0.02	5.0	1.08
1500	0.03	5.5	1.11
1500	0.04	5.8	1.14
1250	0.04	6.8	1.13
1000	0.04	8.3	1.13
680	0.05	8.8	1.16

* Taken from Manufacturer's Calibration Sheet.

Table 2.1 Typical Operating Conditions and Particle Characteristics.

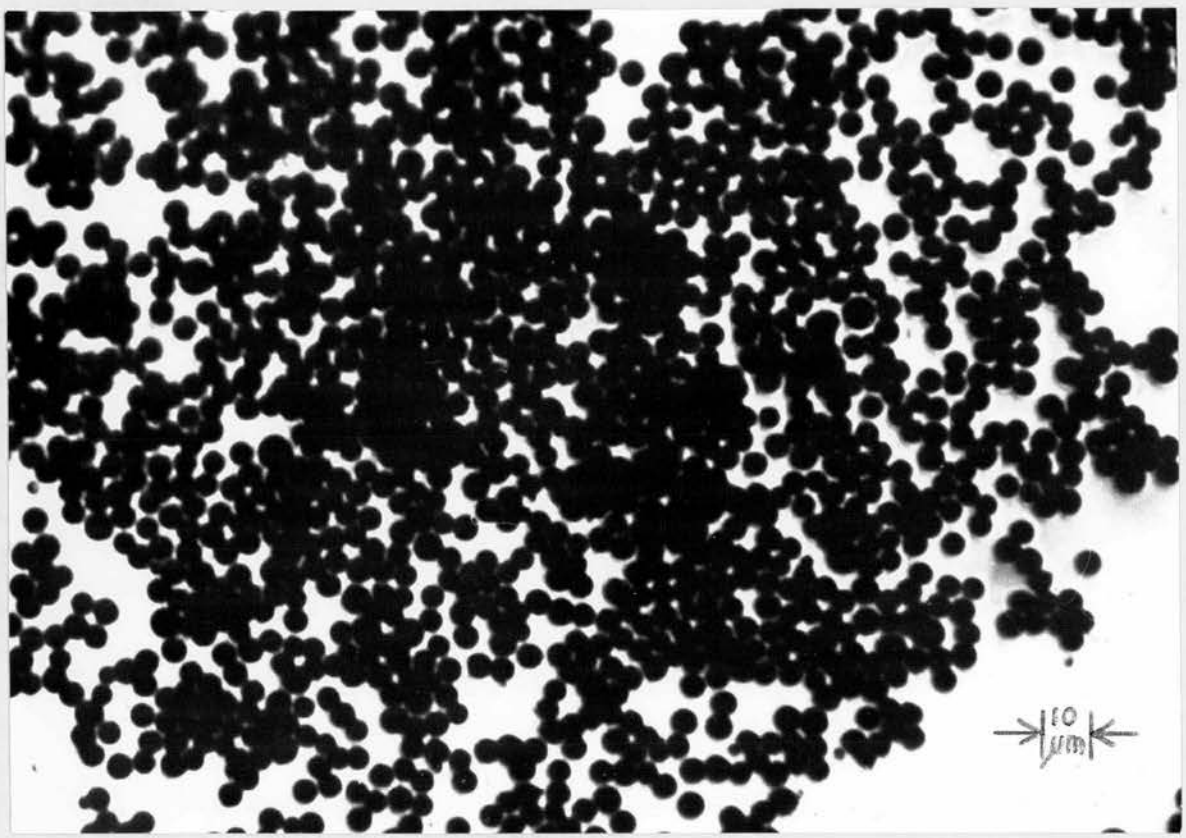

Fig. 2.10 Example of Particles obtained with Spinning Disk.

particles used. When these conditions obtained, samples of the aerosol were taken with the Konimeter and size analysis performed using a TIMBRELL Double-Image micrometer (FLEMING INSTRUMENTS, STEVENAGE), a device which gives a direct dial reading of the particle diameter. The performance of the generator could be assessed (with respect to reproducibility) by comparison of the "mean" size calculated from the Double-Image micrometer with that obtained by the "rigorous" method of cumulative sizing performed at an earlier date. The exception to this "rule" obtained when the generator was set to yield 5μm diameter particles. The graticule of the Konimeter was used for size checking in this instance.

Table 2.1 shows the particle sizes obtained at the various operating conditions while fig. 2.10 shows typical examples of the particles obtained.

Two further points are worthy of attention. Firstly, the bipolar atmospheres were most effective in preventing the inconsistencies in particle production mentioned in the previous section. Throughout the duration of this study no multiplet production and no impairment of particle sphericity were observed which could possibly cause serious doubts as to the correct operation of the generator as a whole.

Secondly, while the Konimeter was in use for monodispersity and sizing checks, it doubled as a device for assessing when the generator needed cleaning. The build-up of solute on the stator and disk caused the aerosols to become progressively more polydisperse. If this effect occurred during an experiment, the results were ignored. The generator was then stripped down for cleaning etc., and the experiment repeated.

2.4 DENSITY OF THE AEROSOL PARTICLES

A knowledge of particle density allows the aerodynamic characteristics of a sphere to be determined. Since the density of the particles may not be the density of the parent material (RAABE, 1970) it becomes important that the density value of any test aerosol be clearly known.

One problem arising with uranine/methylene blue aerosols is that no accurate listing of the density exists. STEIN et al (1966) calculated the density of spherical uranine particles (generated by nebulisation) to be $0.58 \times 10^{3} kgm^{-3}$. The bulk density of the powder used to make up their solutions was determined to be $1.53 \times 10^{3} kgm^{-3}$ by a pycnometer technique.

A spinning disk apparatus was utilised by SEHMEL (1967) to generate monodisperse particles of uranine or uranine cum methylene blue in the size range 3 to 15 μm diameter. Results indicated that the density of the particles lay in the range 1.25×10^{3} to $1.5 \times 10^{3} kgm^{-3}$ i.e. somewhat less than the theoretical density.

McKNIGHT and TILLERY (1967) used a conifuge and a MILLIKAN oil drop apparatus in their investigations into the uranine particulate density problem. The deposition pattern in the conifuge inferred that the uranine density lay in the range 1.3×10^{3} to $1.4 \times 10^{3} kgm^{-3}$. The oil drop apparatus yielded a value for the density in the range 1.3×10^{3} to $1.5 \times 10^{3} kgm^{-3}$.

The rate of drying of the primary droplets of the solutions used by these investigators was reckoned to be an important factor governing the value of the resultant density of the uranine particles.

In this study the density value for the experimental particles was checked by two independent techniques.

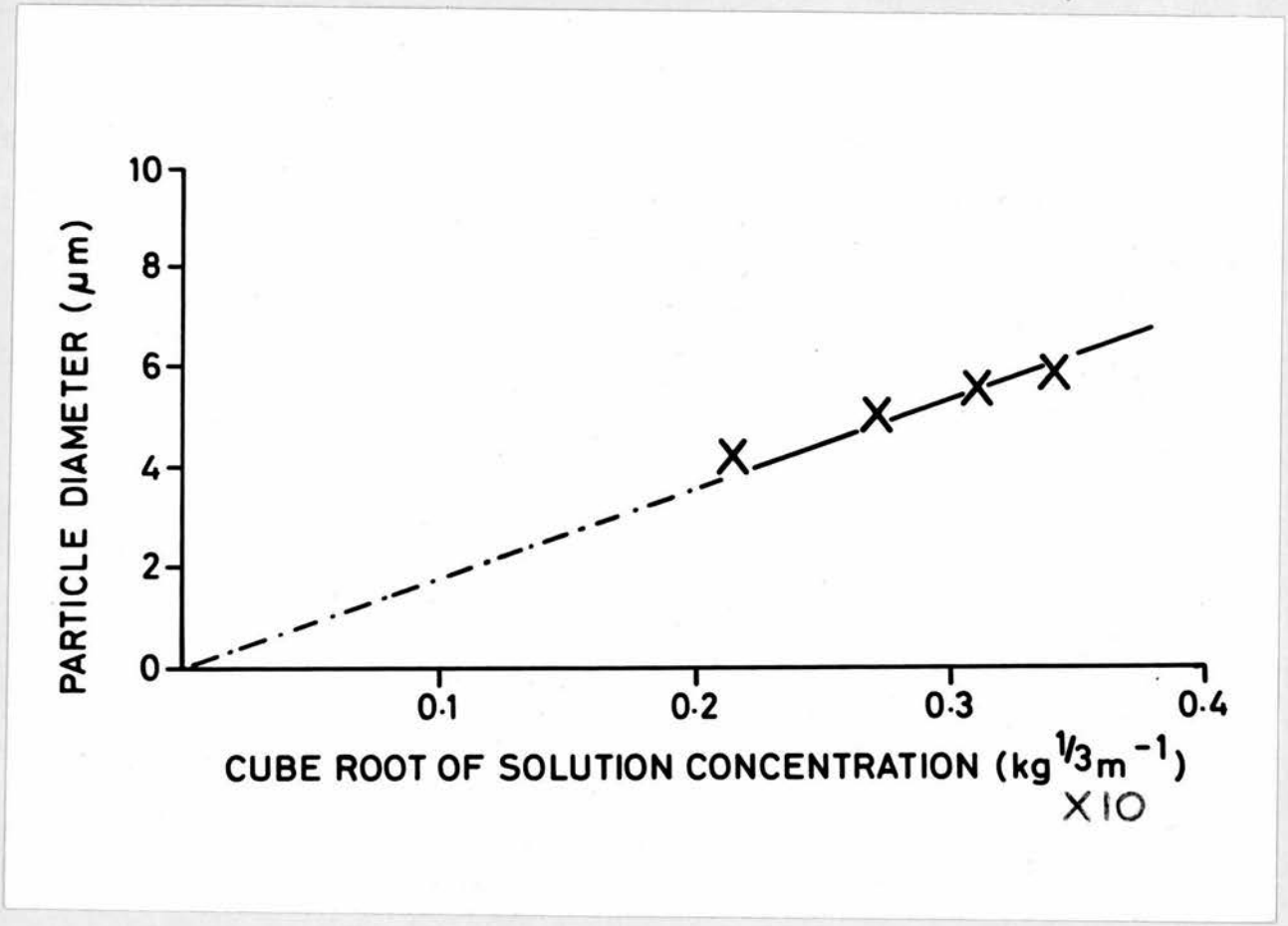

Fig. 2.11 Graph for Inferring Particle Density

The first method was indirect and involved the generation of several sizes of particles with the spinning disk apparatus. The rotational speed was fixed throughout, the different particle sizes being obtained by varying the concentration of the sprayed solution.

Since resultant particle size is related to sprayed droplet diameter, solution concentration and particle density

viz. $d_p/d = (c/\rho_p)^{1/3}$

where d_p = particle diameter (m)

d = droplet diameter (m)

c = solution concentration (wt./vol.) (kgl^{-1})

ρ_p = density of particles (kgm^{-3}),

a plot of measured particle size against cube root of solution concentration should theoretically be a straight line, of gradient $d/\rho_p^{1/3}$

Measurement of droplet diameter (the disk speed was constant) allowed the particle density to be calculated.

The disk pressure was held fixed at $13.8 \times 10^{-4} Nm^{-2}$, resulting in spun droplets of 19.8μm diameter. This diameter was measured by impacting the droplets against a slide covered with magnesium oxide, (MAY, 1945) and correcting the resultant crater diameter to give the true droplet diameter. Sizes were measured with the previously calibrated TIMBRELL Double-Image micrometer.

Figure 2.11 shows the graph of mean particle diameter versus cube root of concentration for solutions of 1,2,3 and 4 per cent (weight/volume) of the binary mixture.

Regression analysis (through the origin) yielded a value of 17.99 for the line slope.

i.e. $d/\rho_p^{1/3} = 17.99$

This implied that $\rho_p = 1.33 \times 10^3 kgm^{-3}$

A more direct method was to float the particles in liquids of known density in which they were insoluble and note the density value at which they remained stable (MAY, 1972).

Particles were collected using a midget impinger containing known mixtures of carbon tetrachloride and petrol i.e. of known density. Uranine and methylene blue are insoluble in such mixtures.

Samples of the liquids were drawn from the impinger and inserted into a thin-walled cell of about 1ml capacity located on the substage of a microscope, the latter being used in the horizontal position. Several minutes were allowed for temperature stabilising to take place before examining the liquids.

If the particles were of greater density than the liquid, STOKES law shows that they will sediment out; a density of particle less than that of the liquid will cause them to rise; equalisation of the densities causes the particles to remain stationary in the fluid.

For each size of particle in the range 5 to 10μm diameter the latter criterion was adopted to give the density. A particular field of view containing several particles was "located" in the liquid using a line or mark on the eyepiece graticule. The net motion of the particles as a function of time was noted. The procedure was repeated for different fields of view.

Experimental results for the particles used in this study indicated that a value of $1.3 \times 10^{3} kgm^{-3}$ for the density was representative. This value agreed well with SEHMEL (1967), McKNIGHT and TILLERY (1967), and MAY (1972).

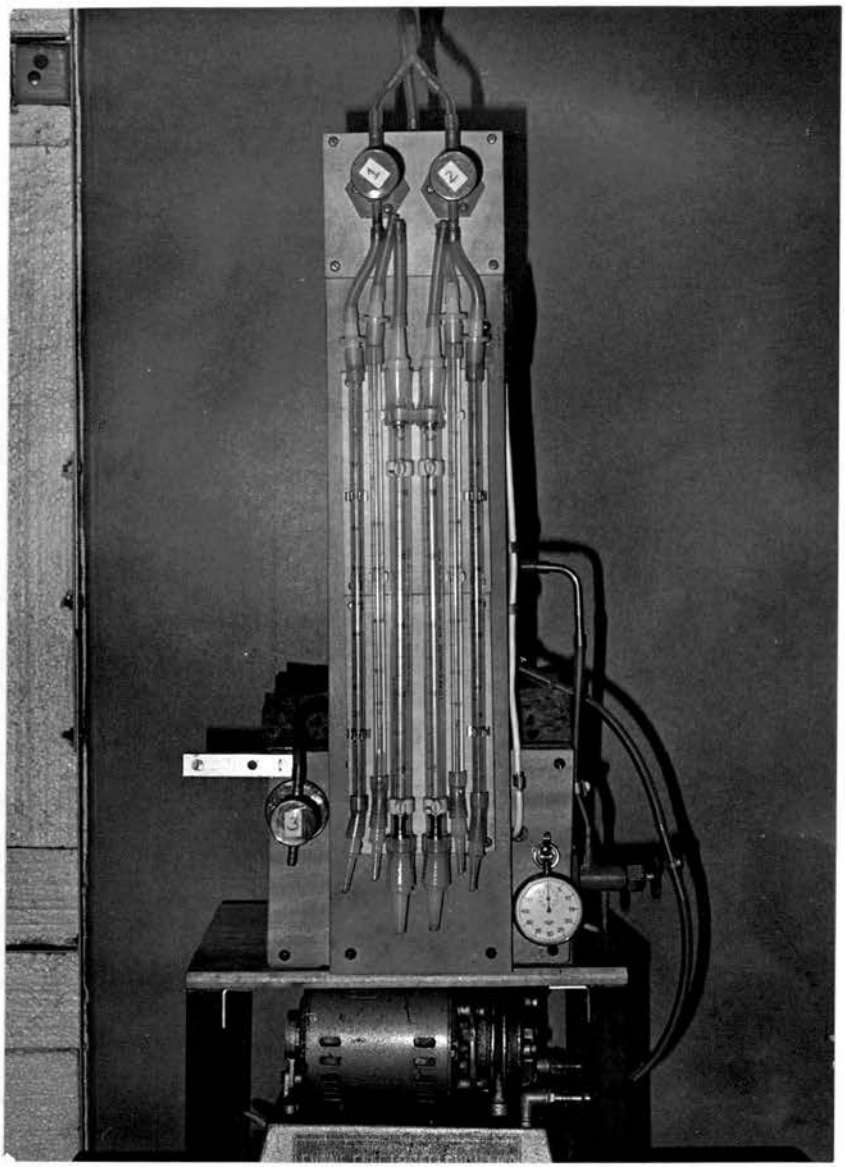

Fig. 2.12 The Steady Flow System

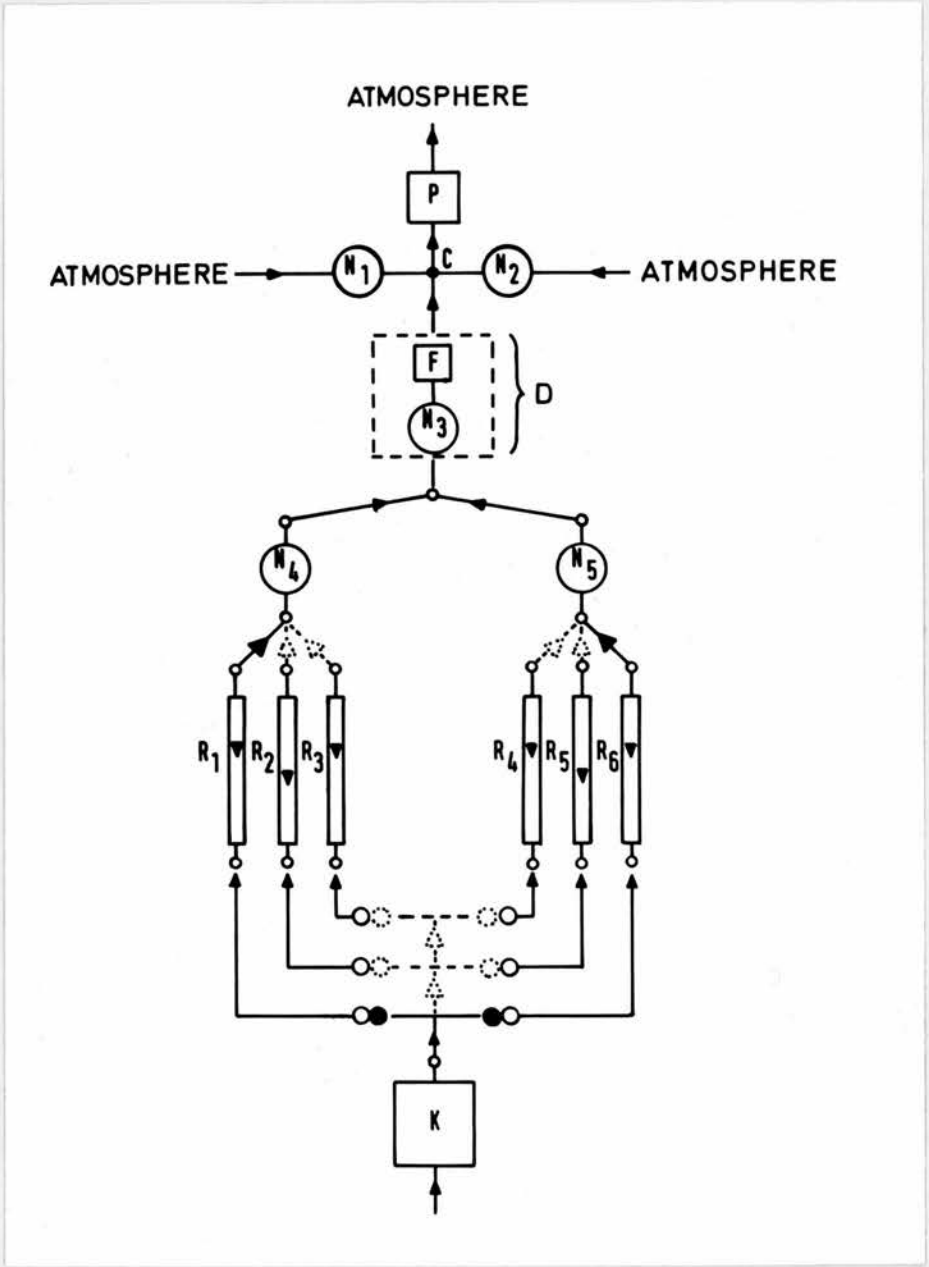

Fig. 2.13 Schematic of Steady Flow System

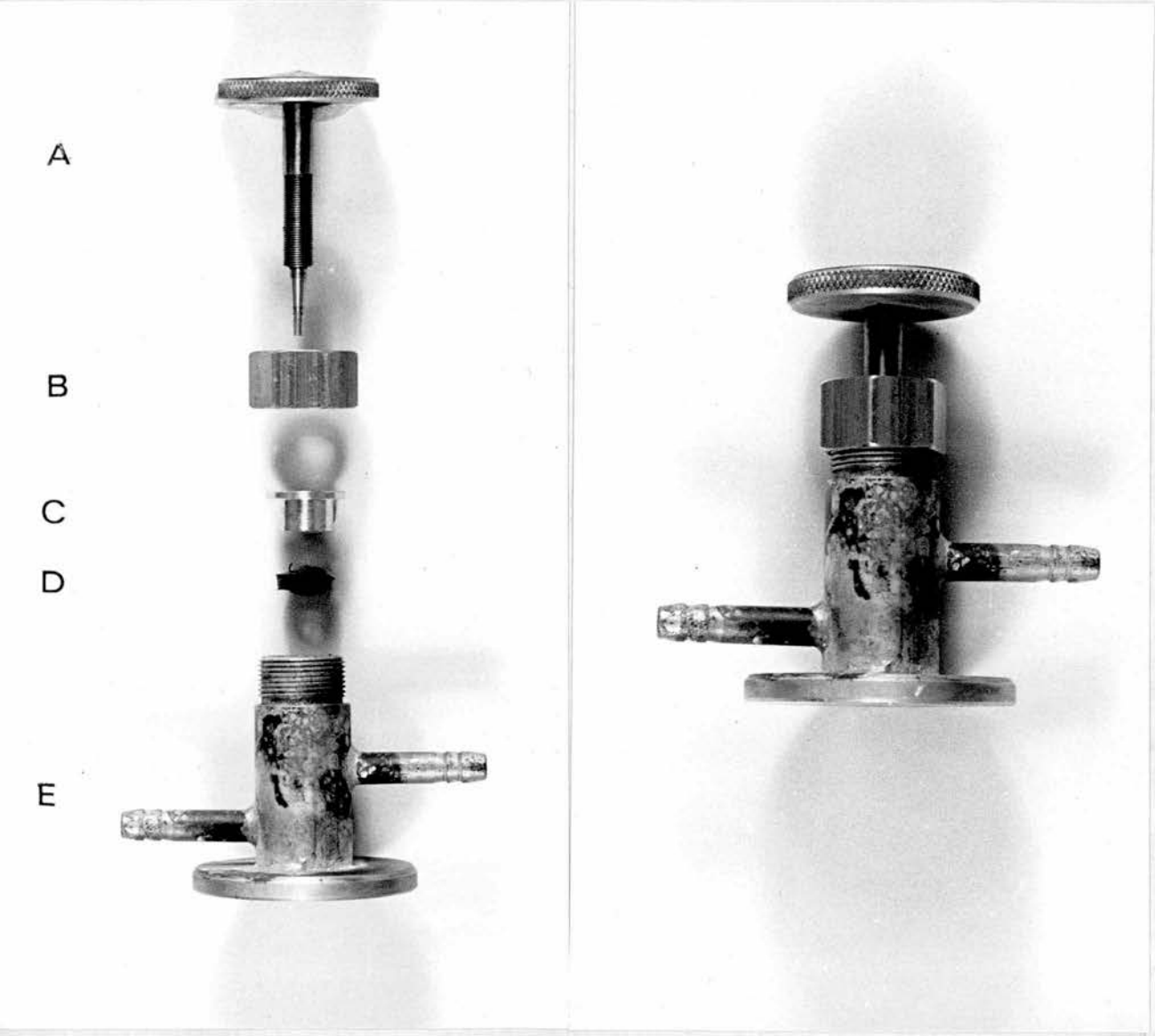

(i)"Exploded" (ii) Assembled

Fig. 2.14 The Needle Valve

(ii) STEADY FLOWS AND QUANTITATIVE MEASUREMENTS

2.5 PRODUCTION OF STEADY FLOWS

Since all the air flows in this study were steady i.e. non-pulsating, it was imperative that during the performance of any particular experiment the flow being used remained constant, adequately controllable and of necessity capable of reproduction at any later date.

A flow-indicating system permitting these conditions to be met was designed which had the added advantage of extreme ease of operation (fig. 2.12).

An Air-Compressor/Vacuum Pump (P) of the rotary sliding vane type (EVANS ELECTROSELENIUM LTD., HALSTEAD) capable of sustaining an 11-12l/min suction rate was joined to a three-way connection (C) (See schematic fig. 2.13). Two of the arms of this connector were led to atmosphere via needle valves (N_1 and N_2) and the third arm joined to a filter (F) and needle valve (N_3). The latter pair acted as a combined throttle and pulsation damper (D). In turn, D made union with another pair of needle valves (N_4 and N_5) via a two-way connector. N_4 and N_5 could be used independently or simultaneously depending on the experimental requirements.

Fig. 2.14 (i) shows an "exploded" photograph of one of the needle valves used. The whole assembly was made in brass and functioned as follows. A, the regulator, mated with the main body (E) via their respective male and female threads, the tapered end of A allowing air to pass through the valve. Fine control of the throughput was obtained by screwing A in or out of E. The rubber ring D, compressed by plug C when B was screwed on to the main body acted in conjunction with light greasing of all threads to leak-proof the assembly.

In use, each or either (depending on the requirements) of the needle valves N_4 and N_5 were connected to one of an array of flow-meters (Rotameters — GEC-ELLIOTT PROCESS INSTRUMENTS LTD., CROYDON) mounted on a vertical unit (fig. 2.12). These Rotameters (Series 1100 - individually calibrated) allowed a flow range of about 30ml min^{-1} to 10l min^{-1} to be covered.

To set up the system for operation, the pump was allowed to suck at maximum throughput. The filter F and needle valve N_3 acted to dampen any pulsations in the flow which would have been propagated through the unit to the Rotameters in question (thereby causing erratic behaviour). The needle valves in the system between the damper and Rotameters were then set to give the approximate flow required (COARSE).

Valves N_1 and N_2 at the three-way connector C, acted as fine controls to the flow thereby enabling the required settings of the Rotameter floats to be exactly (and reproducibly) attained.

Rotameters R_1,R_2 and R_3 each covered a different range, but were identical to R_6,R_5 and R_4 respectively. These devices could either be connected singly or in pairs to produce a known flow through the experimental arrangement K.

The manufacturers supplied their Rotameters calibrated at 288°K. These flow measuring devices had an inherent inaccuracy which was defined as

$$\pm \text{ (m \% indicated flow + 0.3\% full scale)}$$

where m was 2 or 3 depending on the Rotameter.

Another potential source of inaccuracy lay in the effect of the ambient temperature of the working air. In the laboratory this temperature lay within the range 288°K to less than 298°K.

Any increase in the temperature of the working fluid causes a Rotameter (calibrated at a given lower temperature) to read incorrectly. Accordingly, the manufacturers were asked to supply a correction factor which would enable any of their 288°K devices to be read at an elevated 298°K (maximum). It was indicated that the scale reading should be multiplied by the factor 0.96 to give the true "free air" reading at 298°K. As temperature decreased to 288°K this factor approached unity.

The most "unfavourable error" in a given Rotameter reading was therefore 6 to 7 per cent i.e. a combination of inherent error and temperature effect. The most "favourable" error was 2.3 to 3.3 per cent i.e. ignoring temperature effect.

Atmospheric pressure also plays a part in the accuracy of any Rotameter system, although of a secondary nature to the temperature effect.

2.6 FILTERS AND HOLDERS

In later sections, experiments will be described which basically consisted of drawing known-sized aerosol particles through a particular geometrical system and finding what fraction of the cloud was deposited. It will be seen that knowledge of the total quantity of aerosol entering the given system was essential. The problem resolved itself, in every case, to determining the fraction deposited and the fraction which would be transmitted in the absence of any collection device.

i.e. Amount entering = Amount deposited + Amount "Transmitted".

Assay of the deposited fraction was easily accomplished by washing the relevant portions of the experimental assembly in known volumes of solvent.

The fraction of the aerosol cloud which would have been transmitted was accounted for by collecting the particles on glass fibre filters

Facing Page 35

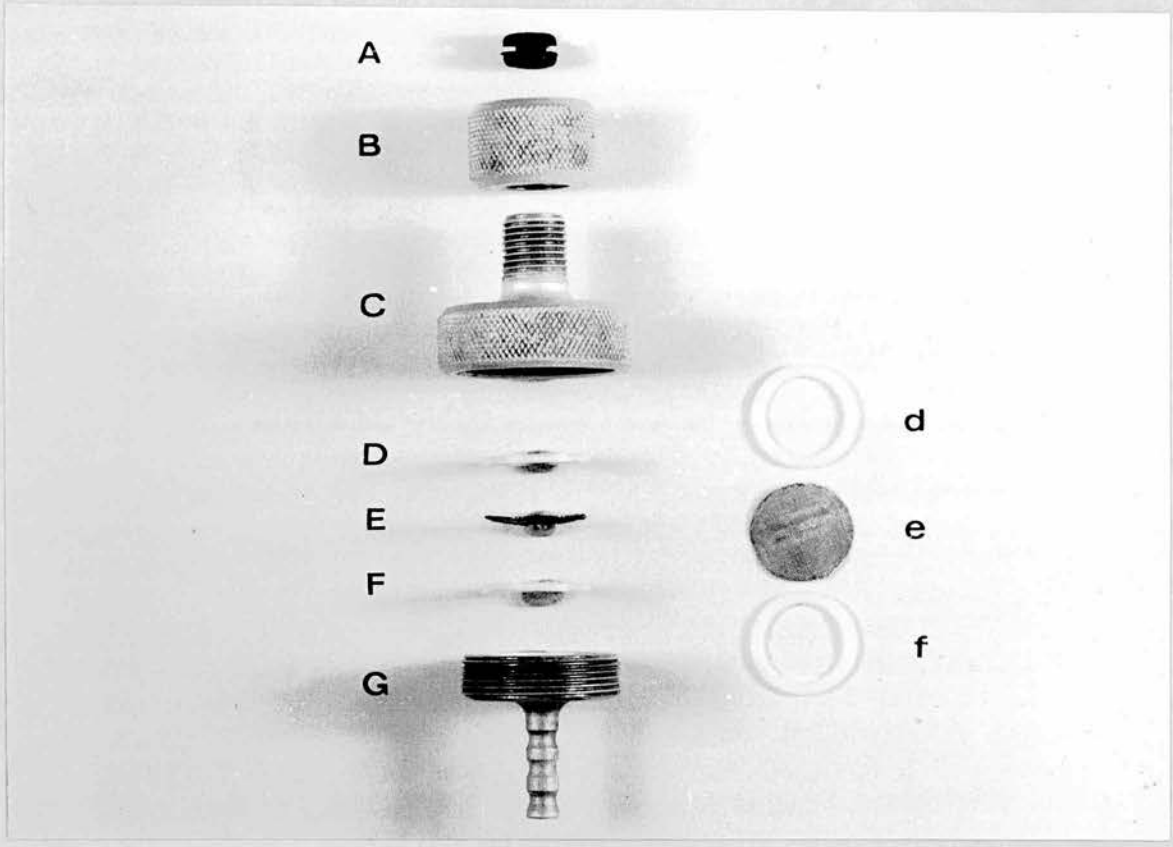

(i) "Exploded"

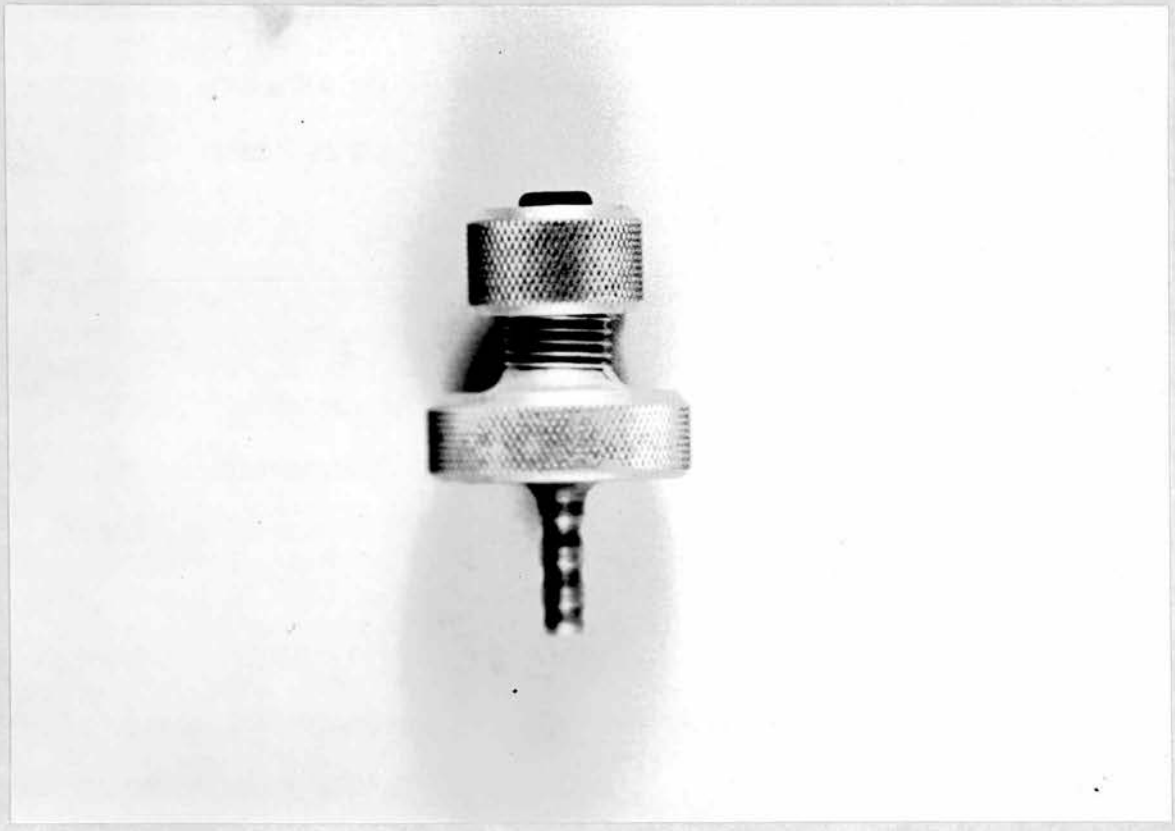

(ii) Assembled

Fig. 2.15 The Filter Holder

(SEHMEL, 1970). The latter proved extremely efficient over the range of sizes and air flows in this study, and had the obvious advantage of being readily amenable to rinsing.

The WHATMAN GF/C filters used (A. GALLENKAMP & CO. LTD., GLASGOW) were of 0.021m diameter and housed between D and E (d and e in plan view) in the holder shown in fig. 2.15. The fine mesh gauze E(e) acted as an inflexible, but flow transmitting backing which acted in conjunction with the P.T.F.E. washers D and F (d and f) to prevent the filter being warped by the air flow through the holder, with subsequent impairment of the collection efficiency.

Simple unscrewing of base G from body C allowed access for loading or removal of the filters.

Since the non-deposited fraction of the aerosol exiting the experimental system had to be collected immediately and not allowed to traverse any path wherein indeterminable losses might have occurred, the holder was designed so that the body C and cap B slid over the exit end of the tube assemblies studied, to such a depth that the latter were in close proximity to the filter. The rubber grommet A prevented any leakage around the entry point of the holder and a thin layer of Apiezon M Grease on all threads sealed the whole unit.

To test the collection efficiency, a filter holder was assembled for a "dummy" run, the outlet (sucking) end of G being connected to a secondary filter consisting of a length of wide bore glass tubing partially plugged with cotton wool. The exit end of this was connected to the steady flow system (fig. 2.12). A length of plastic tubing was slid into the holder to meet the filter (as would occur in normal operation) and the former presented to an atmosphere of known-sized fluorescent particles; a known suction rate was then applied to the filter test unit. Particular attention was paid to the most demanding condi-

tions that the glass fibre filters and holder would have to cope with i.e. high flow throughputs and smaller sized particles.

Any inefficiency in operation would be apparent if fluorescence was detected "beyond" the filter. Accordingly, after a test, the "post-filter" parts of the holder and the cotton wool of the secondary filter were washed in water and a sample of the solution checked using a fluorimeter. This procedure was repeated for several particle sizes and flow rates.

The negative results obtained in all cases, indicated that the filters (and assembly) could be treated as "absolute" throughout the range of conditions envisaged in the study.

On occasion, when examining the filter it was noted that a certain fraction of the aerosol deposit was in contact with the P.T.F.E. washer D. This was caused by too large a gap between the exit end of the experimental tube and the filter. A small gap was usually preferable on assembly since the danger of holing the filter arose if a zero gap was present. On a routine basis, the upper washers and filters were therefore rinsed together.

The possibility of aerosol particles bouncing back from the filter on to the body C was also considered when testing the filter holders. At the flow rates used, the problem did not manifest itself.

Since the fluorimetric analysis was of extremely high sensitivity all experiments were run for short periods (minutes). The problem of filter clogging was accordingly of little importance.

2.7 THE FLUORIMETER

For quantitative measurement of all fluorescent solutions obtained in the course of this experimental investigation, a commercially available

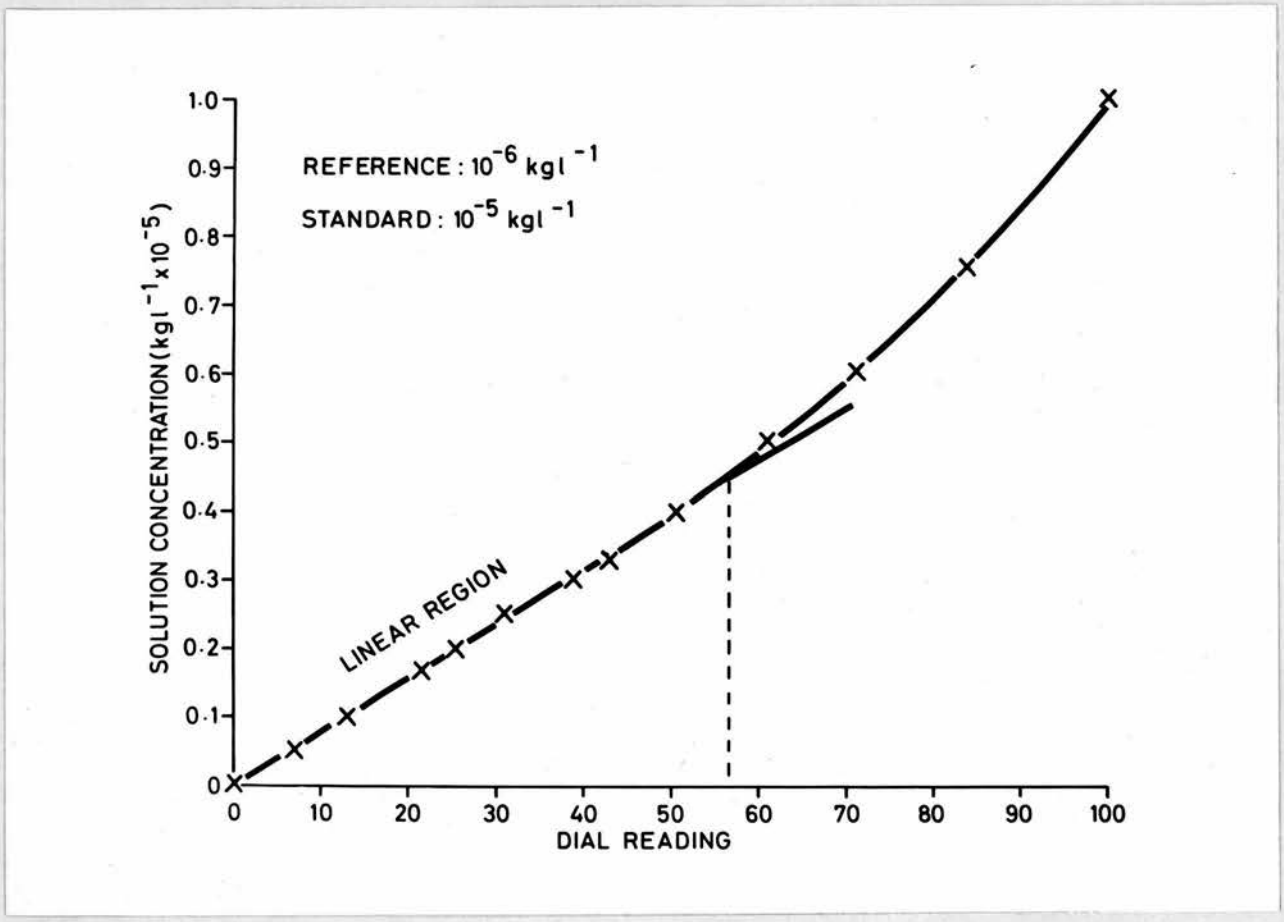

Fig. 2.16 Fluorimeter Calibration Curve

"EEL" Fluorimeter (EVANS ELECTROSELENIUM LTD., HALSTEAD) was used. This device employed a mercury vapour lamp which delivered spectral energy of known wavelength to the unknown solution of interest. The emitted fluorescent light passed via a secondary filter to a high sensitivity photo-multiplier tube, the electrical output being fed to a galvanometer.

In operation the fluorimeter was used as a null-deflection instrument with the unknown fluorescence being balanced against a known reference solution whose emitted light impinged on a second photo-multiplier. Both photo-multipliers were connected in opposition to a null-point galvanometer and balance obtained by means of a high precision potentiometer whose 0-100 division scale gave a reproducibility of ± 1 per cent.

A sample holder containing three matched cuvettes could be rotated to allow irradiation of any one. These cuvettes contained a blank solution, standard solution and the unknown solution respectively. The purpose of the blank and the standard was to allow hand setting of zero and full scale reading respectively on the potentiometer dial (scale 0 and 100) relative to a given reference solution.

Calibration of the instrument was performed by making up accurately known solutions of sodium fluorescein and finding the dial readings which indicated balance i.e. for known standard and reference.

Fig. 2.16 shows a typical calibration curve obtained. Linearity between solution concentrations and dial readings ceased to exist beyond a dial value of about 56.

In the straightline region,

$$\text{Dial Reading } (R) = \text{Constant } (k) \times \text{Concentration } (c)$$

$$\text{i.e. } R = kc$$

$$\text{Now } c = \frac{\text{mass of solute}}{\text{volume of solution}} = \frac{m}{v}$$

$$R = k\frac{m}{v}$$

$$\text{or/ } m = \frac{v}{k}R \quad \text{.....2.7.1}$$

Accordingly, when comparison of two fluorescent solutions was performed on a relative basis i.e. to obtain a fraction, the constant of proportionality k was no longer of importance as it disappeared from the analysis.

Any reading obtained which lay outwith the linear region could be accommodated, since known dilution of the "rogue" solution would allow balance at a lower "linear" dial reading.

The calibration could be performed with distilled de-ionised water or 2 per cent volume to volume aqueous Decon - 75 concentrate (MEDICAL - PHARMACEUTICAL DEVELOPMENTS LTD., BRIGHTON) as solvent for the sodium fluorescein, with no alteration to the shape of the graph or the "critical" dial reading.

In practice, any solution leading to a dial reading greater than 50 was taken as unacceptable, and further diluted prior to assay.

CHAPTER THREE

SINGLE BENDS

3.1 INTRODUCTION AND EXPERIMENTAL PROCEDURE

Calculations concerning the quantitative aspects of inertial impaction in the human lung are primarily possible due to the work of FINDEISEN (1935), LANDAHL and HERRMANN (1949) and LANDAHL (1950). The latter two investigators, both theoretically and experimentally, were concerned with the efficiencies of various collection systems in an attempt to characterise inertial impaction under a variety of conditions.

The results obtained in the case of tube bends of known geometry enabled calculation of a parameter whose magnitude was indicative of the impaction efficiency of the bend in question. LANDAHL (1950) utilised this parameter in establishing a relationship which was assumed to characterise the inertial deposit in branching conduits similar to those found in the lung.

The purpose of this study was to attempt to supply the experimental evidence which would verify or negate the assumption that a bifurcation was, in fact, a straightforward extension of a single bend, as regards the magnitude of aerosol deposition.

Accordingly, before proceeding with an analysis of branching systems, a series of experiments was performed in which particle impaction was measured in single tube assemblies.

The information to be gleaned from this preliminary investigation was of a dual nature. Firstly, it would enable calculation of the factor obtained by LANDAHL and HERRMANN (1949), and show clearly, in a qualitative manner, which parameters were relevant i.e. of primary importance,

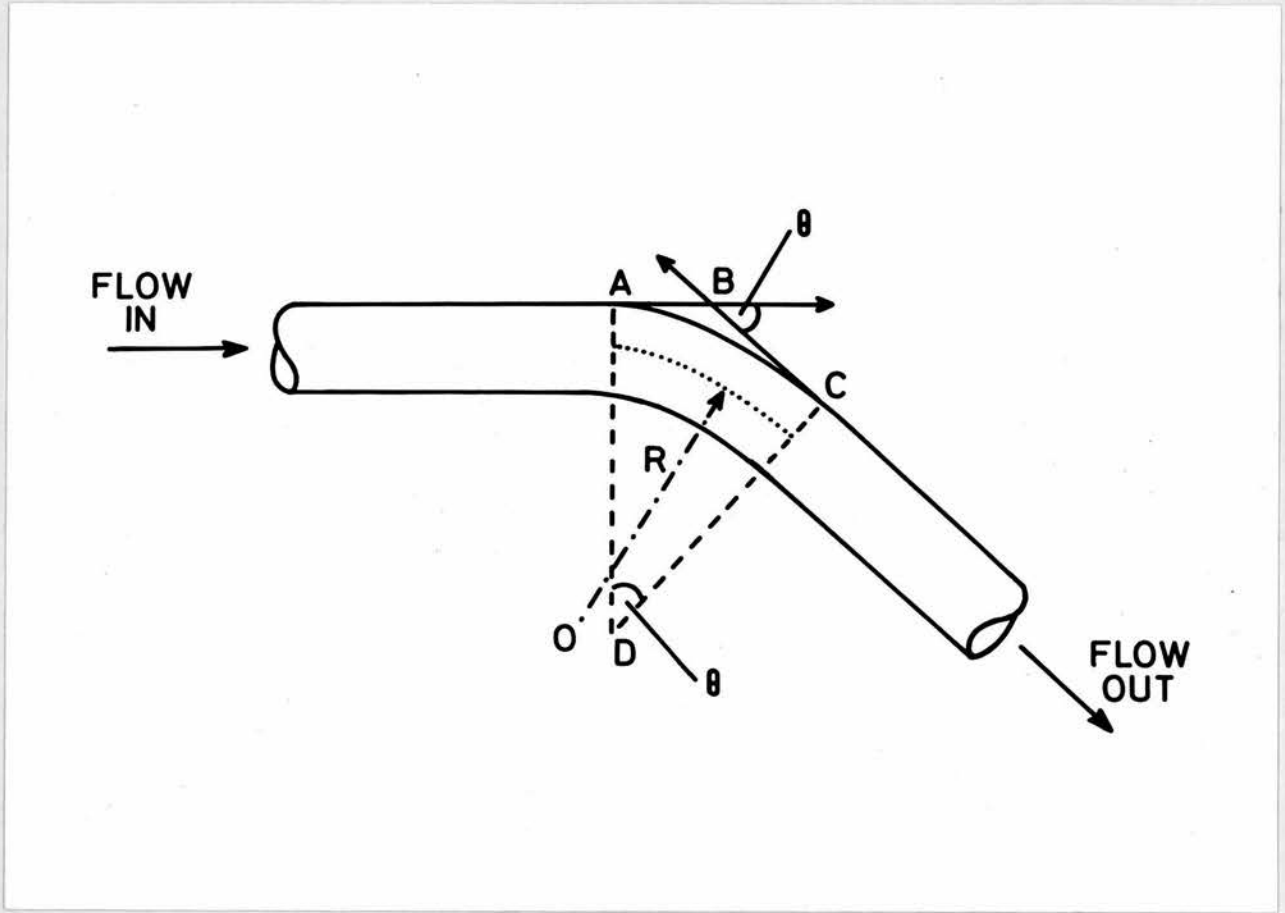

Fig. 3.1 Definition of Geometric Bend of Angle θ and Axial Radius of Curvature R

when the inertial deposition mechanism was the predominant method of particle removal.

For a tube of given bore, two parameters were adopted to define a geometric bend, viz. the angle of the bend and its radius of curvature. Fig. 3.1 illustrates these criteria in the case of an arbitrary bend. It can be seen that θ is the angle formed by the intersection of the tangents on the "input" and "output" sides of the outer wall of the bend i.e. AB and CB. Since quadrilateral ABCD is cyclic, the angle of the bend may also be defined as that formed by the intersection of the perpendiculars to the tangents AB and CB, from A and C respectively.

The radius of curvature was usually defined as one half of the diameter of the circle which had part of its circumference synonymous with the axis of the given bend as defined by the angle θ. When tubes of differing bore were compared, however, the radius of curvature of the inside wall of the bend was normally used. R and θ were capable of independent variation.

Bends of known geometry were constructed using polyethylene tubing of uniform internal diameter, and whose wall thickness allowed a considerable range of curvatures to be achieved with no accompanying "kinking" of the tube bore, (A. GALLENKAMP & CO. LTD., GLASGOW). The translucence of this material enabled external visual inspection of the internal walls.

To form any given bend, a copper sleeve was mounted on to a piece of matrix board using Terry clips. The internal diameter of this sleeving corresponded to the external diameter of the polyethylene tubing which could be inserted into its bore. Using a Stereo microscope (EALING BECK LTD., LONDON) to check for possible distortions,

Facing Page 41

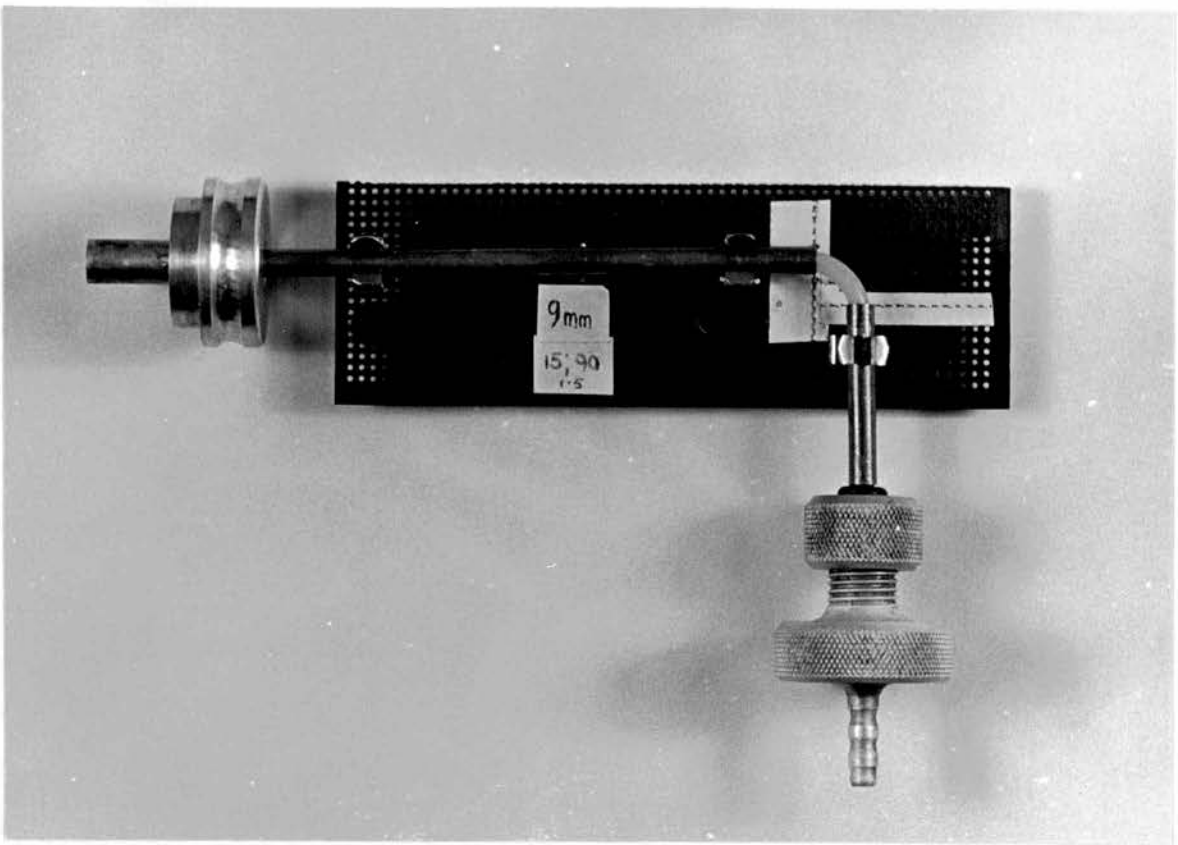

Fig. 3.2 An Assembled Model

and circular stencils of known diameter, the polyethylene tubing could be bent into various configurations which conformed to the criteria pertaining to θ and R previously mentioned. The position of the copper guide sleeve ends i.e. pre- and post-bend, could be reproduced by suitable markings on the matrix board.

The exit lengths of any of the experimental bends terminated in one of the filter holder units described in Section 2.6.

All air flows studied in the single bends lay within the laminar flow regime. The parabolic velocity profile characteristic of fluid motion in this range takes a finite transition length before becoming fully developed (BOUSSINESQ, 1890, 1891). This length is a function of the input characteristics to the tube and of the velocity of propagation of the fluid. DAVIES (1973) gives a brief summary of the criteria for calculation of laminar flow distortions in the entry length of any simple tube assembly.

As a general rule (SCHROTER, 1972), every entry length in the matrix board models was one hundred diameters long and had, at the input end, a "bell-mouth" arrangement whose internal surface was a paraboloid of revolution. This helped to establish the steady parabolic velocity profile in the tube proper. Figure 3.2 shows one particular model fully assembled for operation. The large plug at the input was purely for positioning of the model at a sampling-port of the aerosol holding chamber.

Unless otherwise specified, the axis of the entry lengths of the experimental tubes and the axis of the symmetry of the filter holders lay in the vertical plane. For the sizes of particles, range of air flows and diameters of tubes used, deposition of particles by sedimentation in the input length would be minimal (NATANSON (FUCHS, 1964)). Later experimental evidence confirmed this theoretical prediction.

The correct length of plastic tubing for a particular bend of known geometry had previously been established when designing the system. Accordingly, this length was cut from a coil of the tubing using a scalpel, to give clean flat ends.

The internal walls were then coated with a layer of Aerosol 2A-X (ELECTROLUBE LTD., SLOUGH), an antistatic agent dispensed from a pressurised canister. This substance had the advantage of existing in the liquid state, on being deposited on the tube walls, for a sufficiently long enough time to entirely cover them, when the tube was inverted several times. When the solvent evaporated, the coating remained as a pseudo-greasy layer which would act as a sink for any particles impinging on it. This minimised the possible occurrence of particle bounce (or skid) from the actual deposition site (JORDAN, 1954; GILLESPIE and RIDEAL, 1955; GALLILY and LA MER, 1958).

One end of the treated tubing was then inserted into the input "bell" and plug unit, care being taken to ensure that the internal union was perfect. The tubing was then slipped through the guiding copper sleeves and clamped firmly in position in the Terry clips attached to the matrix board, making sure that the bend, by definition, was suitably set up. In the meantime, the filter holder had been assembled and it, in turn, was connected to the exit end of the tubing.

Connection of the output of the filter holder to a low-range rotameter on the steady flow system, (figs. 2.12 & 2.13) via a length of plastic tubing, permitted the whole assembly to be tested for leaks. In this instance, the procedure was to set the vacuum pump at full throughput i.e. pumping through the rotameter via fully opened needle valves, N_3 and N_4 (or N_5); N_1 and N_2 were fully closed. Since the whole

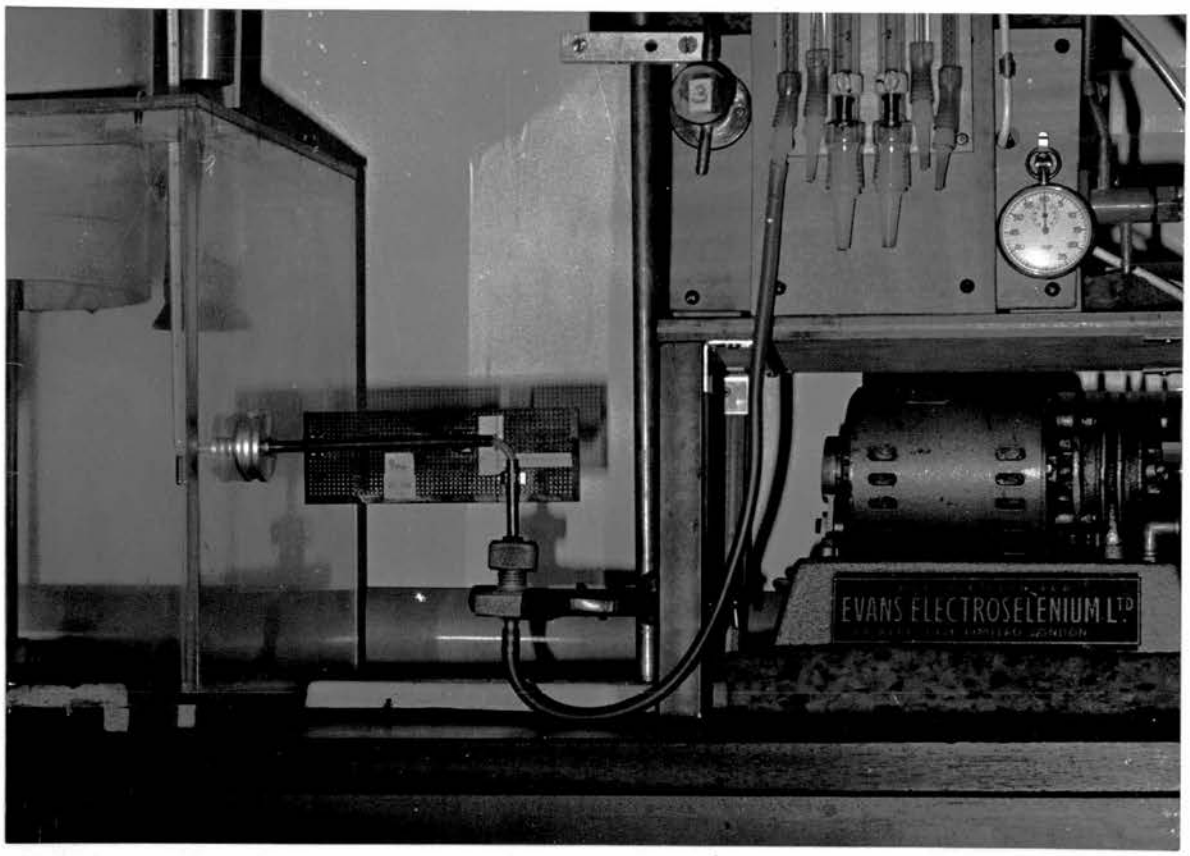

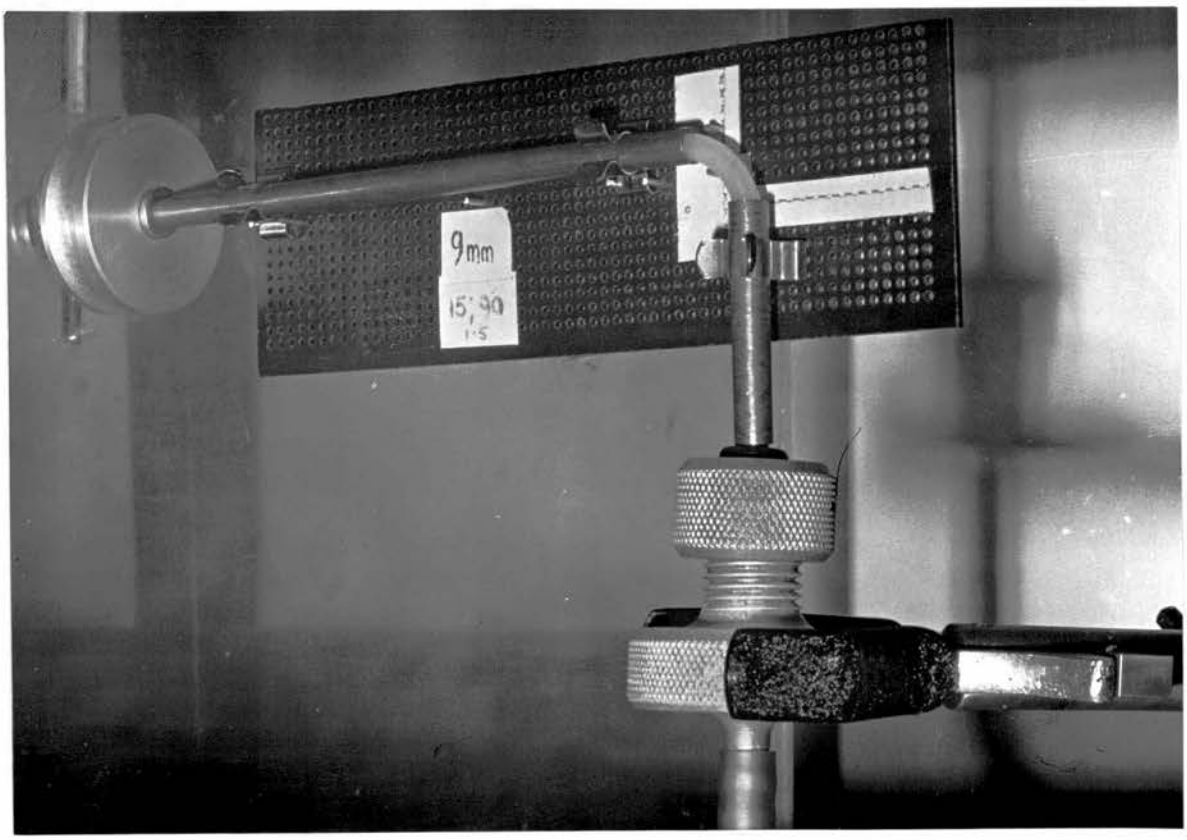

Fig. 3.3 Two Different Views of a Model connected to the Aerosol Chamber

assembly was thereby connected to atmosphere, only at the input "bell" of the tube system, closing-off this opening automatically reduced the flow through the test rotameter to zero, if and only if no leaks were present. In operation, if it was found that a leak existed, the system could be easily broken down into stages, working forward from the rotameter to the input bell, and tested individually. The source of leakage which occurred most often lay in the threads of the filter holder. Regreasing with Apiezon M invariably eliminated this trouble.

The unit was now ready for use.

To set up for an actual experiment the plastic tubing was disconnected from the input end of the leak testing rotameter and re-connected to another rotameter which would indicate the required air flow for the particular experiment in question. The plug at the input was then inserted into a suitable port in the aerosol chamber and the whole configuration held rigid and correctly aligned using a lens clamp (fig. 3.3).

Once the experimental flow was established through the tube system under study, the PALMER Injector Apparatus was switched on to feed a uranine/methylene blue solution of known concentration to the spinning disk. By light-aided evaporation, a flux of aerosol particles was accordingly generated. The temperature of the ambient air, the temperature of the air in the holding chamber (and its relative humidity) were consequently recorded and a stopwatch started to give an indication of the experiment duration. These criteria were not critical, serving mainly for comparison when reproducing a particular experiment.

As expected, especially at the higher flows, build-up of particles at the bend could be clearly seen through the translucent tubing.

Facing Page 44

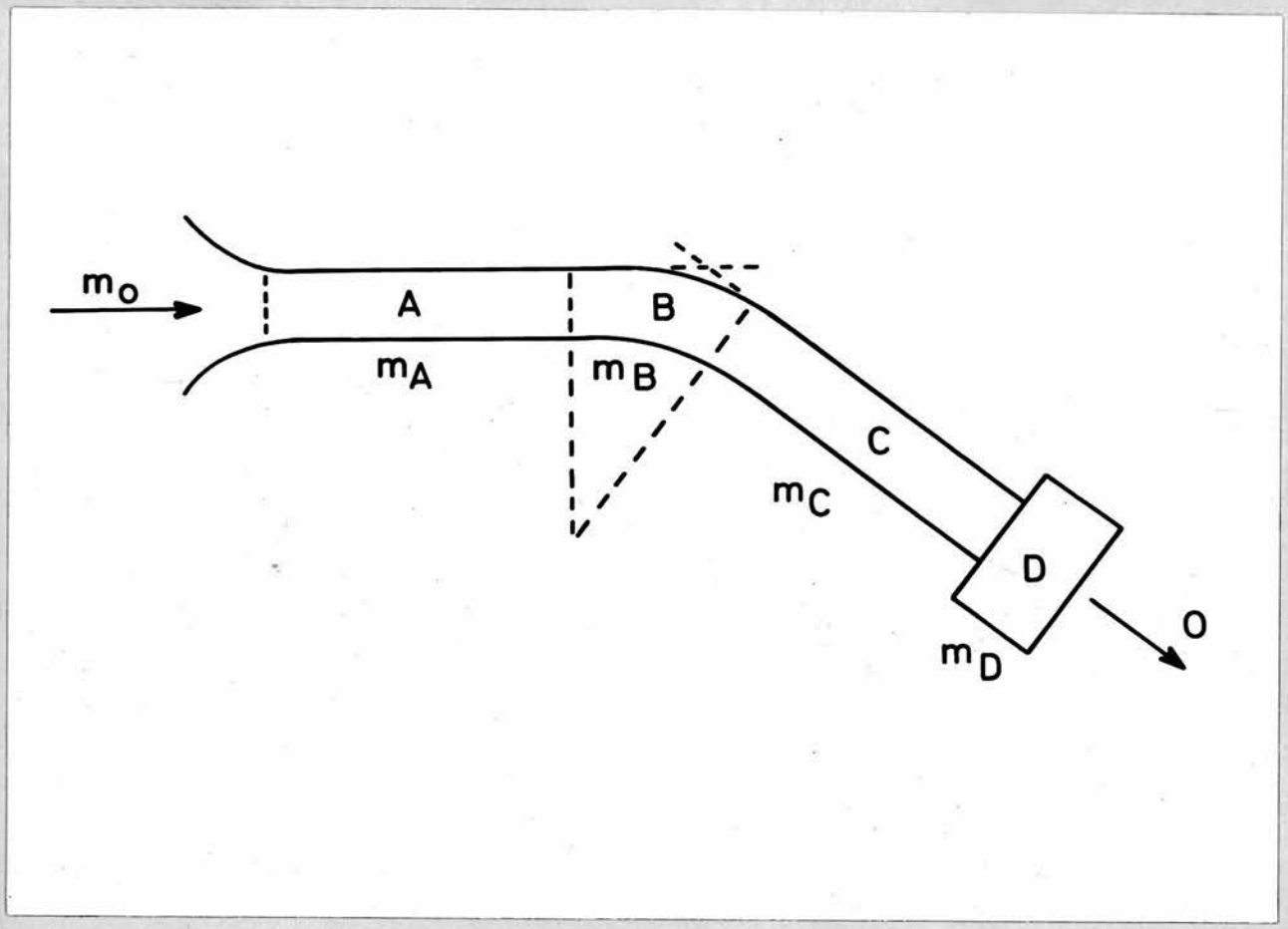

Fig. 3.4 Deposition Regions of a Bend Unit

Since the characteristics of the aerosol were known, it was necessary only to sample the cloud exiting the holding chamber with the Konimeter, as a check on the monodispersity.

Several minutes after the start, the experiment was terminated by switching off the rotameter pump and PALMER Injector.

While in situ, the geometric bend was marked off using a scalpel blade; this enabled the tube assembly to be totally disconnected and the bend cleanly severed once the tubing was extracted from the confines of the copper sleeves. The filter holder was dismantled and the filter and P.T.F.E. washers carefully removed using tweezers; these were then immersed in a known volume of aqueous Decon-75 solution contained in a beaker placed on a magnetic stirrer.

Each experimental tube assembly was divided into three separate sections for assay purposes. The one hundred diameter input served as the pre-bend length with the post-bend tubing leading to the filter and the filter itself as another: The geometric bend acted as the major region of interest.

The essence of the measurement technique was to determine the amount of deposited fluorescein in each section and perform a mass balance to calculate deposited fractions (SEHMEL, 1970).

Each section was rinsed out with accurately known volumes of Decon-75 solution dispensed with a 1000μl EPPENDORF pipette (V.A. HOWE and CO. LTD.). The purpose of the Decon-75, which is a surfactant, was to remove all traces of the Aerosol 2A-X coating on the lumen walls.

Figure 3.4 shows the relevant deposition regions of an arbitrary bend and the mass of aerosol deposited in each.

If mass m_0 of aerosol particles enters the system, mass m_A will

deposit in the one hundred diameter entry length A, mass m_B will impact in the geometric bend B and mass m_C will deposit in the post-bend length C. Any particles escaping deposition will be retained by the filter D. Let this mass be m_D.

Since the assembly was leak-tight, and the filters used were absolute over the range of operating conditions,

$$m_0 = m_A + m_B + m_C + m_D$$

Thus the fraction of aerosol entering the tube which deposited in the bend was m_B / m_0.

Now m_A was the mass of aerosol deposited in the entry length.

Accordingly $m_0 - m_A$ was the mass of aerosol presented to the bend. The fraction of the incident aerosol which impacted was therefore

$$\frac{m_B}{m_0 - m_A} \quad \text{or} \quad \frac{m_B}{m_B+m_C+m_D}$$

Experimentally, m_A was invariably found to be extremely small,

Thus $$\frac{m_B}{m_0} \simeq \frac{m_B}{m_B+m_C+m_D}$$

(m_C and m_D were usually treated together to give mass m_E).

As explained in Section 2.7, when working in the linear region of the fluorimeter, knowledge of the volume of solution and precision potentiometer dial reading was sufficient to determine the mass of fluorescein present. The constant k (equation 2.7.1) disappeared from the calculation.

Thus, if v_n and R_n refer to the volume of solution and dial reading respectively, for mass of fluorescein m_n, the fraction of incident aerosol deposited (F) is

$$\frac{v_B R_B / k}{v_B R_B / k + v_C R_C / k + v_D R_D / k}$$

$$\text{i.e. } F = \frac{v_B R_B}{v_B R_B + v_C R_C + v_D R_D} \quad \text{.....3.1.1}$$

This technique was used to determine how aerosol deposition in geometric bends was affected by air flow rate, particle size, tube diameter, angle of bend and its radius of curvature.

3.2 EXPERIMENTAL RESULTS

In all experiments, the independent variable was taken as the fluid Reynolds Number (Re) with the dependent (measured) variable being the percentage of aerosol deposited in the geometric bend.

The mode of variation of the Reynolds Numbers was by alteration of the rate of air flow through the tube system in question.

Since $Re = \frac{\sigma \bar{V} D}{\eta} = \frac{\bar{V} D}{\nu}$ 3.2.1

where σ = air density (kgm^{-3})

$\bar{V}$ = average velocity of air (ms^{-1})

D = tube diameter (m)

η = air viscosity (Nsm^{-2})

ν = kinematic viscosity of air ($m^2 s^{-1}$)

and $\bar{V} = 4\dot{V} / \pi D^2$ 3.2.2

where $\dot{V}$ = volumetric flow rate of air.

Then $Re = 4\dot{V} / \pi D \nu$ 3.2.3

With the spinning disk aerosol generator used in this study, it was impractical to generate aerosols in different carrier gases, e.g. He and SF_6. Since these gases and air have similar dynamic viscosities but different densities, this would have been an alternative method of varying the Reynolds Numbers.

Accordingly, it was concluded that the Reynolds Number of the air was a reasonable parameter to adopt as long as it was realised that density may be relevant when dealing with other gases.

Facing Page 47

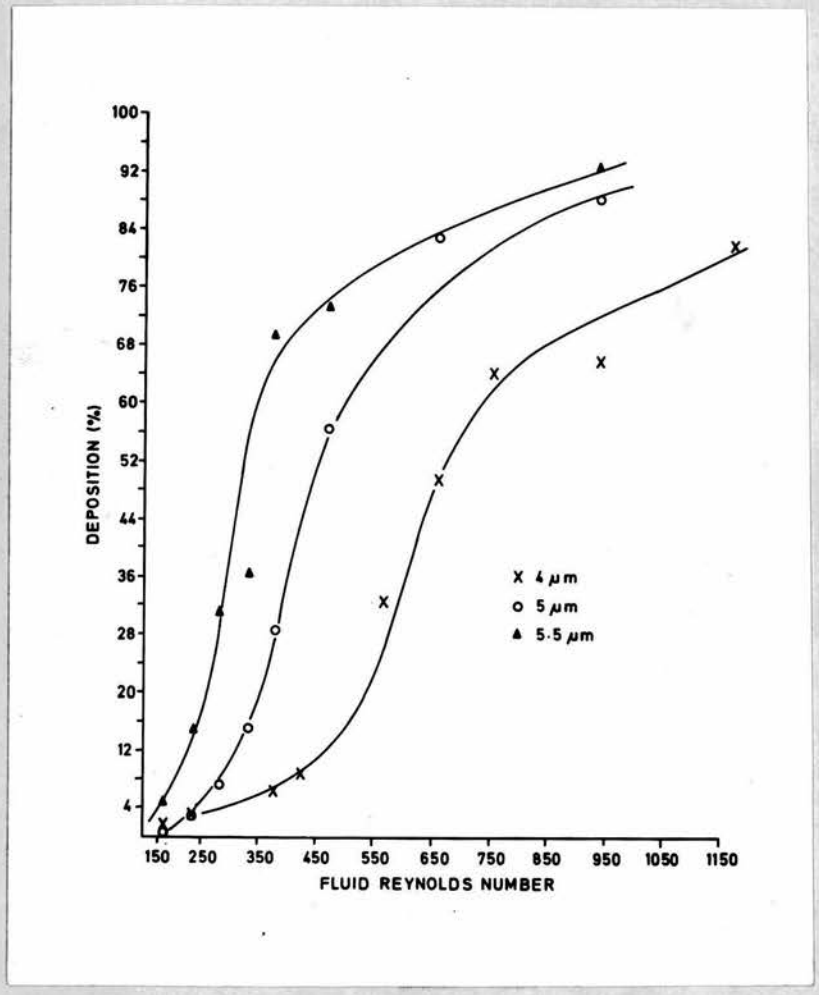

Fig. 3.5 Effect of Particle Size on Deposition

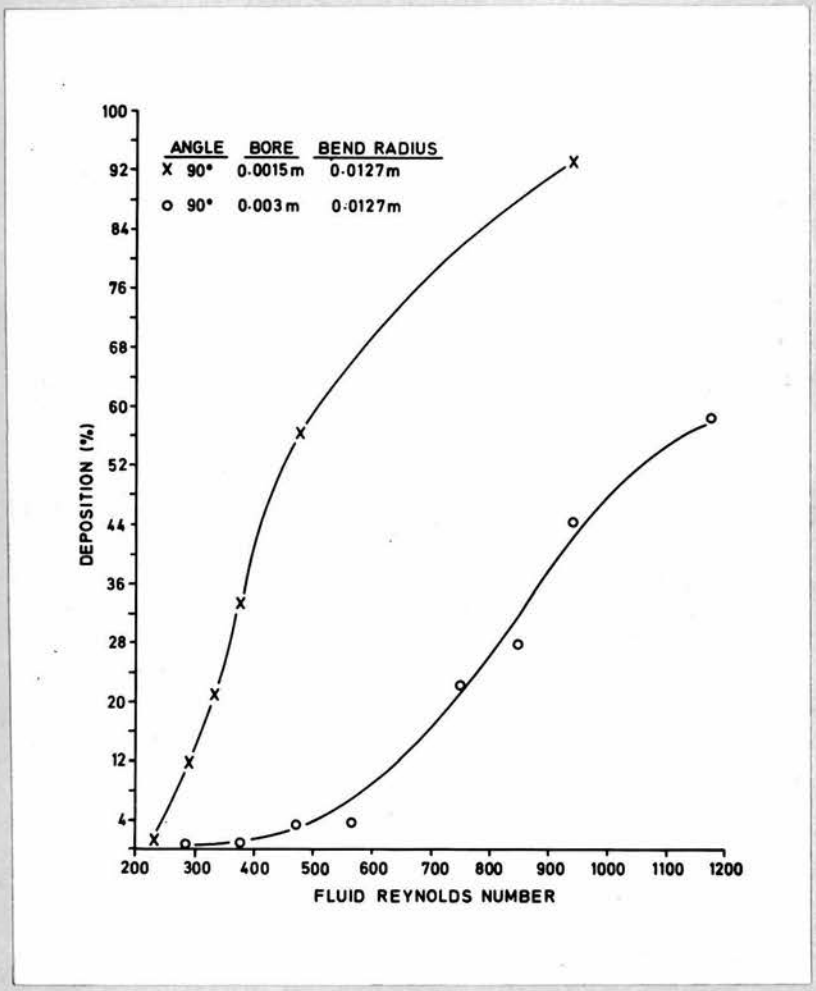

Fig. 3.6 Effect of Tube Bore (i) on Deposition

The polyethylene tubing used for the majority of experiments was of 0.0015m bore and identical wall thickness.

Since each experimental tube was destroyed by the sectioning procedure, it was imperative for reproducibility sake, that the tubing material be of consistent uniformity and be readily available commercially.

The polyethylene tubing used was opted for, since these criteria were satisfied.

a. Effect of Particle Size

Fig. 3.5 shows a plot of percentage deposition against Reynolds Number for three sizes of particle.

The experimental $\pi/2$ radian (90°) bend used, was of 0.0015m bore and 10 diameter axial radius of curvature.

It can be clearly seen that for a fixed particle size, deposition increased non-linearly with fluid Reynolds Number. Increase of particle size kept the characteristic sigmoid shape of the curve but increased the deposition for any given Re.

b. Effect of Tube Diameter

Two similar bends were constructed having $\pi/2$ radian angle and inside bend radius of 0.0127m: The bore diameters of the polyethylene tubes however were in the ratio 2:1 i.e. 0.003 and 0.0015m. All experiments were carried out using 5μm diameter particles. Equation 3.2.3 shows that increasing bore diameter reduces the Reynolds Number by the same factor. Accordingly, to keep Re similar in both tubes, the volumetric flow rate in the large bore was double that in the small.

The sigmoid shape of either curve (fig. 3.6) was evident, with the larger bore tubing giving the lesser deposition at a fixed Re.

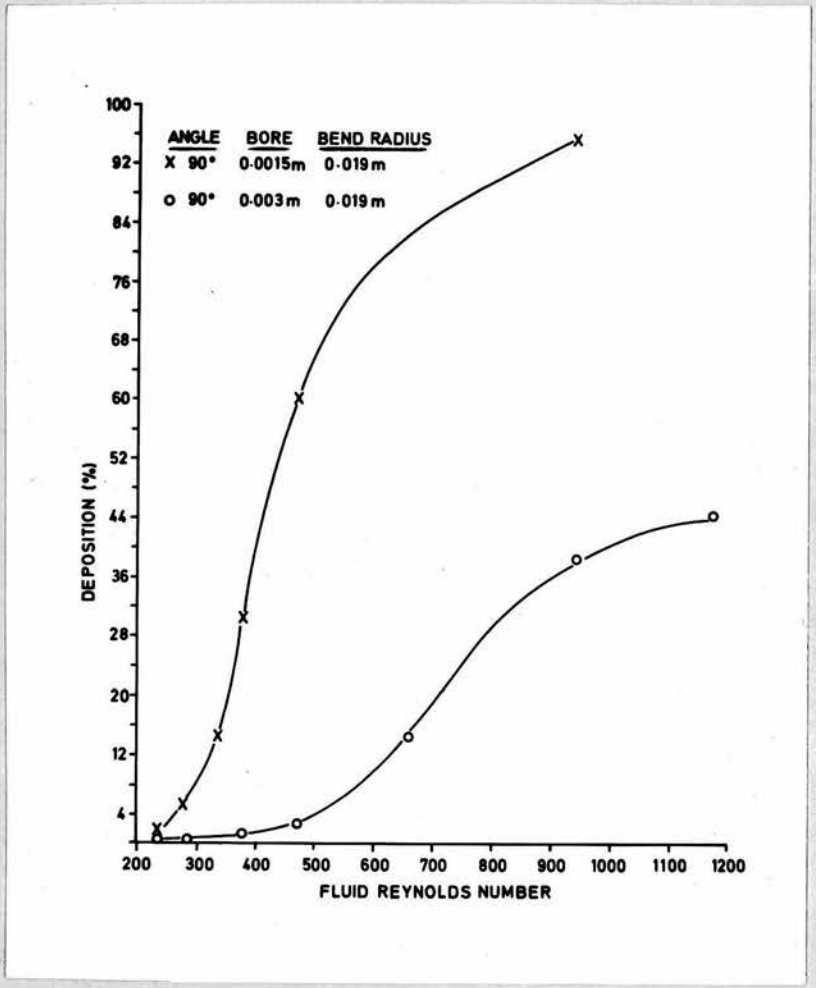

Fig. 3.7 Effect of Tube Bore (ii) on Deposition

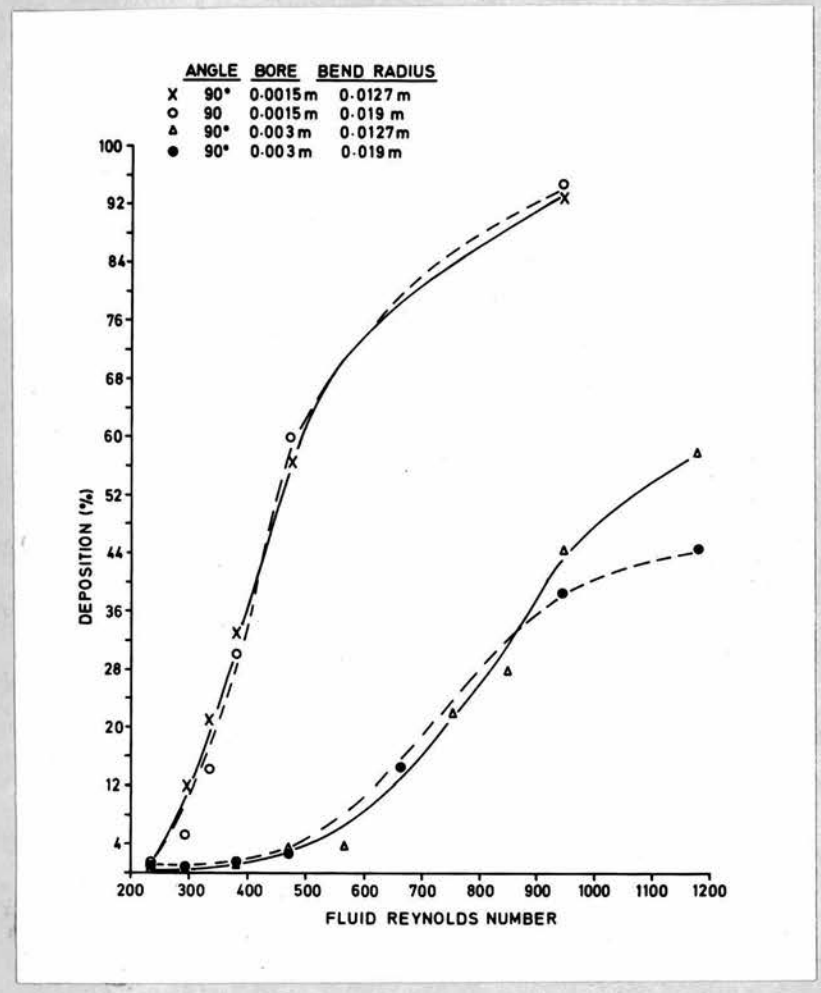

Fig. 3.8 Effect of Bend Radius on Deposition

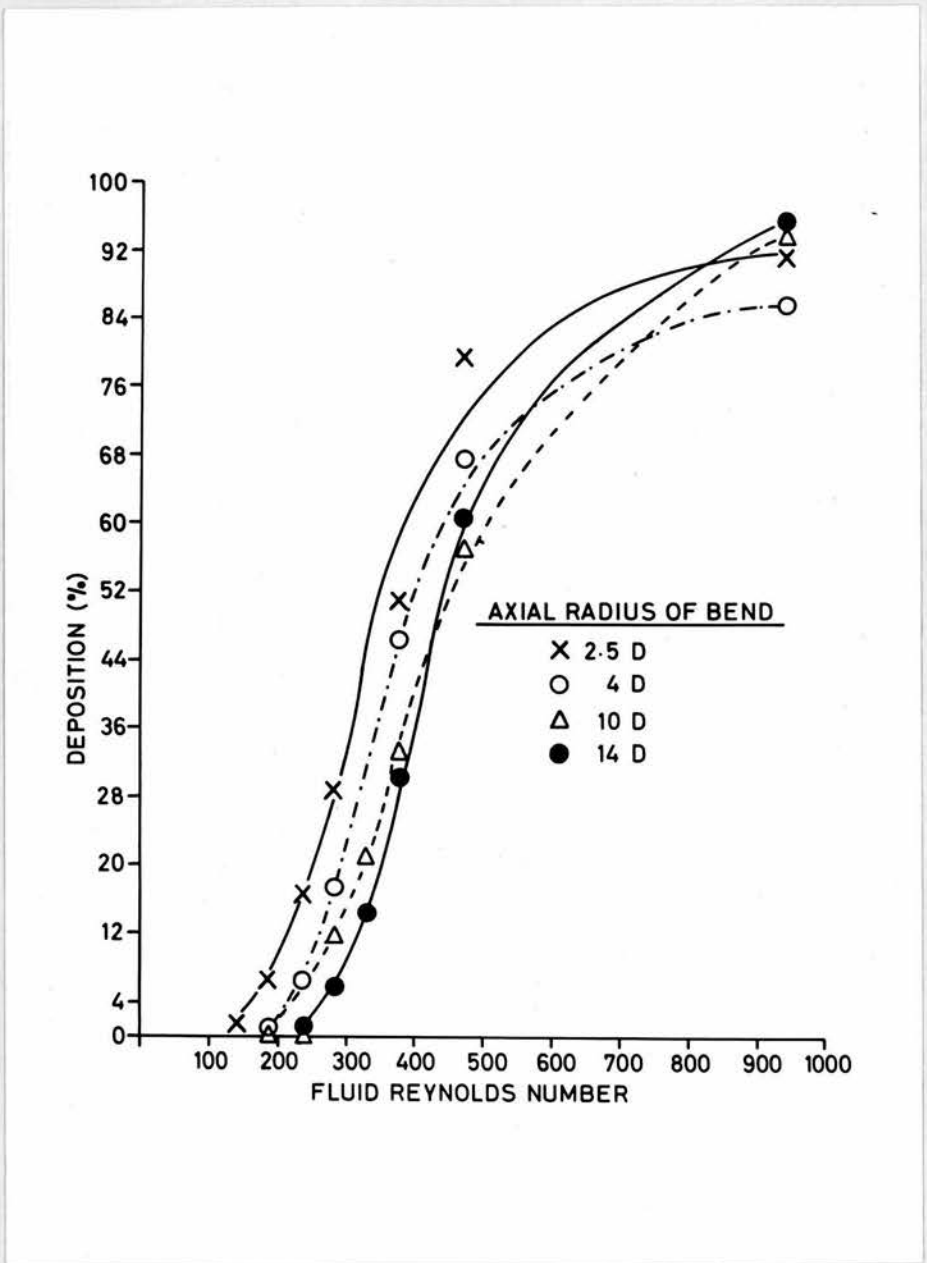

Fig. 3.9 Effect of Bend Curvature on Deposition

It should be noted, that for an identical flow through each tube, any Re in the 0.0015m bore tube was twice that in the 0.003m tube. Examination of the two deposition curves however, showed that the value of deposition at any Re on the small bore curve (X) was not double that of the deposition corresponding to one half of this Re on the large bore curve (O).

Fig. 3.7 is of similar nature to fig. 3.6 except that the inside bend radius studied was of different numerical value.

c. Effect of Radius of Curvature of the Bend

Fig. 3.8 shows a combination of figs. 3.6 and 3.7 and illustrates that, at the two values of inside bend radius used, deposition of aerosol was relatively insensitive to the curvature of the bend.

Two other models of 0.0015m bore were constructed, having angle of $\pi/2$ radians but lower axial radii of curvature than the same bore models of fig. 3.8.

The combined results are illustrated in fig. 3.9. Deposition of the 5μm particles used was greatest in the model with the greatest curvature particularly at the smaller values of Reynolds Number. Decreasing the curvature slightly decreased the deposition. As the magnitude of particle deposition tended to one hundred per cent the effect of bend curvature became less important and the deposition curves tended to overlap.

d. Effect of Angle of Bend

The angle of a bend and its radius of curvature are not inter-dependent. For a fixed angle, an infinite number of bend radii are possible.

To test the relative effect of these variables on particle deposition, two models were constructed out of 0.0015m diameter bore tubing,

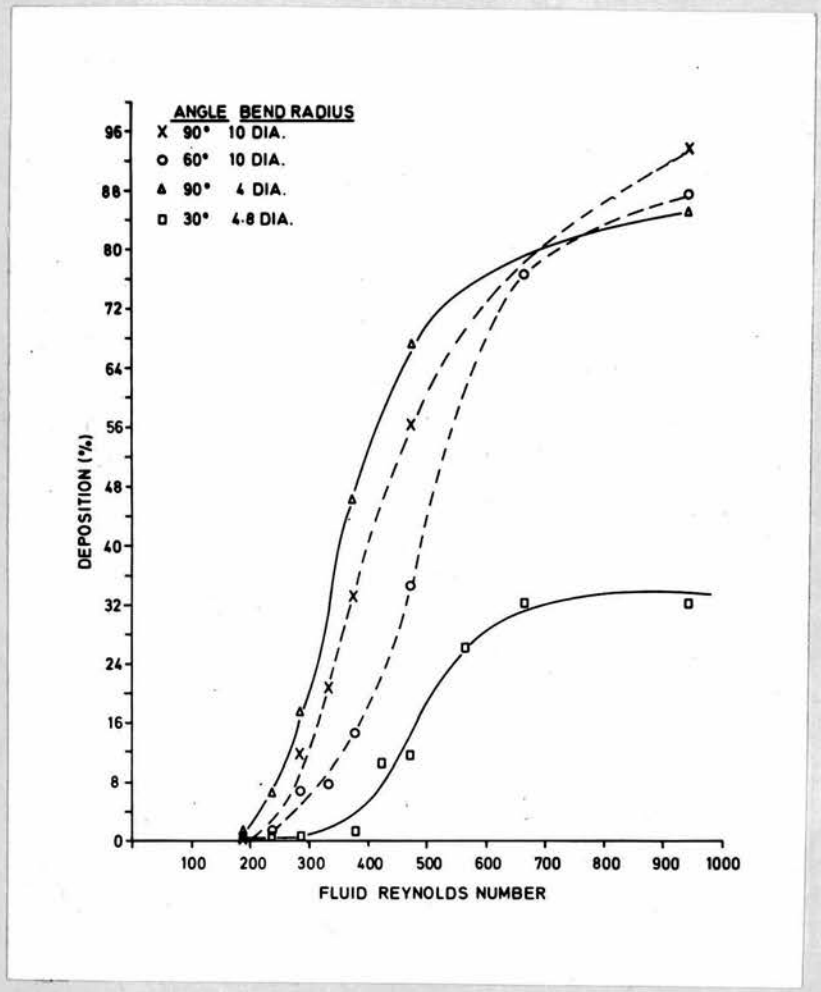

Fig. 3.10 Effect of Bend Angle on Deposition

their bend angles being $\pi/6$ and $\pi/3$ radians (30° and 60°). The curvatures of the bends of these models were similar to those of two $\pi/2$ radian models previously used.

The aerosol particles used were again of 5μm diameter.

Fig. 3.10 shows the deposition curves obtained for the four models.

For the two tubes of $\pi/2$ radians, the lower radius of curvature tended to enhance the deposition slightly more than the larger (see previous section). When the radius of curvature remained fixed at 10 diameters and the bend angle changed to $\pi/3$ radians, deposition was consistently smaller in the lower angle model. At the Reynolds Numbers tending to yield one hundred per cent deposition the two $\pi/2$ radian models and the $\pi/3$ radian model yielded similar values for the particle deposition.

On the other hand, the $\pi/6$ radian model exhibited noticeably smaller deposition than the $\pi/2$ radian model of similar curvature.

It would thus appear that angle of bend and bend curvature have independent effects on the particle deposition, with angle effect between $\pi/6$ and $\pi/3$ radians predominating at the higher Reynolds Numbers.

To summarise the experimental results in a qualitative manner, consider passage of an aerosol flux through a conduit containing a bend. It is desired that by the design of this conduit, minimal deposition of particles should occur, in the bend region.

Accordingly, the aerosol particles should be of small diameter, and travelling at low velocities: The bend itself should have large bore, and be of low curvature and angle.

These criteria for minimal deposition, as deduced from the experimental results, in no way contradict what might be expected intuitively.

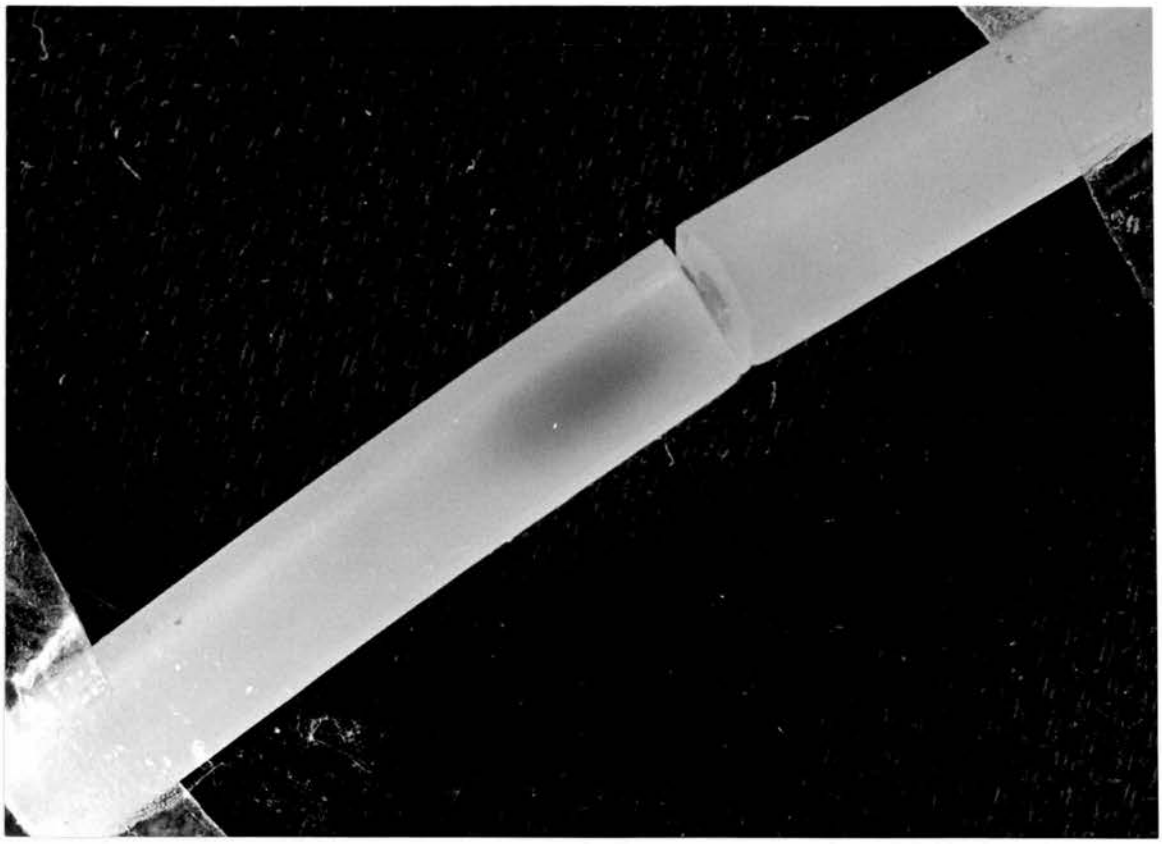

(i) Outer Wall (Classical)

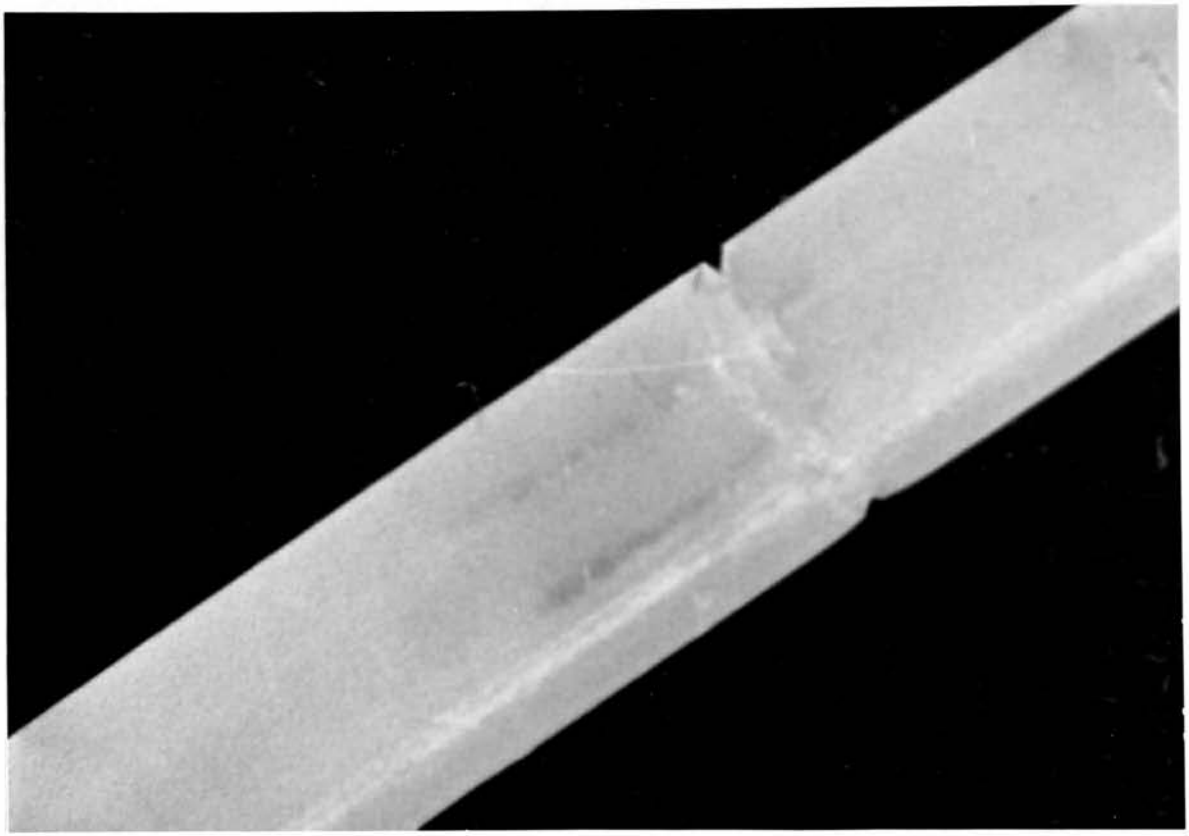

(ii) Inner Wall

Fig. 3.11 Bend Deposition

3.3 OBSERVATIONS AND CONCLUSIONS

When fluid flows through a bent tube, a radial pressure occurs owing to the flow. This pressure gradient induces secondary motions to balance the centrifugal force. A double helical flow pattern is accordingly established and propagated beyond the bend (DEAN, 1927; DAVIS, 1964; ROWE, 1970).

Classical inertial deposition theory as applied to bends, implies that any particles entrained in the fluid will tend to move in an orderly fashion towards (and possibly deposit on) the outer wall of the bend, as the fluid changes direction.

In addition to this deposit, the induced rotational motion, in many of the experimental bends studied, was sufficient to cause a deposit to build up on the inside wall of the bend. This invariably appeared in the form of two narrow parallel lines. Fig. 3.11 illustrates the two kinds of deposit for one particular bend.

This "vortex-deposition" was found to occur in both diameters of tube studied, and appeared in most cases complementary to the outer wall deposit. Occasionally, however, only one species of deposit was visible to the naked eye. This may have been due partially to the experiment duration at that particular flow.

Numerous investigators have performed experiments in which the deposition of particles in simple bends was measured. (SCHWENDIMAN et al, 1964; STRÖM, 1972). No comment was possible on the deposition pattern in these studies, since the experimental tubes were metallic, and obviously impervious to external visualisation of the inside walls.

One important point arising from this investigation which should not be ignored, was that in certain cases, both or either of the deposits extended beyond the geometric "confines" of the bend, in some cases 10

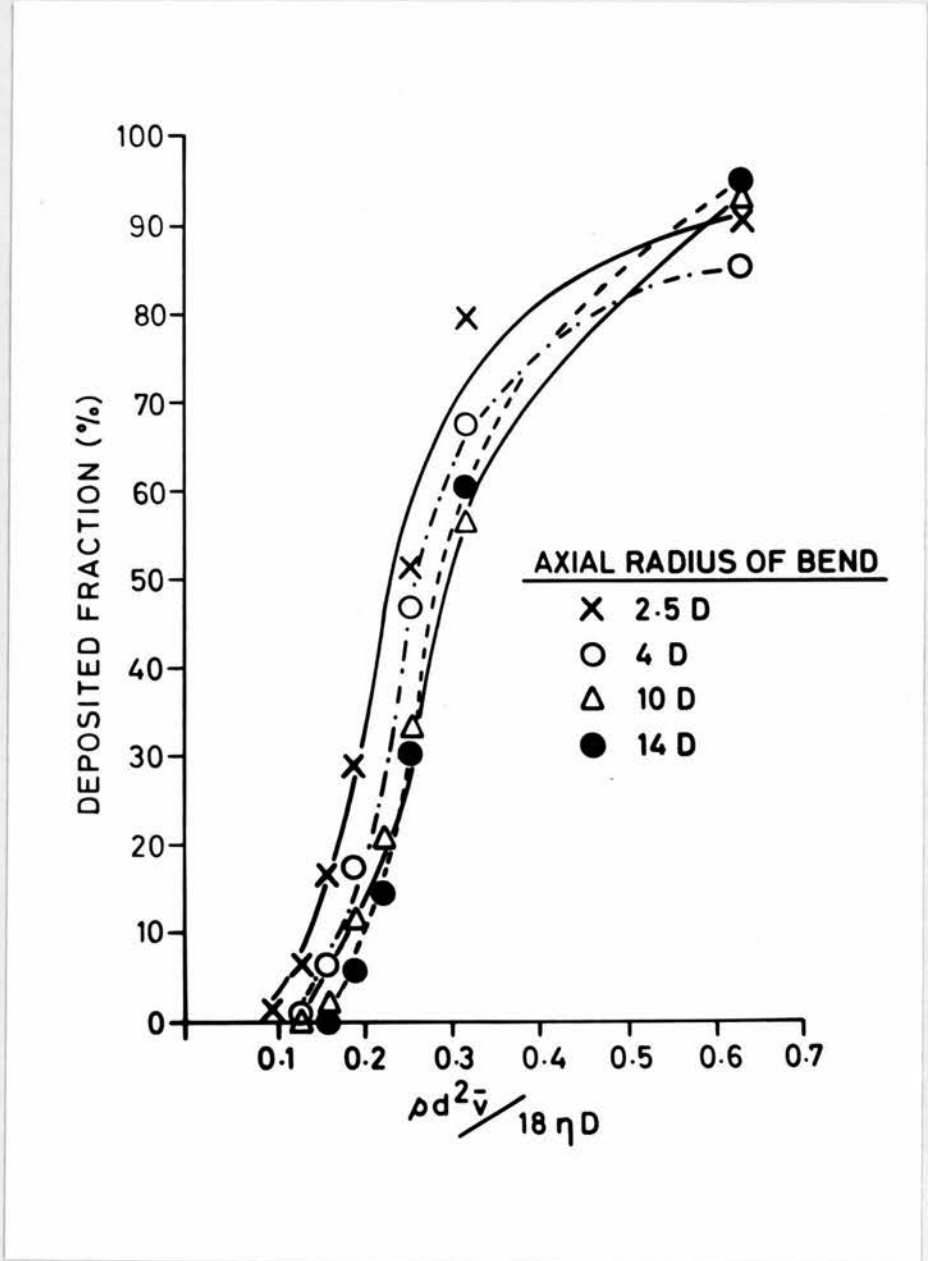

Fig. 3.12 Graph of Deposition against Impaction Parameter

to 15 diameters downstream.

This immediately poses the difficulty of accurately defining a bend: Geometric bend may not be adequate from the point of view of particle deposition. Any future experimental studies on bend deposition should carefully bear this point in mind.

All experimental results quoted in this chapter refer to geometric bend deposition to enable comparison with previous work.

LANDAHL and HERRMANN (1949), defined their inertial parameter as

$$\frac{\rho d^2 \bar{V}}{18 \eta D}$$

where ρ = particle density (kgm^{-3})

d = particle diameter (m)

$\bar{V}$ = average velocity of fluid (ms^{-1})

η = viscosity of fluid (Nsm^{-2})

D = tube diameter (m)

This parameter is the ratio of the stop distance of the particle to the diameter of the tube (See Section 1.2) and is similar to the STOKES Number which is usually defined with tube radius in place of diameter.

In fig. 3.9, a plot of Deposition against fluid Reynolds Number is shown for four right-angled bends of differing curvatures. Simple manipulation of the variables common to Reynolds Number and the impaction parameter enabled fig. 3.9 to be converted to fig. 3.12 which shows the same experimental deposition values plotted against their corresponding impaction parameters.

As before, the non-linearity is self-evident.

Theoretically, for a $\pi/2$ radian bend LANDAHL and HERRMANN (1949) constructed a similar sigmoid correlation between Deposition and

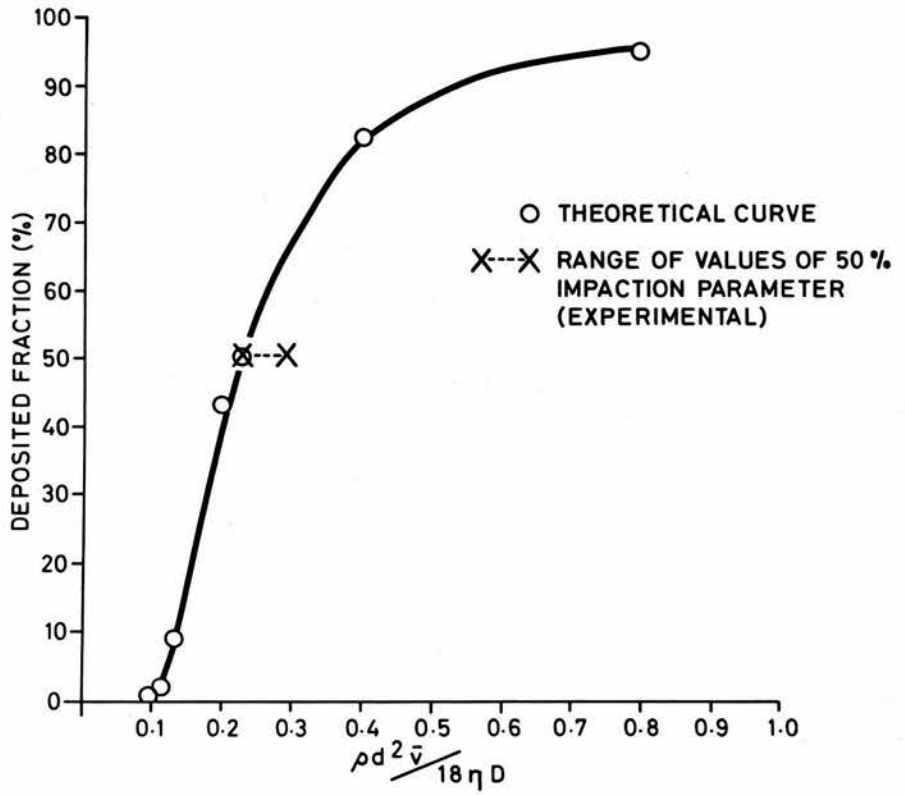

Fig. 3.13 Theoretical Deposition Curve

Impaction Parameter: The value of the latter at 50 per cent deposition was found to be 0.23.

Fig. 3.12 indicates that, in this study, $\rho d^2 \bar{V} / 18 \eta D$ lay in the range 0.23 to 0.3 when a 50 per cent deposition obtained.

For sake of comparison, this range of values is superimposed on the theoretical deposition curve (fig. 3.13). The similarity between the theoretical and experimental points at 50 per cent deposition is apparent.

It can therefore be concluded that in the preliminary series of impaction experiments reported in this chapter, qualitative understanding of the impaction variables has been attained, and the work of LANDAHL and HERRMANN (1949) verified in the case of right-angled bends.

CHAPTER FOUR

BIFURCATIONS

4.1 INTRODUCTION

Experimental assessment of regional or total aerosol deposition in the human lung may be accomplished using two main techniques.

Firstly, measurements are obtainable by in vivo experiments with volunteer subjects, using radionuclide methods (LIPPMANN and ALBERT, 1969) or inert particles (MUIR and DAVIES, 1967; HEYDER et al, 1973). Secondly, rigid (TIMBRELL et al, 1970) or flexible (EISMAN, 1970) hollow replicas of lung airways can be manufactured which permit passage of particle-laden air. The retention in the different regions of these and more idealised models can be assayed. (SCHLESINGER and LIPPMANN, 1972; MARTIN and JACOBI, 1972).

Mathematically, it is possible to construct models which enable the derivation of equations, permitting the calculation of total (or regional) aerosol deposition, under a variety of physiological conditions (ALTSHULER, 1959; BEECKMANS, 1965; DAVIES, 1972). Such models, of necessity, are highly dependent on a knowledge of the physical entities tending to cause deposition, and their inter-relationships.

The magnitude of deposition by impaction in the lung has been primarily assessed, in the past, by using the results of LANDAHL and HERRMANN (1949), which were obtained from single bend experiments. No work on actual bifurcations was performed by these investigators.

This chapter describes a series of experiments involving several branching tubes, modelled on anatomical data pertaining to the airways of the human lung.

As these different models had geometries which were closely related, it was possible to assess the quantitative effects of the pertinent variables.

4.2 EXPERIMENTAL PROCEDURE

Since the geometry of any branching airway is complex, certain well-defined criteria had to be adopted which would be reproducible in the manufacture of the models and yet would not interfere with the effect of the variable of interest. These rigid criteria were not entirely arbitrary, but based on the available anatomical details of bronchial bifurcations.

Although the models tended to have generalised values for the primary variables, all the important features of relevance as regards geometric detail were retained.

The models, five in number, were symmetrical and had dimensions chosen to be generally compatible with the Model "A" of WEIBEL (1963). The "Parent" tube of diameter (D) determined the diameters of its two "Daughter" tubes (D_d), since the area ratio of the models was held fixed throughout, (WEIBEL, 1963; HORSFIELD and CUMMING, 1967).

i.e. $$\frac{\text{Area of combined daughter tubes}}{\text{Area of Parent}} = 1.2$$

$$\frac{2.\pi D_d^{\,2} / 4}{\pi D^2 / 4} = 1.2$$

$$D_d \simeq 0.78D \qquad \ldots\ldots\ldots\ldots\ldots\ldots\ldots\ldots 4.2.1$$

In line with PEDLEY et al (1970a) the lengths of a given parent and its attendant daughters were defined as 3.5 times their respective diameters. This compared well with the mean value of 3.25 found by WEIBEL (1963).

OLSON et al (1970) and HORSFIELD et al (1971), discuss the effect

of different kinds of bifurcating spur (e.g. sharp, blunt, flaccid) on the fluid motion at the branching point of an airway. The models of this study had sharp flow dividers (as defined by eye) i.e. of high curvature relative to the diameter of the daughter tubes.

The radius of curvature of the outer wall of any junction was held constant at four times the radius of the parent tube. At this value of curvature ratio , no separation of flow was observed in the experiments of SCHROTER and SUDLOW (1969).

The foregoing criteria were fixed throughout this study, leaving the effect on deposition of the following primary variables to be investigated.

1. Fluid flow rate (Laminar)
2. Particle size
3. Branching angle
4. (Parent) tube diameter

To manufacture a model, a "master" was made out of Wood's Metal, a low melting point alloy, and hand fashioned to attain the correct geometry. This solid Y-piece was subsequently polished to remove any surface imperfections.

Nickel was electroplated on to four of the masters while successive layers of acrylic were built-up on the fifth.

Immersion of the Nickel/Wood's Metal and Acrylic/Wood's Metal models in a hot water bath, melted out the master material, leaving a hollow replica of the bifurcating model.

After careful polishing and checking of the interiors, the ends of the parent and daughter tubes of the metal models were turned on a lathe, or collars added. This enabled attachment of tubes of simi-

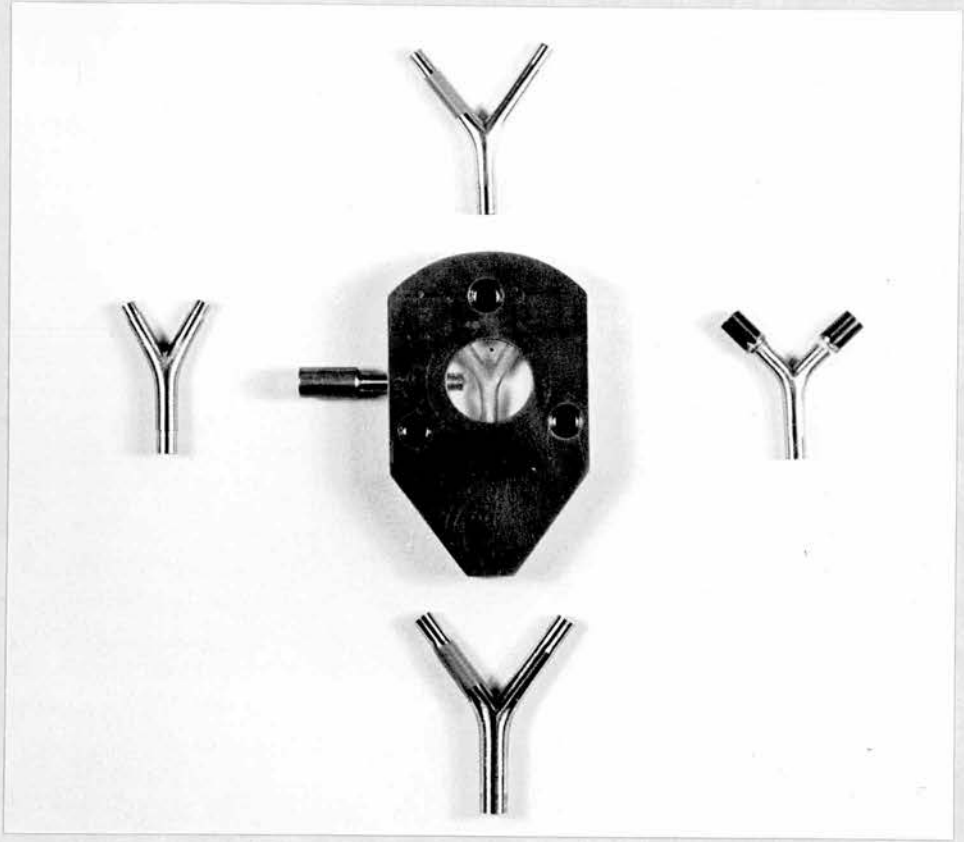

Fig. 4.1 **The Model Bifurcations**

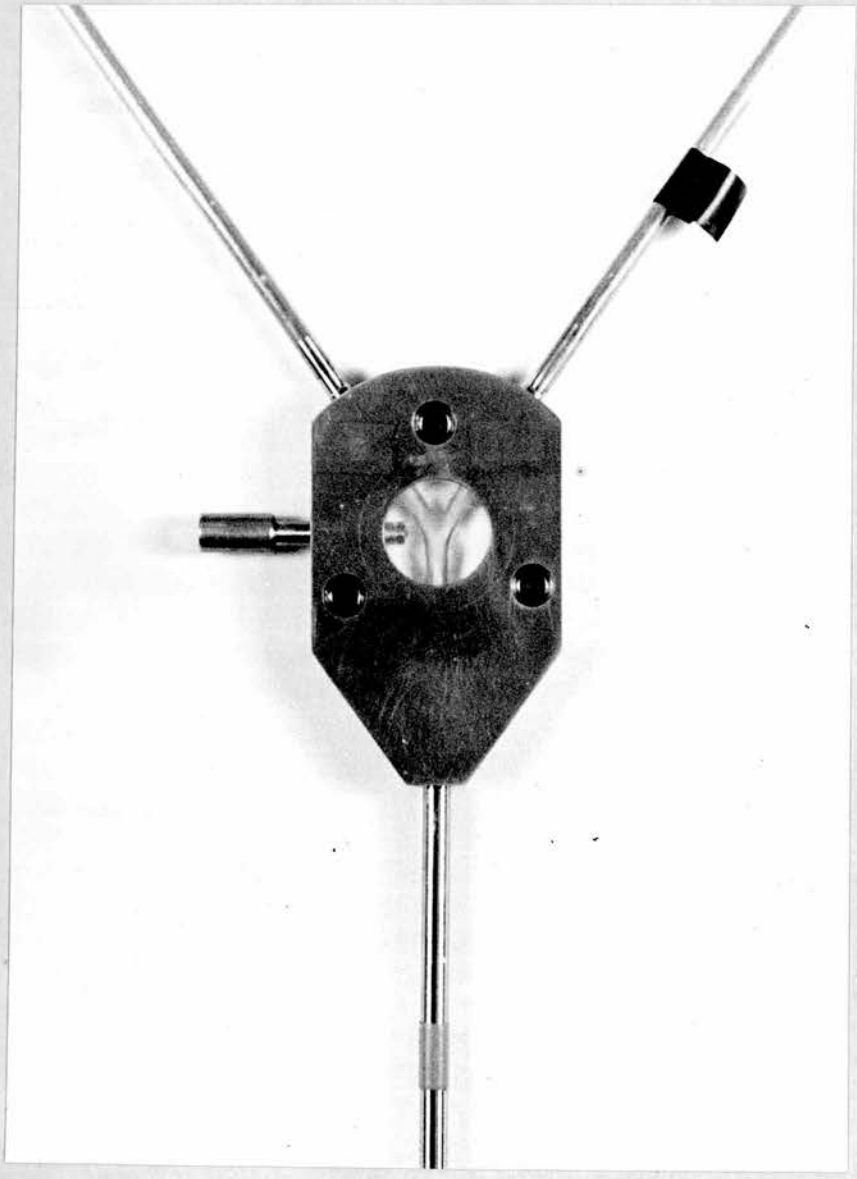

Fig. 4.2 **The Acrylic Model**

lar internal diameter. The acrylic bifurcation was housed in a brass holder, carefully drilled and machined to allow insertion of tubing to mate with the parent and daughters.

Fig. 4.1 shows the five models used: These were of similar design etc., to the scaled-up models of lung airways used by SCHROTER and SUDLOW (1969) for air flow studies.

The surface roughness of the interior walls was considered constant for all models, since the mode of manufacture was identical for each. In laminar flow, any remaining minor corrugations will have little effect on the bulk flow profile unless a critical protuberance height is attained (SCHILLER, 1932). Since the models were sprayed internally with Aerosol 2A-X (See Section 3.1) before use, any irregularities would be "smoothed-out", owing to the fluid-spread of this agent on inversion of the models.

One bifurcation was manufactured in acrylic (fig. 4.2) to enable visualisation of the deposition pattern of the particles. The values of the geometric variables of the other four models were chosen to range the equivalent values of the acrylic model; the latter was accordingly treated as the "primary unit" of this study.

The procedure adopted for experimentation with the bifurcation units was basically similar to that of the single bends, with appropriate measures taken to deal with the double flow-splitting in the former.

To avoid any possible complications due to gravitational effects at the bifurcations, all experiments were performed with the axes of symmetry of the models in the vertical plane (FRIEDLANDER and JOHNSTONE, 1957). This necessitated the mounting of the bifurcations

Facing Page 57

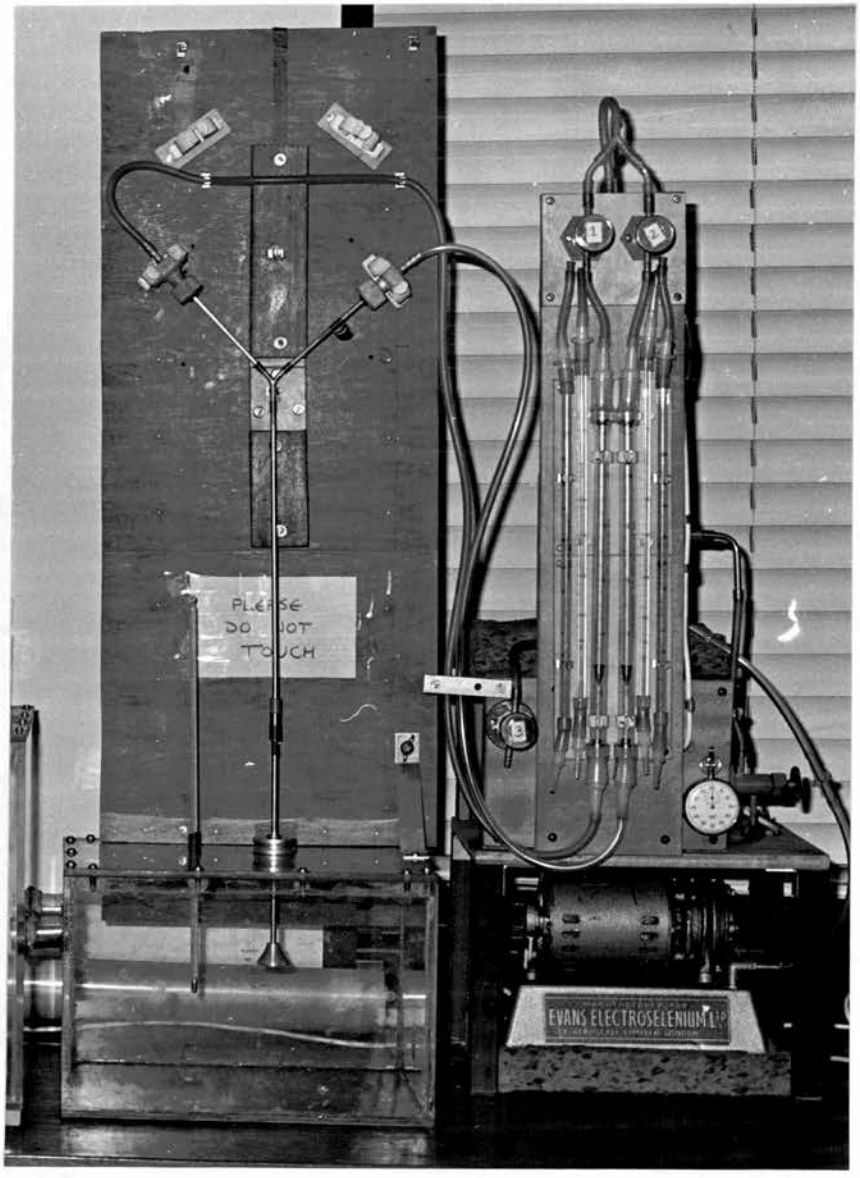

Fig. 4.3 Mounting of the Bifurcations

on a vertical wooden board: The latter was rigidly attached to a secondary aerosol holding chamber, connected directly to that of the aerosol generator proper (fig. 4.3).

All air flows were produced by the steady flow apparatus of Section 2.5 using a bell-mouth at the input of the system to establish the flow profile. The subsidiary tubing abutting the parent and daughters of a given model served as the appropriate input length ($\geqslant$ 100 diameters) and as connectors for the filter holders (Section 2.6) respectively.

By using two similar rotameters, each attached by suitable tubing to a filter holder unit on one daughter leg and setting identical flows, the upward flow through the parent tube could be regulated. The Reynolds Number corresponding to this was taken, as in the single bend experiments, to be the independent variable, with deposition (in the model) as the dependent.

Prior to an experiment, the given model was thoroughly coated (internally) with Aerosol 2A-X to facilitate retention of any deposited particles. The filter holders had previously been carefully assembled and mounted in position on the vertical board.

By working down from the filter holders to the input tubing the whole assembly could be leak-tested, low reading rotameters being used for null-flow indication.

Once the model unit had been satisfactorily checked, the particular Reynolds Number under study was set, by adjusting the flows through each daughter tube.

The aerosol generator was accordingly operated to yield a flux of known sized particles, and the relevant temperatures, flows etc., noted.

Facing Page 58

(i) Method "A" Assembly

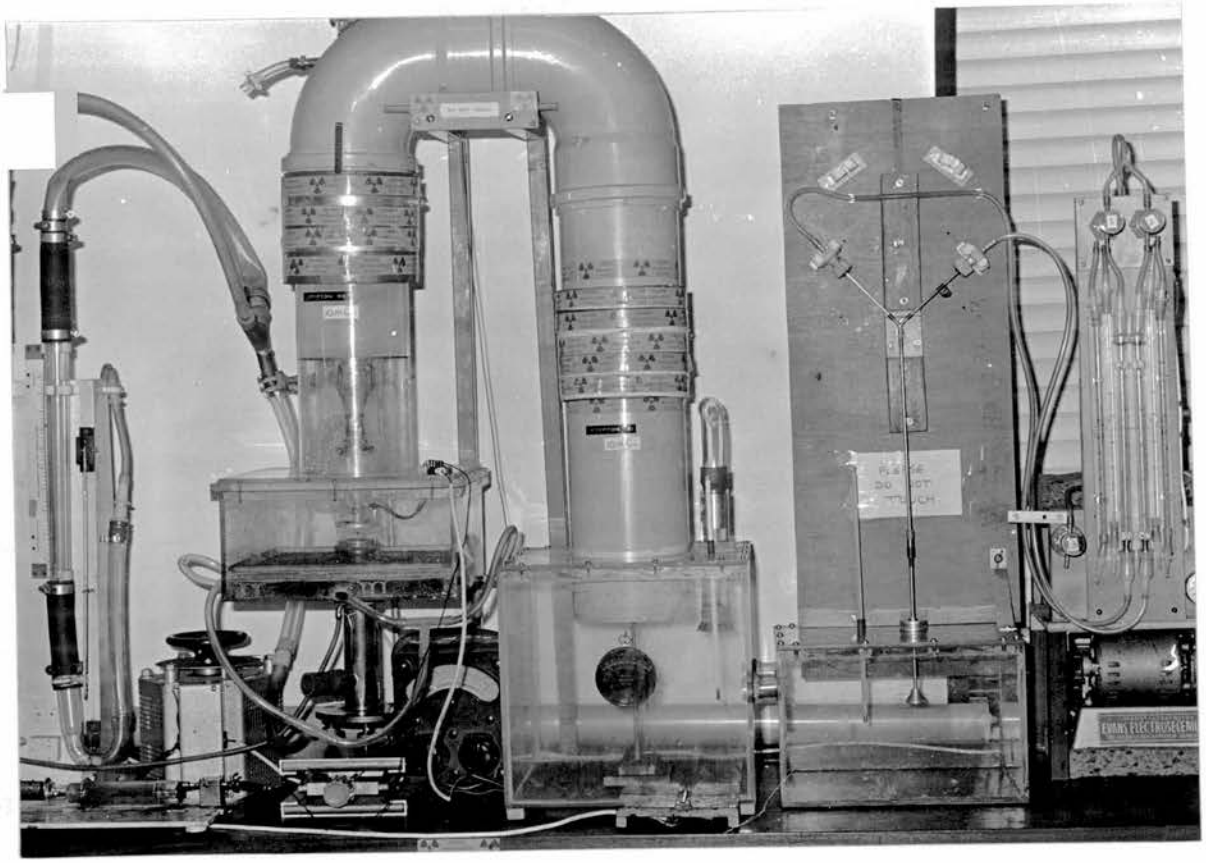

(ii) Method "B" Assembly

Fig. 4.4 Complete System for a Bifurcation Experiment

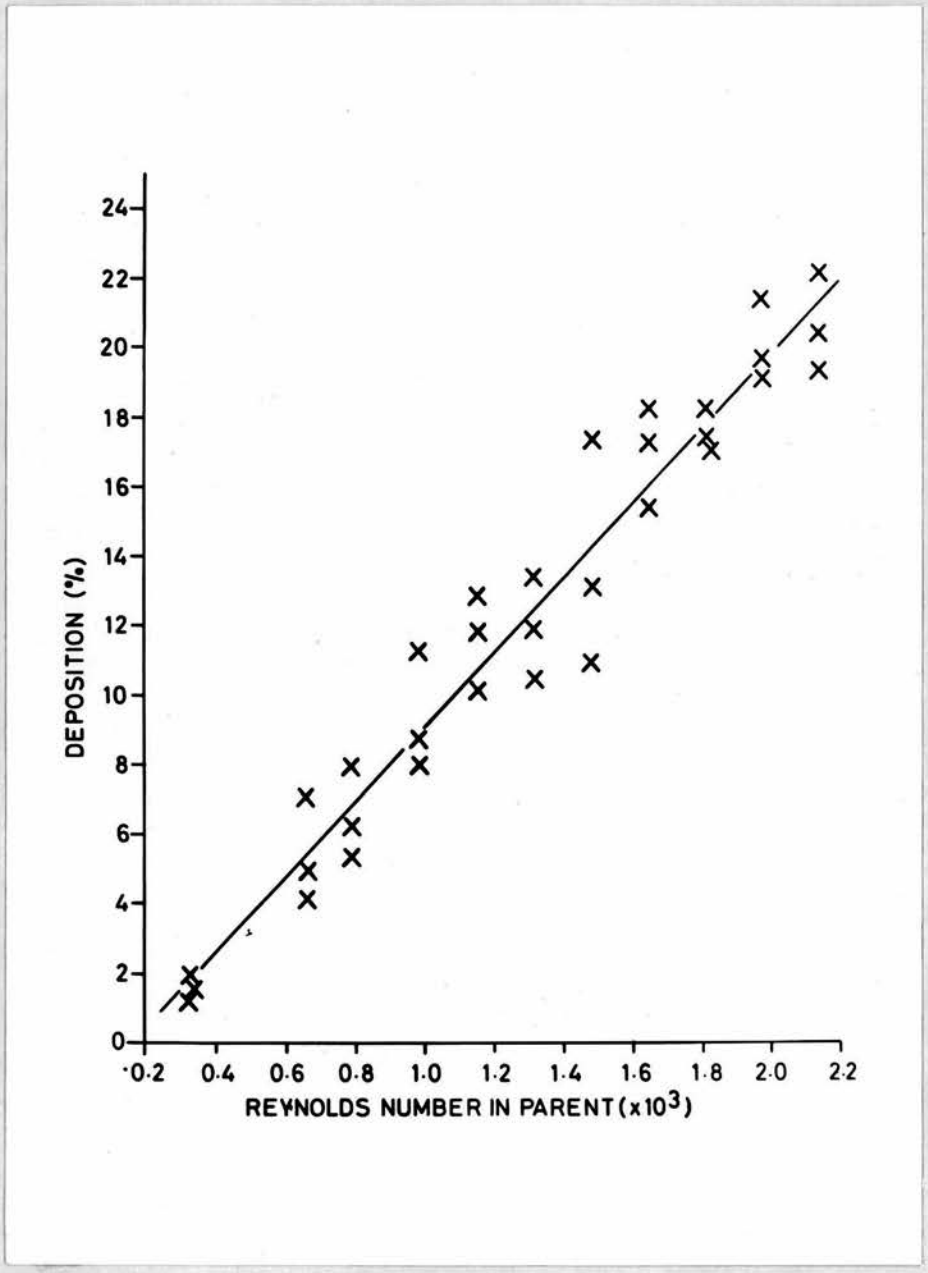

Fig. 4.5 Deposition as a function of Reynolds Number

Fig. 4.4 shows the complete aerosol generating and measuring systems used in the bifurcation series of experiments.

To assay the deposited quantity of aerosol, the procedure was identical to that of the single bends. Since the whole assembly was "absolute" over the conditions studied, measurement by fluorimetry of the amount deposited in each section enabled calculation of the fractional deposit in the model itself. As before (Section 3.1), the quotient of the mass of aerosol deposited in the model to the mass of aerosol approaching the model (total mass minus amount deposited in entry length) yielded the appropriate value.

Unless otherwise stated, all flows refer to particle motion towards the bifurcating spur i.e. equivalent to inhalation.

4.3 EXPERIMENTAL RESULTS

The ease of production of 5μm particles and their rapid size measurement using the Konimeter, were deemed sufficient reasons for choosing particles of this size as the "standards" for the bifurcation work.

The primary model studied was the acrylic, having parent tube diameter of 4.3×10^{-3}m and branching angle of 0.6109 radians (35°) (semi-inclusive angle).

Quantitative measurements were obtained and deposition patterns noted throughout.

a. Effect of Fluid Flow Rate

Fig. 4.5 shows a plot of Percentage Deposition of 5μm particles as a function of the Reynolds Number of the fluid in the parent tube (acrylic model).

Regression analysis showed a linear effect with the following

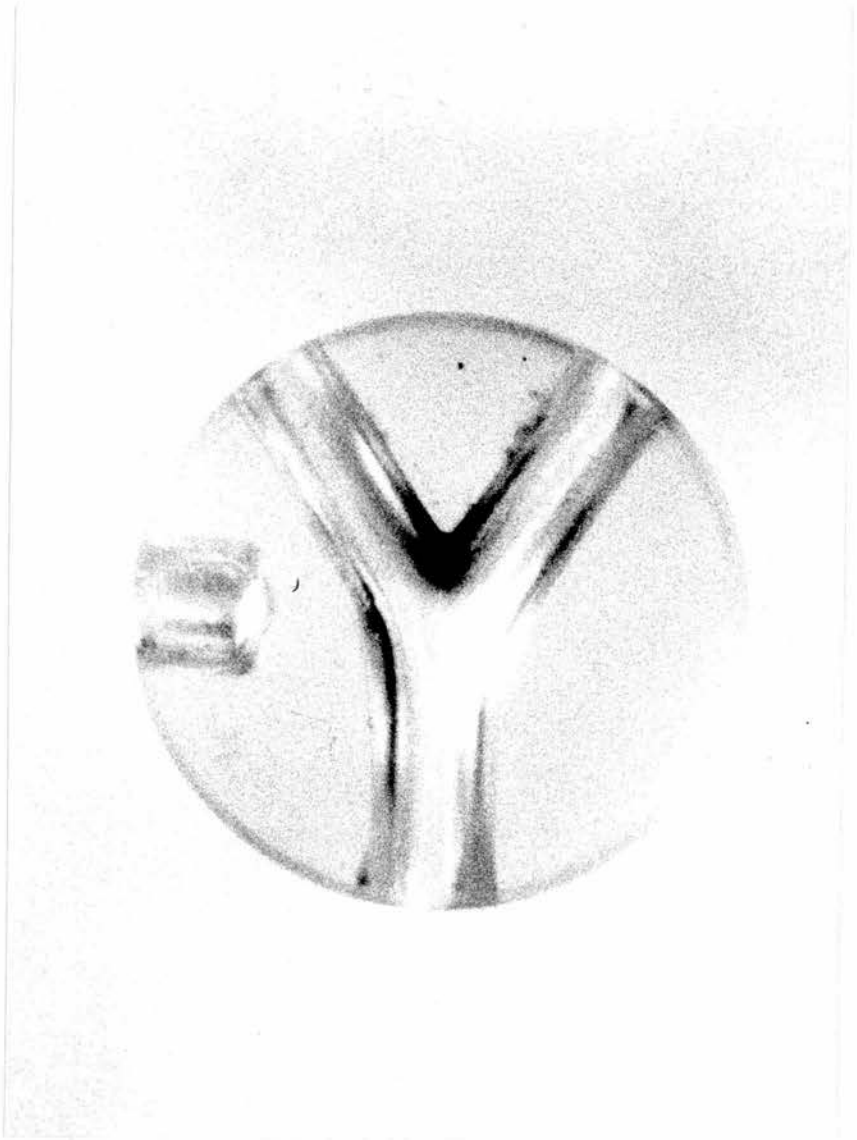

Fig. 4.6 Deposition at the Flow Divider

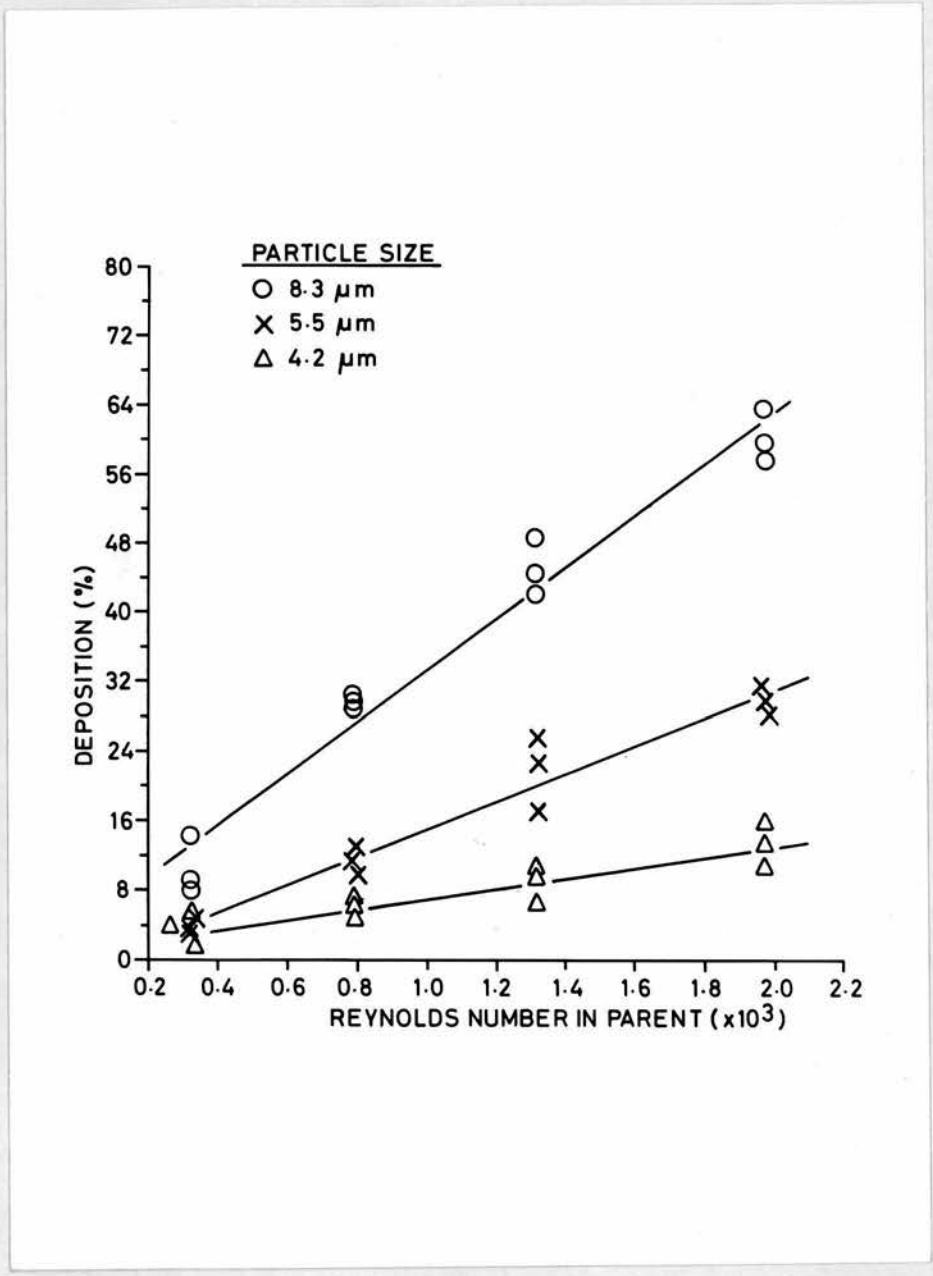

Fig. 4.7 Effect of Particle Size on Deposition

relationship between the ordinate and the abscissa.

$$D^* = 0.01077\ Re_p - 1.6965 \quad \ldots\ldots 4.3.1$$

(Residual Standard Deviation = 1.58)

where D^* = Percentage Deposition

Re_p = Reynolds No. of fluid in Parent Tube

This line accounted for about 96 per cent of the variability of D^*.

The pattern of deposition was observed in all cases to be in the region of the flow divider (fig. 4.6), with no evidence of the vortex deposition effect arising in certain of the single bend experiments.

To show that the linearity was present at other particle sizes, four representative Reynolds Numbers were adopted and the percentage deposition measured using three different sizes of particle. Fig. 4.7 illustrates the results obtained.

The fitted lines were as follows:-

$d = 4.2\mu m$; $D^* = 0.00606\ Re_p + 0.8658$ 4.3.2

(Variance Accounted for, 84%)

$d = 5.5\mu m$; $D^* = 0.01599\ Re_p - 0.8845$ 4.3.3

(Variance Accounted for, 96%)

$d = 8.3\mu m$; $D^* = 0.0296\ Re_p + 3.7500$ 4.3.4

(Variance Accounted for, 97%)

Deposit, once again, was observable only at the "carina" of each model.

b. Effect of Particle Size

A series of experiments was performed using the acrylic model, in which Reynolds Number in the parent tube was held constant and the size of the aerosol particles varied.

Fig. 4.7 has already been referred to as illustration of the linearity of Deposition with Reynolds Number.

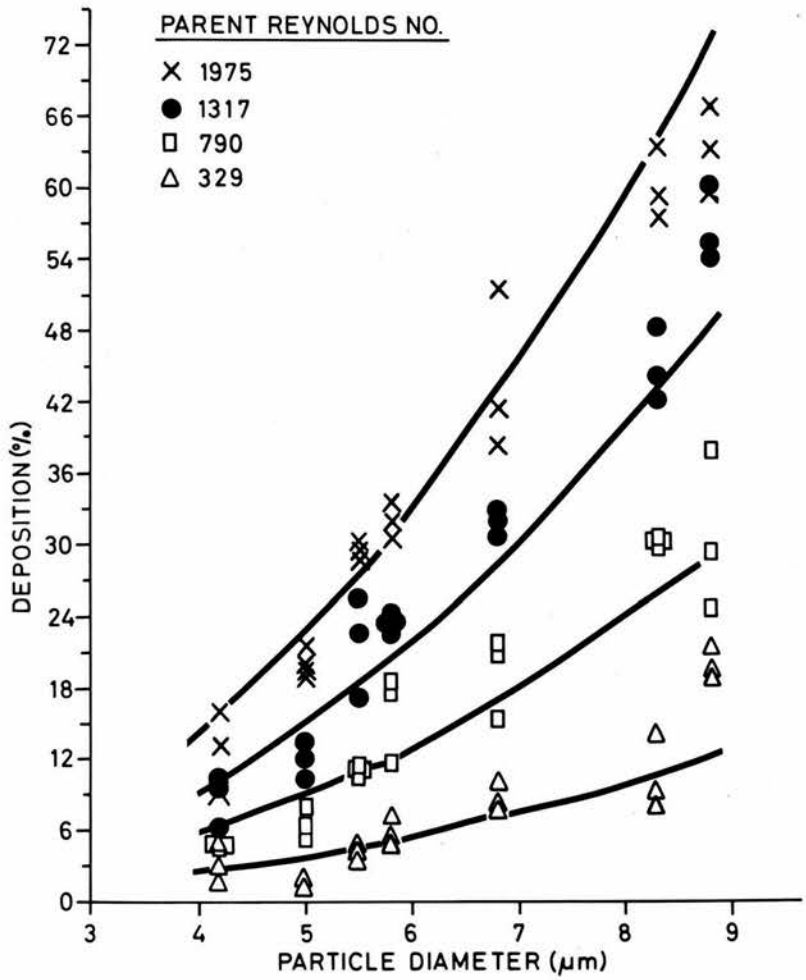

Fig. 4.8 Deposition as a function of Particle Size

A plot of Percentage Deposition against mean particle diameter (d) however, was non-linear, as seen in fig. 4.8. Regression analysis yielded the equation, for d in metres

$$D^* = (490d^2 - 0.00014d).10^6.Re_p \quad \text{.....4.3.5}$$

The percentage of variance accounted for in this instance was about 98 per cent.

A simpler expression, namely

$$D^* = 470x10^6 d^2 Re_p \quad \text{.....4.3.6}$$

could be used as an alternative to 4.3.5 with little error involved.

Deposit was observable only at the flow divider.

c. Effect of Bifurcating Angle

To assess the effect on deposition of altering the angle of branching of an airway, two metallic models of $4.3x10^{-3}$m parent diameter (i.e. that of the Acrylic Model) but semi-inclusive branching angles of 0.7854 radians (45°) and 0.4974 radians ($28^\circ30'$), were studied. Particles of 5μm dia. were again used.

For each bifurcation, deposition was linear with Reynolds Number, the regression lines being

Θ = 0.4974 radians; $D^* = 0.00875\ Re_p - 2.8770$ 4.3.7
(Residual standard deviation = 2.44)

Θ = 0.7854 radians; $D^* = 0.02216\ Re_p - 1.3614$ 4.3.8
(Residual standard deviation = 3.99)

Fig. 4.5 shows the Deposition/Reynolds Number line for the 0.6109 radian (acrylic) model. If the deposition values at the Reynolds Numbers used with the other two models are noted and a linear regression line fitted to these points, then for Θ = 0.6109 radians,

$$D^* = 0.01117\ Re_p - 2.2973 \quad \text{.....4.3.9}$$

(Residual standard deviation = 1.16)

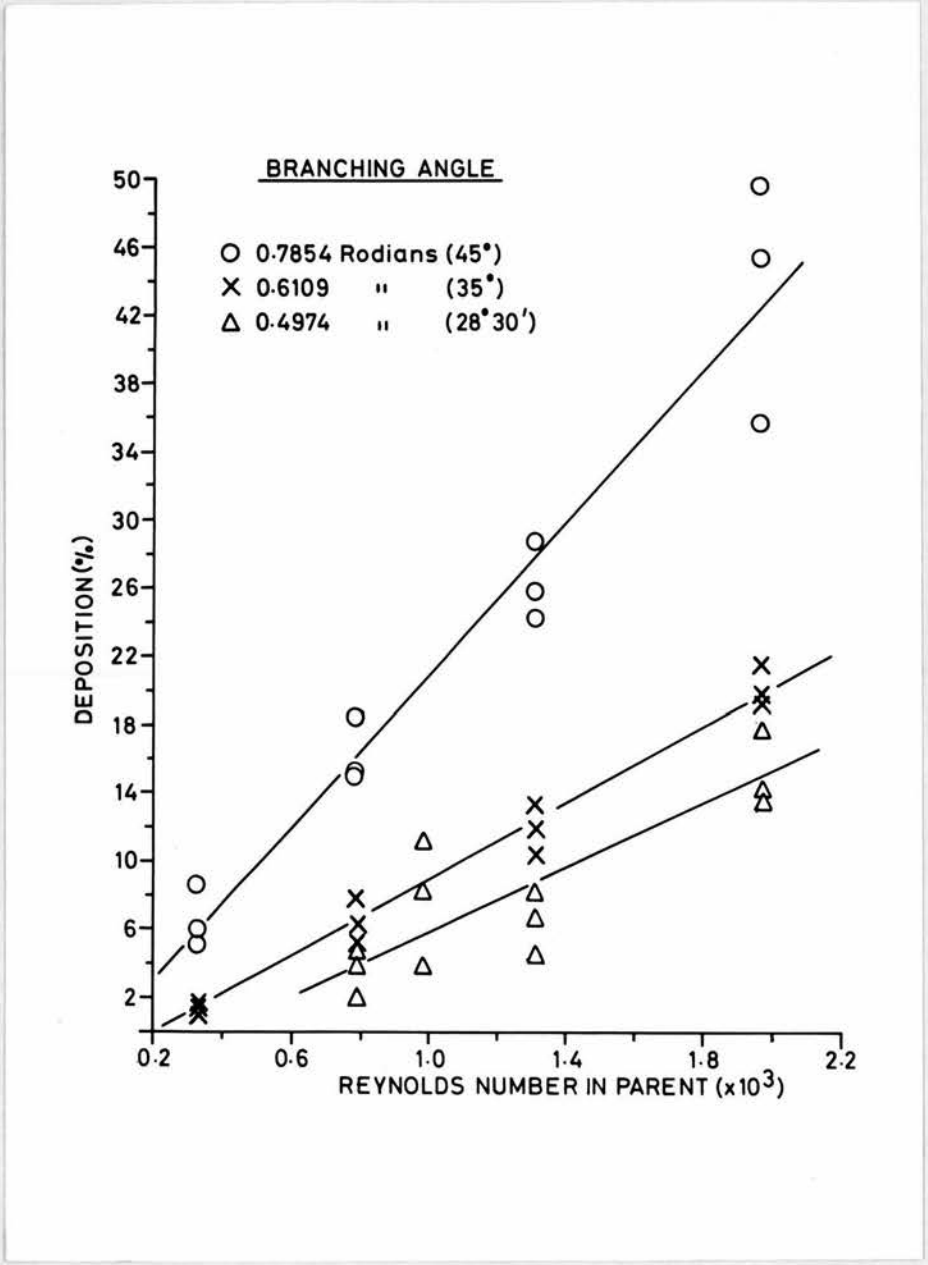

Fig. 4.9 Deposition as a function of Branching Angle

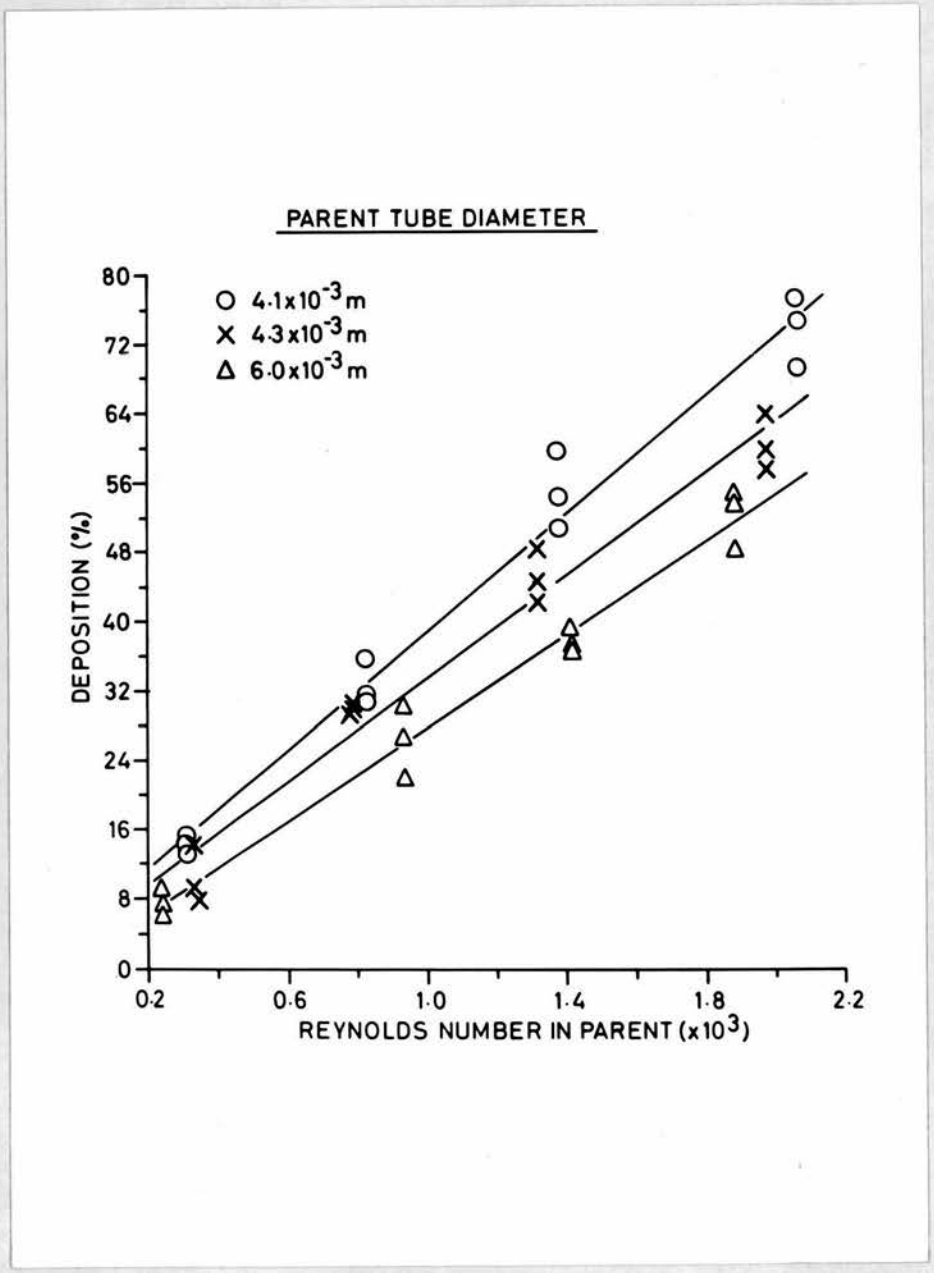

Fig. 4.10 **Deposition as a function of Parent Tube Bore**

Fig. 4.9 shows the effect of bifurcating angle on percentage deposition.

A model which satisfied all three straight lines, accounting for over 97 per cent of the variability was

$$D^* = (0.31707 \sin^3\theta - 0.30643 \sin^2\theta + 0.08815 \sin\theta).\ Re_p \quad \text{.....4.3.10}$$

A more simple model, almost as good a fit to the experimental data was

$$D^* = 0.05827\ Re_p \sin^3\theta \quad \text{.....4.3.11}$$

d. Effect of Parent Tube Diameter

The "primary" acrylic model of 0.6109 radian semi-inclusive branching angle had parent tube diameter of 4.3×10^{-3}m. Two other models were available which had the same angle but different parent tube bore; viz. 4.1×10^{-3}m and 6.0×10^{-3}m.

Using 8.3μm particles in an attempt to cover the whole spectrum of deposition values, graphs of percentage deposition against parent tube Reynolds Number were constructed.

$D = 4.1 \times 10^{-3}$m; $D^* = 0.0339\ Re_p + 4.8344$ 4.3.12

(Residual standard deviation = 3.38)

$D = 4.3 \times 10^{-3}$m; $D^* = 0.0296\ Re_p + 3.7500$.....4.3.13

(Residual standard deviation = 2.71)

$D = 6.0 \times 10^{-3}$m; $D^* = 0.0265\ Re_p + 1.0099$ 4.3.14

(Residual standard deviation = 2.88)

These linear fits are shown in fig. 4.10. Calculation of a general expression to satisfy all three equations yielded, for D in metres

$$D^* = 10^{-4} Re_p / (-36.1D^2 + 0.835D) \quad \text{.....4.3.15}$$

This fit accounted for about 99 per cent of the variability of the deposition values.

4.4 THEORETICAL ANALYSIS

The results of the single bend experiments inferred, primarily in a qualitative manner, that the magnitude of particle deposition by inertial precipitation increased directly with the fluid flow rate, particle size and angle of bend: An inverse relationship obtained with tube bore diameter.

Applying dimensional analysis to the problem of deposition in a bifurcation, yielded a group of dimensionless parameters which could be related quantitatively by the experiments described in the previous section.

Let $D^* = f(\bar{V}, D, \rho, d, \eta, \sigma, \delta)$ 4.4.1

where D^* = Deposition (%)

$\bar{V}$ = Average velocity of carrier fluid

D = Bore of Parent tube (in this study, daughter bores were related to that of the parent)

ρ = Particle density

d = Particle diameter

η = Dynamic viscosity of carrier fluid

σ = Density of carrier fluid

δ = A characteristic length of the bifurcation system which would alter as angle of branching or bore of parent tube changed.

$f(x)$ = Some function of x

Since there are 7 independent variables, and 3 primary dimensions (mass M, length L, and time T), then by BUCKINGHAM'S π Theorem (1914), 4 dimensionless groups exist.

Taking $D^* = k\bar{V}^x D^y d^z \rho^p \eta^q \sigma^r \delta^s$ 4.4.2

where k is a dimensionless parameter, and reducing the variables to their fundamental dimensions,

then $M^0L^0T^0 = k(LT^{-1})^x(L)^y(L)^z(ML^{-3})^p(ML^{-1}T^{-1})^q(ML^{-3})^r(L)^s$

$= k\, M^{p+q+r} L^{x+y+z+s-3p-3r-q} T^{-x-q}$

Equating indices,

$p+q+r = 0$ .....(i)

$x+y+z+s-3p-3r-q = 0$ .....(ii)

$-x-q = 0$ .....(iii)

From (iii) $-x = q$

Therefore in (i) $x = r+p$

Hence, in (ii) $s = 3r + 3p+q-x-y-z$

$= x-y-z$

or, $y = x-s-z$

Accordingly, in 4.4.2

$D^* = k\bar{V}^x D^{x-s-z} d^z \rho^p \eta^{-x} \sigma^{x-p} \delta^s$

$\therefore D^* = k \left(\frac{\sigma \bar{V} D}{\eta}\right)^x \left(\frac{d}{D}\right)^z \left(\frac{\delta}{D}\right)^s \left(\frac{\rho}{\sigma}\right)^p$

i.e. $D^* = f\left(\frac{\sigma \bar{V} D}{\eta}; \frac{d}{D}; \frac{\delta}{D}; \frac{\rho}{\sigma}\right)$

Now $\frac{\sigma \bar{V} D}{\eta}$ is Reynolds Number (by definition, of the Parent Tube)

Therefore, $D^* = f\left(Re_p; \frac{d}{D}; \frac{\delta}{D}; \frac{\rho}{\sigma}\right)$ 4.4.3

In this study, since the densities of the particulates and carrier fluid did not vary, $\frac{\rho}{\sigma}$ was constant.

Thus $D^* = f'\left(Re_p; \frac{d}{D}; \frac{\delta}{D}\right)$ 4.4.4

If δ is defined by the distance along the axis of the parent tube from the flow divider to the point of intersection of the axes of the parent and daughter tubes, then

$$\frac{\delta}{D} \propto \frac{1}{\sin\theta}$$

where θ is the branching angle.

Accordingly, $D^* = f''(Re_p; \frac{d}{D}; \sin\theta)$ to comply with the experimentally observed dependence of deposition on the quantities in parenthesis.

A general equation was obtained which related deposition to the relevant variables. Before describing the method of obtaining this and comparing the deductions with existing theory, certain points should be observed regarding the format of several of the regression lines previously noted.

Equations 4.3.(2,4,12,13 and 14) were all of the form

$$D^* = A\ Re_p + B \quad \text{.....4.4.5}$$

where $B \lesssim 5$

This general equation represented a good fit to the points obtained for the series of experiments in question.

Theoretically, however, a positive intercept is unacceptable. This arises from the manner in which the deposition experiments were performed. All flows were in the upward direction through a 100 diameter input length of tubing. The particles used, ranged from about 5 to 10μm aerodynamic diameter. This implies settling velocities in the order of 0.75×10^{-3} to $3 \times 10^{-3}\ ms^{-1}$. Consequently, a "critical" flow must exist which has to be attained before a given particle in the holding chamber will move against the force of gravity and through the tube. (This critical flow has no connection with that characterising the onset of turbulence).

The actual magnitude for 10μm dia. unit density spheres in the 6×10^{-3}m tube (the "worst" possible in this study) is about $8 \times 10^{-5}\ ls^{-1}$ ($Re_p \simeq 1.2$).

Although small, this infers that a Reynolds Number of zero in equation 4.4.5, with an accompanying positive value for deposition, is fundamentally erronecus.

To establish a general relationship between deposition, particle size, angle of branching and fluid flow rate (Re_p) it was necessary to mathematically combine the three general equations.

viz. $D^*_{d,D} = (0.31707\sin^3\theta - 0.30643\sin^2\theta + 0.08815\sin\theta).Re_p$

$D^*_{\theta,D} = (490d^2 - 0.00014d).10^6.Re_p$

and $D^*_{\theta,d} = 10^{-4}Re_p \,/\, (-36.1D^2+0.835D)$ **

where $D^*_{a,b}$ = Percentage deposition for fixed a and b

θ = radians

d = metres

D = metres

Re-arranging **

$$D^*_{d,D} = 0.31707\sin^3\theta\,(1 - \frac{0.9663}{\sin\theta} + \frac{0.2780}{\sin^2\theta}).Re_p$$

$$= 0.31707\,\sin^3\theta.f_1(\theta).Re_p \quad \ldots\ldots 4.4.6$$

$$D^*_{\theta,D} = 490.10^6d^2(1 - \frac{2.857\times10^{-7}}{d}).Re_p$$

$$= 490.10^6d^2.f_2(d).Re_p \quad \ldots\ldots 4.4.7$$

$$D^*_{\theta,d} = 0.0277\times10^{-4}Re_p \,/\, D^2(\frac{2.313\times10^{-2}}{D} - 1)$$

$$= 0.0277\times10^{-4}Re_p \,/\, D^2.f_3(D) \quad \ldots\ldots 4.4.8$$

where $f_x(y)$ = function x of variable y.

By consideration of the qualitative effects of the different variables and the existence of the "critical" (entry) flow, the following model was postulated.

$$D^* = \frac{k\,d^2.\sin^3\theta.\,Re_p}{D^2}\,.\,F(\theta,d,D) - C \quad \ldots\ldots 4.4.9$$

where $F(\theta,d,D) = f_1(\theta).f_2(d) \,/\, f_3(D)$ and C = constant

Equation A: $D^* = 1324.1 \times 10^3 \frac{d^2_{min}{}^3 \theta}{D^2} Re_p^* F(\theta, d, D) - 0.525$

Equation B: $D^* = 1306.7 \times 10^3 \frac{d^2_{min}{}^3 \theta}{D^2} Re_p^* F(\theta, d, D)$

Parent Tube Diameter D(m)	Particle Size d(m)	Branching Angle θ (rad)	Reynolds No. in Parent Tube	Values Predicted by equation A	(Mean) Experimental Values	Values Predicted by equation B
4.3×10^{-3}	5.0×10^{-6}	0.4974	790	6.0	3.6	6.4
			987	7.6	7.7	8.0
			1317	10.3	6.5	10.7
			1975	15.7	15.1	16.0
4.3×10^{-3}	5.0×10^{-6}	0.6109	329	3.3	1.6	3.8
			790	8.7	6.5	9.1
			1317	14.8	11.9	15.2
			1975	22.5	20.1	22.7
4.3×10^{-3}	5.0×10^{-6}	0.7854	329	8.0	6.6	8.4
			790	19.9	16.1	20.1
			1317	33.5	26.2	33.5
			1975	50.5	43.4	50.3
4.3×10^{-3}	4.2×10^{-6}	0.6109	329	2.2	3.5	2.6
			790	5.9	4.9	6.3
			1317	10.2	8.6	10.6
			1975	15.5	13.2	15.9
4.3×10^{-3}	8.8×10^{-6}	0.6109	329	11.7	19.8	12.0
			790	27.5	30.5	27.6
			1317	48.3	56.6	48.2
			1975	72.7	63.1	72.3
4.1×10^{-3}	8.3×10^{-6}	0.6109	311	10.1	14.4	10.5
			829	27.8	32.6	27.9
			1390	46.6	54.7	46.5
			2071	70.2	73.3	69.8
6.0×10^{-3}	8.3×10^{-6}	0.6109	236	5.6	7.4	6.0
			934	23.7	26.2	23.9
			1416	36.2	37.1	36.2
			1887	48.4	51.9	48.3

Table 4.1 Comparison of Theoretical and Experimental Deposition.

The values of deposition at the lowest and highest values of θ, d and D, were used, in conjunction with deposition values obtained using the primary acrylic model, to compute k and C.

k was found to be 1324.1×10^{3} with C equal to 0.525.

i.e. $$D^{*} = \frac{1324.1 \times 10^{3} d^{2} \sin^{3}\theta \; Re_{p}}{D^{2}} \cdot F(\theta, d, D) - 0.525 \quad \text{.....4.4.10}$$

with greater than 93 per cent of the variability accounted for.

If the constant C was ignored in equation 4.4.9,

i.e. $$D^{*} = \frac{k' d^{2} \sin^{3}\theta \; Re_{p}}{D^{2}} \cdot F(\theta, d, D) \quad \text{.....4.4.11}$$

and the appropriate values of the relevant parameters submitted (as before) then

$$k' = 1306.7 \times 10^{3}$$

i.e. $$D^{*} = \frac{1306.7 \times 10^{3} d^{2} \sin^{3}\theta \; Re_{p}}{D^{2}} \cdot F(\theta, d, D) \quad \text{.....4.4.12}$$

This fit accounted for about 97 per cent of the variability.

Table 4.1 shows the experimentally found mean values of deposition compared with the values predicted by the two general equations.

The above calculations were performed using a DATA 100 computer; simultaneous variation of the primary variables was accounted for by this method.

Manual computation of the numerical coefficient necessitated the use of the three generalised equations for θ, d and D. The basic principle involved substituting the values of two of the variables into the composite equation (4.4.11 for ease of calculation) and comparing the resultant coefficient with that of the general equation of the remaining third variable. A unique value of k' was accordingly not possible.

The order of magnitude however, was similar to the computerised solution for k', the three values being 1089×10^3; 1375.9×10^3 and 1309.2×10^3 (mean value 1258×10^3).

In the previous chapter on Single Bends, the inertial parameter $\rho d^2 \bar{V} / 18\eta D$ was defined, for a right angled bend, and a numerical value found which was indicative of 50 per cent deposition.

This value was approximately 0.25.

Let $\rho d^2 \bar{V} / 18\eta$ = S = Particle Stop Distance.

Now $S/D \doteq 0.25$ 4.4.13

Then, since D = 2R where R is the tube radius

$S/R \doteq 0.5$ 4.4.14

In an attempt to quantify inertial deposition at a bifurcation, LANDAHL (1950) quoted the results of his single bend analysis (LANDAHL and HERRMANN, 1949) in the form

$S/R = 1$, for a $\pi/2$ radian bend 4.4.15

The incompatibility of the latter two statements, in the light of the experimental results has been pointed out by JOHNSTON and MUIR (1973)*.

Using the concept of S/R = 1, LANDAHL (1950) stated an equation which was assumed to be applicable to a branching tube system such as found in the lung.

viz. $\rho d^2 V_p \sin\theta / 18\eta R_D = 1$, for 50% Deposition 4.4.16

where V_p = average velocity of air stream in parent tube (inhalation)

R_D = radius of daughter tube

θ = (semi-inclusive) branching angle

or/ $S \sin\theta / R_D = 1$ 4.4.17

where $S = \rho d^2 V_p / 18\eta$

* IN APPENDIX

The general equation representing the experimental results of this investigation

i.e. $$D^* = \frac{1324.1\times10^{3} d^2 \sin^3\theta \ Re_p}{D^2} . F(\theta, d, D) - 0.525$$

was manipulated algebraically to yield the inertial parameter, and suitable values inserted for quantitation.

Since $Re_p = \frac{\sigma V_p D}{\eta}$, where the symbols have their previous meaning,

$$\frac{d^2 \sin^3\theta \ Re_p}{D^2} \equiv \frac{d^2 \sin^3\theta}{D^2} \cdot \frac{\sigma V_p D}{\eta} \cdot \frac{(\rho . 18)}{(\rho 18)} \quad \ldots\ldots\ldots 4.4.18$$

where ρ, the particle density, and the number 18 are introduced since they appear theoretically.

Thus $$\frac{d^2 \sin^3\theta \ Re_p}{D^2} \equiv \frac{\rho d^2 V_p \sin\theta}{18 \eta D} \cdot \left(18\sin^2 . \frac{\sigma}{\rho}\right) \quad \ldots\ldots\ldots 4.4.19$$

Now $$\frac{\rho d^2 V_p \sin\theta}{18 \eta D} \equiv \frac{S \sin\theta}{D}$$

Accordingly,

$$D^* = 1324.1\times10^{3}\left(\frac{S\sin\theta}{D}\right).18\sin^2\theta . \frac{\sigma}{\rho} . F(\theta, d, D) - 0.525 \quad \ldots\ldots\ldots 4.4.20$$

To establish the range of $\left(\frac{S\sin\theta}{D}\right)$, it was necessary to use the experimental values of θ, d and D which would

a. Maximise and

b. Minimise the impaction parameter.

To maximise, the largest size of particle (8.8×10^{-6} m), the greatest branching angle (0.7854 radians) and the minimum parent tube diameter (4.1×10^{-3} m) were substituted into the general equation.

This yielded

$$\frac{S\sin\theta}{D} = \frac{D^* + 0.525}{434.9} \quad \ldots\ldots\ldots 4.4.21$$

At $D^* = 50$, $\frac{S\sin\theta}{D} = 0.116$

In the models used, $R_D = 0.39D$

Thus $$\frac{S\sin\theta}{R_D} \simeq 0.3 \quad \text{.....4.4.22}$$

To minimise, the smallest size of particle (4.2×10^{-6}m), the smallest branching angle (0.4974 radians) and the maximum parent tube diameter (6.0×10^{-3}m) were used, to give

$$\frac{S\sin\theta}{D} = \frac{D^* + 0.525}{320.6} \quad \text{.....4.4.23}$$

At $D^* = 50$, $\frac{S\sin\theta}{D} = 0.158$

Since $R_D = 0.39D$

$$\frac{S\sin\theta}{R_D} \simeq 0.4 \quad \text{.....4.4.24}$$

Thus $$0.3 \lesssim \frac{S\sin\theta}{R_D} \lesssim 0.4 \quad \text{.....4.4.25}$$

This should be compared with the similar parameter of LANDAHL (1950) which had value of unity.

The anatomical model used by the latter investigator had values for the dimensions of the conducting airways similar to those of FINDEISEN (1935). The approximate relationship between succeeding generations was

$$R_D \simeq \tfrac{1}{2}R_p \quad (R_p = \text{parent radius})$$

Because of the different parent/daughter relationships of the LANDAHL/FINDEISEN model, and that of the present study, the relevant impaction parameters are worthy of comparison only when referred to the parent tubes.

Accordingly, for the LANDAHL (1950) model

$$\left(\frac{S\sin\theta}{R_p}\right)_{\text{LANDAHL}} = 0.5 \text{ for 50\% impaction} \quad \text{.....4.4.26}$$

while for the general equation

$$\left(\frac{S\sin\theta}{R_p}\right)_{\blacksquare\blacksquare\blacksquare\blacksquare} = 0.23 - 0.31 \quad \text{.....4.4.27}$$

The average branching angle of the lung was taken by FINDEISEN (1935) and LANDAHL (1950) to be $\pi/6$ radians.

Since $\sin \pi/6 = \frac{1}{2}$

$$\left(\frac{S}{R_p}\right)_{LANDAHL} = 1 \quad \text{.....4.4.28}$$

while

$$\left(\frac{S}{R_p}\right)_{EXPERIMENTAL} = 0.54 \text{ (Mean)} \quad \text{.....4.4.29}$$

It is obvious that the value of the impaction parameter at 50 per cent deposition is highly dependent on the geometric model adopted to represent a typical lung bifurcation.

A general expression for impaction efficiency based on the 50 per cent parameter, was derived by LANDAHL (1950). This had the form

$$I = \frac{x}{1 + x} \quad \text{where } x = \frac{S \sin\theta}{R_D}$$

and I = fraction removed from airstream.

When $x = 1$, $I = \frac{1}{2}$ or 50 per cent.

Consider any given size of particle in transit through a particular generation in the conducting airways.

$$\text{Since } x = \frac{S \sin\theta}{R_p} = \frac{\rho d^2 V_p \sin\theta}{18 \eta R_D}$$

$$\text{and } Re_p = \frac{V_p D}{\nu} \quad \text{where } \nu \text{ is the kinematic viscosity}$$

$$\text{then } x = \frac{\rho d^2}{18} \cdot \frac{\sin\theta}{R_D} \cdot \frac{Re_p}{\sigma D}$$

where σ is the air density.

As $R_D = 0.39D$ (In this study)

$$x = \rho d^2 Re_p \sin\theta \,/\, \sigma\, 18 \times 0.39 D^2$$

$$\text{or/ } x = B.Re_p \sin\theta \quad \text{.....4.4.30}$$

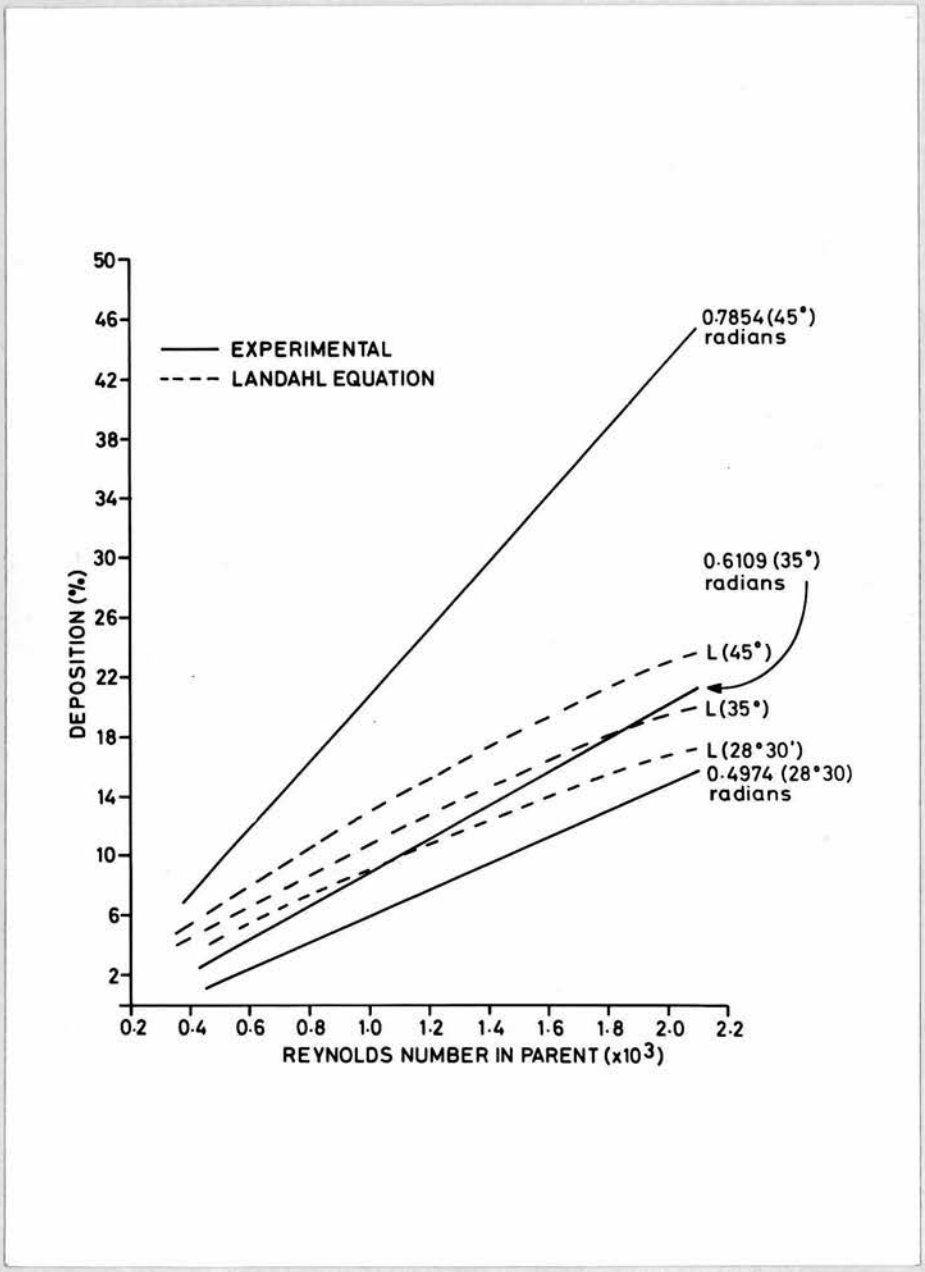

Fig. 4.11 **Comparison of Theoretical and Experimental Impaction Efficiencies**

Re_p	LANDAHL'S $x/(1+x)$	General Equation for Θ
329	3.3	2.3
790	7.6	5.6
987	9.3	7.0
1317	12.1	9.4
1975	17.1	14.0

Table 4.2 Predicted Deposition for $\pi/6$ Radian Branching Angle

where $B = \rho d^2 / 7.02\sigma D^2$

$= \text{Constant}$

Thus $I = B.Re_p \sin\theta / (1 + B.Re_p \sin\theta)$ 4.4.31

Fig. 4.9 graphically illustrates the effect of bifurcating angle on the deposition of fixed size particles, in three models whose geometries differed only by θ.

Equation 4.4.31 was applied to the three branching angles and Deposition plotted against fluid Reynolds Number as before. The results are shown in figure 4.11. The notation $L(A^\circ)$ denotes the predicted LANDAHL value for the deposition in the bifurcation of angle A; the full lines are those obtained experimentally for the particular angle shown.

For the angles of 0.4974 and 0.6109 radians, experimental and theoretical deposition efficiencies show very little difference.

In the bifurcation of angle 0.7854 radians, however, the theoretical equation seriously underestimates, particularly at the higher values of Reynolds Number.

The average branching angle of the lung adopted by FINDEISEN (1935) and LANDAHL (1950) was substituted in the general equation,

$D^* = (0.31707\sin^3\theta - 0.30643\sin^2\theta + 0.08815\sin\theta).Re_p$

and in LANDAHL'S theoretical equation, $\frac{x}{1+x}$ (4.4.30/31)

The equations are in good agreement in the $\pi/6$ region as shown in Table 4.2.

Fig. 4.12 "Vortex Redistribution" of Aerosol

(i) Inspiration

4.5 OBSERVATIONS AND REMARKS: VORTEX EFFECT

The five bifurcating models of this study had dimensions generally representative of generations 3 to 6 of the Model "A" of WEIBEL (1963).

In the human lung, at all but the more strenuous breathing rates, laminar flow would be present in this region, although the POISEUILLE parabolic profile would be disturbed by virtue of the flow-splitting at each generation.

The flow patterns in branching airways and the factors affecting the airflow have been of interest in the past (WEST and HUGH-JONES, 1959; CLARKE et al, 1972; OLSON et al, 1972) since much information pertinent to respiratory mechanics e.g. resistance, can be inferred from the experimental results (HYATT and WILCOX, 1963; PEDLEY et al, 1970 (a & b); OLSON et al, 1970).

It has been shown (SCHROTER and SUDLOW, 1969) that downstream of a bronchial bifurcation, in any direction i.e. equivalent to inhalation or exhalation, secondary motions are induced, irrespective of the form of the entry profile.

In this study these complex secondary motions were sufficient, even at the lower values of Reynolds Number, to redistribute the aerosol flux across the lumen of the tube(s).

In the case of "inspiratory" flow, two vortices were generated in each daughter tube. The perturbation to the particulate concentration profile across the tube bore was subsequently propagated downstream, in some cases for about 40 diameters, before the aerosol particles were intercepted by the glass fibre filters housed in the holders.

Figure 4.12 shows a typical pattern observed on examination of the filters (since the bifurcating systems were symmetrical, both filters

showed similar deposits). The diameter of the dark region approximately corresponds to the internal diameter of the daughter tube since the exit end of the latter was in close proximity to the filter. In general the effect of the double vortex formation at the flow divider was clearly evidenced by two distinct areas denuded of particles.

This "vortex redistribution" effect was observed in all the model bifurcation experiments performed. The actual size of the deposit-free regions appeared, however, to be a function of the model used, and the experimental variables under study.

In the human lung, the average length of an airway is of the order of 3.25 diameters (WEIBEL, 1963). Any disturbance to the particle flux profile initiated (on inspiration) at a given bifurcation is capable of being propagated for a much greater distance than the daughter airway length. This redistribution across the lumen will be presented to the post-daughter branching where further deposition will take place and other flow asymmetries generated.

The magnitude of particle deposition by inertial forces at each bifurcation of a multiple branching system remains to be quantified.

Inertial precipitation of aerosol particles on inspiration can be handled theoretically by assuming an orderly movement of the particles towards the carinal region when the parent flow divides into that of the two daughters.

On expiration i.e. when the flows in the daughters join together and pass into the parent, deposition of particles will occur, but would appear to be primarily due to the fluid motions rather than the particle inertia.

As on inspiration, the aerosol flux will be redistributed over the

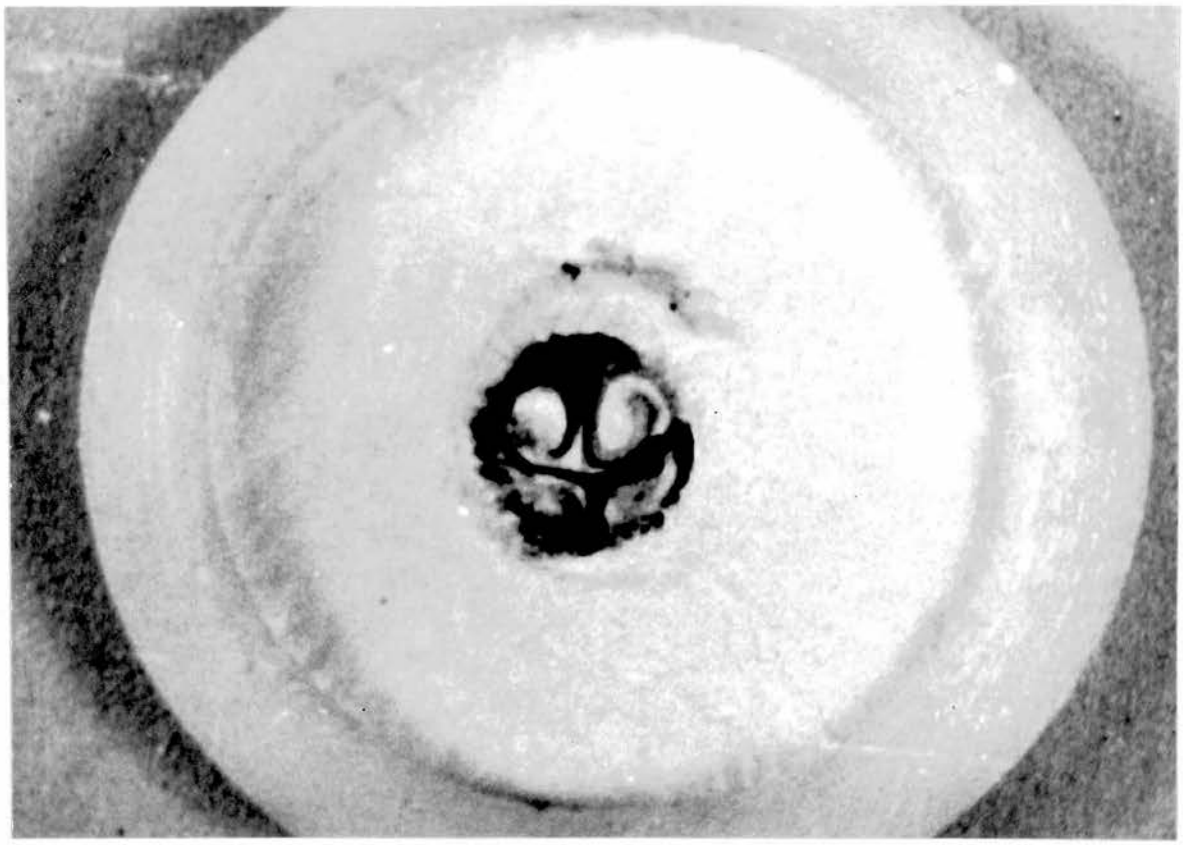

Fig. 4.13 "Vortex Redistribution" of Aerosol

(ii) Expiration

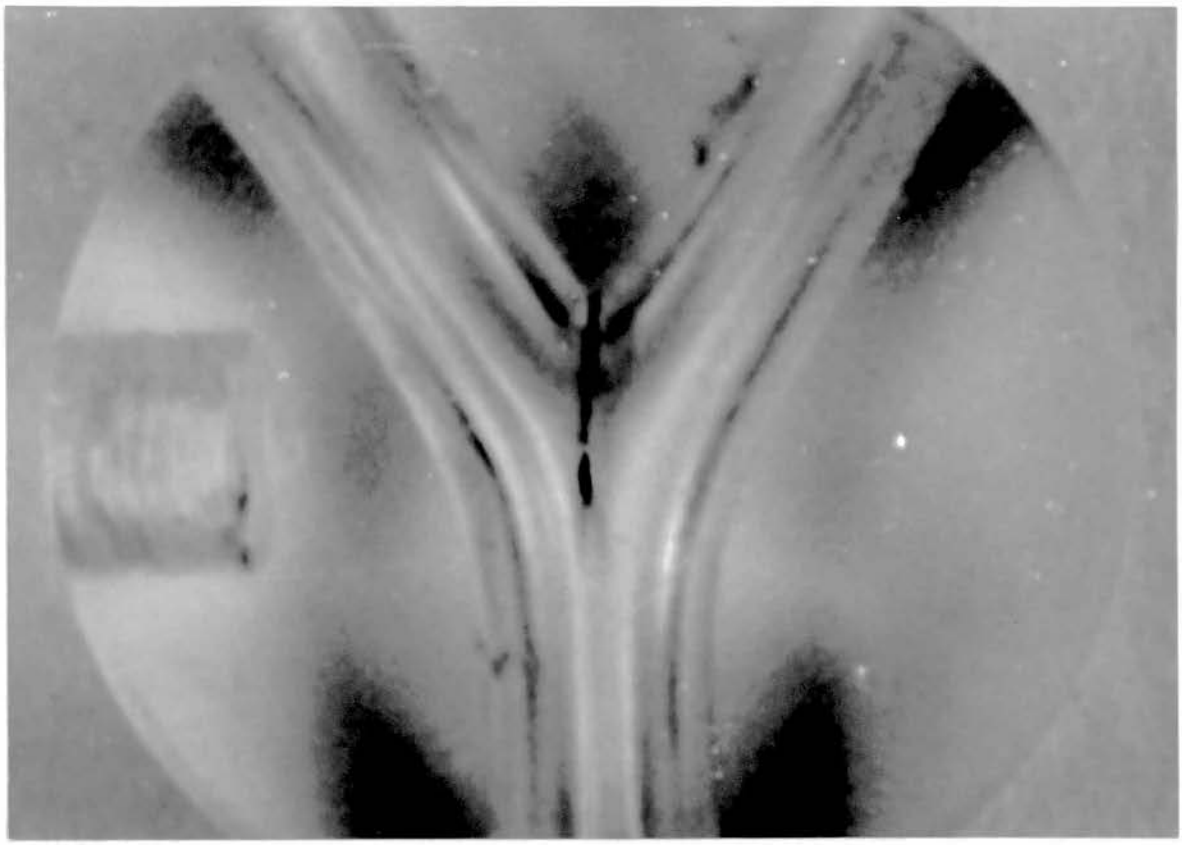

(i) Plan View of Model

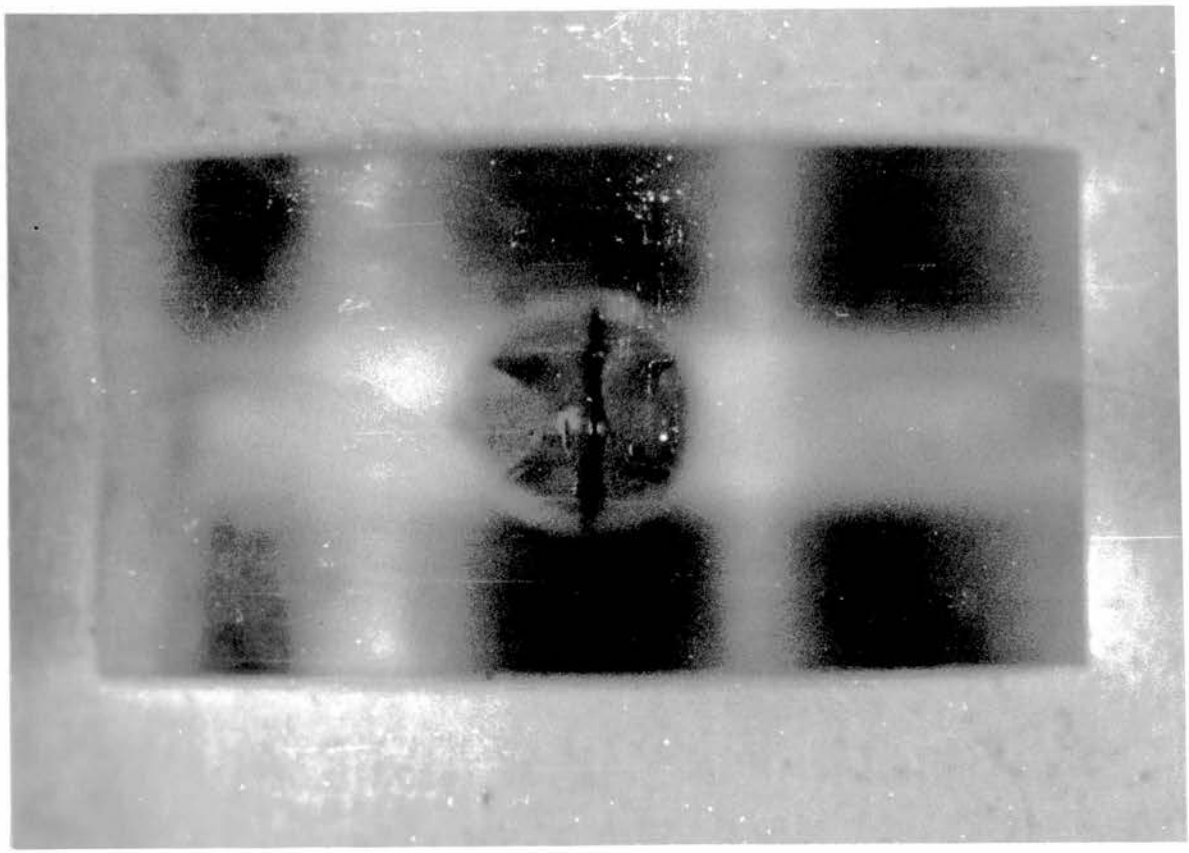

(ii) View looking down Parent Tube

Fig. 4.14 Deposition Site of "Expired" Particles

lumen of the tube but in this instance two sets of balanced vortex pairs (i.e. total of four) obtain (SCHROTER and SUDLOW, 1969; SCHERER, 1972). Fig. 4.13 shows the deposit obtained when a loaded filter holder was placed at the exit end of the parent tube of the acrylic model, and aerosol particles drawn through the system via the daughter tubes. This experiment was performed with the model horizontal (for ease of experimentation), and assumed that the daughter flows were equal.

The actual deposition site of the particles is shown in Fig. 4.14. This differed quite significantly from the deposition site of fig. 4.6. A thin line of deposited particles, running exactly along the flow "divider" extended continuously for about 7.5×10^{-3}m along the axial plane of symmetry of the system, on both the top and bottom surfaces. The site can be understood if the directional motion of the generated vortices is considered: This would be vertically upwards in the axial plane of symmetry for the two vortices of the upper half of the parent tube, and vertically downwards for the pair of vortices of the lower half (SCHERER, 1972).

No rigorous quantitative experiments were performed for the "expiration" mode of deposition, since several assumptions regarding the models would have been necessary. Also, two 100 diameter daughter tubes each at an angle to the vertical would have necessitated, in the case of the larger angle and larger diameter tubes, a relatively broad aerosol holding chamber, to locate the widely spread input ends.

Unlike the "inspiration" series of experiments, it would have been necessary to assume equality of flow through each daughter; also, the particulate flux through each tube could not be regarded as identical, since one daughter would have its bell-mouth facing toward the aerosol

holding chamber proper (fig. 4.3), while the other would face away towards the exit to atmosphere of the secondary chamber.

The experiments of this chapter, while yielding certain qualitative and quantitative results, also serve to highlight the complexities of the lung as a system, and underline the need for improvements to the basic models used.

Further research is necessary on the effects of pulsatile flow on deposition, the multiple generation problem, asymmetric bifurcations and of course expiratory flow.

CHAPTER FIVE

CONCLUSIONS

The general equation

$$D^* = A \frac{d^2 \sin^3\theta \, Re_p}{D^2} \cdot F(\theta, d, D) - B$$

deduced from the results of the bifurcation series of experiments was found to be generally compatible with the existing theoretical equation of LANDAHL (1950), when the average angle of branching of the airways of the human lung was taken to be in the region of $\pi/6$ radians.

The LANDAHL (1950) equation for deposition efficiency,

$$I = x/(1 + x)$$

where $x = \rho d^2 V_p \sin\theta \,/\, 18\eta R_D$

was shown to underestimate the magnitude of inertial precipitation, when branching angle was significantly greater than the average: The discrepancy increased as fluid flow rate increased.

Disagreement arose regarding the value of the inertial parameter (x) characterising 50 per cent deposition in a given bifurcation. It was demonstrated that the model geometry was important in determining the correct value.

ACKNOWLEDGEMENTS

I wish to express my appreciation to Dr. P. Tothill and Dr. D.C.F. Muir for their encouragement throughout the duration of this project. The primary supervision was performed by Dr. Muir and his helpful advice is gratefully acknowledged.

The bifurcation experiments would not have been possible without the skill of Mr. V. Bass who manufactured the models: For advice and many helpful discussions regarding these and the fluid aspects of the deposition problem, I thank Dr. R.C. Schroter.

Due thanks are necessary to Mr. K.D. Isles and Mr. M.D. Attfield for statistical help; Mr. H. Tully and Mr. K. Donaldson for photographic advice; the staff of the Institute of Occupational Medicine workshop, in particular Mr. R.D. Strachan and Mr. G. Lynch for the work performed by them.

Lastly, my wife Ruth, deserves full credit and thanks for her patience in typing this thesis.

REFERENCES

ALDRICH, J.E. and JOHNSTON, J.R. (1974); Int. J. appl. Radiat. Isotopes, 25,15.

ALTSHULER, B. (1959); Bull. math. Biophys., 21,257.

ALTSHULER, B.; YARMUS, L.; PALMES, E.D. and NELSON, N. (1957); A.M.A. Archs. ind. Hlth, 15,293.

ALTSHULER, B.; YARMUS, L.; PALMES, E.D. and NELSON, N. (1959); J. appl. Physiol., 14,321.

AVERY, M.E.; NAI-SAN, W. and TAEUSCH, H.W.Jr. (1973); Scient. Am., April, 75.

BEAMS, J.W. (1937); J. appl. Phys., 8,795.

BEECKMANS, J.M. (1965); Can. J. Physiol. Pharmac., 43,157.

BELL, K.A. (1970); M.Sc. Thesis, California Institute of Technology.

BELL, K.A. and FRIEDLANDER, S.K. (1973); Staub Reinhalt. der Luft (In English), 33,183.

BOUSSINESQ, J. (1890); Comptes Rendus, 110,1160.

" " (1891); ibid. 113,9.

B.S. 4094, Part 1 (1966); Recommendation for Data on Shielding from Ionising Radiation - Part 1. Shielding from γ - Radiation.

BUCKINGHAM, E. (1914); Phys. Rev. Vol.4, Ser.2,345.

CHOW, H.Y. and MERCER, T.T. (1971); Am. ind. Hyg. Ass. J., April, 247.

CLARKE, S.W.; JONES, J.G. and OLIVER, D.R. (1972); Bull. Physio. - path. resp., 8,409.

CODE OF PRACTICE for the protection of persons exposed to Ionising Radiations in Research and Teaching (1968); London, H.M.S.O.

CUDDIHY, R.G.; BROWNSTEIN, D.G.; RAABE, O.G. and KANAPILLY, G.M. (1973); J. Aerosol Sci., 4,35.

CUNNINGHAM, E. (1910); Proc. Roy. Soc. A, 83,357.

DAVIES, C.N. (1945); Proc. Phys. Soc. (London), 57,259.

" " (1961); New Scient., No. 254,782.

" " (1972); J. Aerosol Sci., 3,297.

" " (1973); ibid. 4,317.

DAVIES, G. and REID, L. (1970); Thorax, 25,669

DAVIS, R.E. (1964); Int. J. Air Wat. Pollut., 8,177.

DEAN, W.R. (1927); Phil. Mag., Series 7,4,208.

DUNNILL, M.S. (1962); Thorax, 17,329.

EINSTEIN, A. (1905); Ann. Phys. Lpz., 17,549.

EISMAN, M.M. (1970); J. appl. Physiol., 29,531.

ELLISON, J. M^{c}K. (1967); Ann. occup. Hyg., 10,363.

FINDEISEN, W. (1935); Pflüg. Arch. ges. Physiol. 236,367.

FOWLER, W.S. (1949); J. appl. Physiol., 2,283.

FRIEDLANDER, S.K. and JOHNSTONE, H.F. (1957); Ind. Engng Chem. Fund., 49,1151.

FRY, F.A. (Oct. 1969); A.E.R.E. Report No. R6150.

FUCHS, N.A. and SUTUGIN, A.G. (1966); In Aerosol Science, ed. C.N. Davies, Academic Press, London and New York.

GALLILY, I. and LA MER, V.K. (1958); J. phys. Chem., 62,1295.

GILLESPIE, T. and RIDEAL, E. (1955); J. Colloid Sci., 10,281.

GREEN, H.L. and LANE, W.R. (1964); Particulate Clouds, E. and F. Spon Ltd., New Fetter Lane, London.

HAGEN, G. (1839); Poggendorffs Annalen, 46,423.

HANDBOOK OF RADIOLOGICAL PROTECTION (1971); London, H.M.S.O. Part 1. Data.

HATCH, T.F. and GROSS, P. (1964); Pulmonary Deposition and Retention of Inhaled Aerosols, Academic Press, New York.

HEYDER, J.; GEBHART, J.; HEIGWER, G.; ROTH, C. and STAHLHOFEN, W. (1973); J. Aerosol Sci., 4,191.

HORSFIELD, K. and CUMMING, G. (1967); Bull. math. Biophys., 29,245.

HORSFIELD, K.; DART, G.; OLSON, D.E.; FILLEY, G.F. and CUMMING, G. (1971); J. appl. Physiol., 31,207.

HYATT, R.E. and WILCOX, R.E. (1963); J. clin. Invest., 42,29.

JAEGER, M.J. and MATTHYS, H. (1970); In Airway Dynamics, ed. A. Bouhouys, Charles C. Thomas, Springfield, U.S.A.

JOHNSON, C.G. and WALTON, W.H. (1947); Bull. ent. Res., 38,405.

JOHNSTON, J.R. and MUIR, D.C.F. (1973); J. Aerosol Sci., 4,269.

JORDAN, D.W. (1954); Br. J. appl. Phys., Suppl. No. 3, Paper H.4, S194.

LANDAHL, H.D. (1950); Bull. math. Biophys., 12,43.

LANDAHL, H.D. and HERRMANN, R.G. (1948); J. ind. Hyg. Toxicol., 30,181.

" " " " " (1949); J. Colloid Sci., 4,103.

LIPPMANN, M. and ALBERT, R.E. (1969); Am. ind. Hyg. Ass. J., May - June, 257.

LOVE, R.G. (1973); Ph.D. Thesis, University of Edinburgh.

MARTIN, D. and JACOBI, W. (1972); Hlth. Phys., 23,23.

MAY, K.R. (1945); J. Scient. Instrum., 22,187.

" " (1949); J. appl. Phys., 20,932.

" " (1966); J. Scient. Instrum., 43,841.

MAY, K.R. (1972); Private Communication.

MORROW, P. (1970); In Airway Dynamics, ed. A. Bouhouys, Charles C. Thomas, Springfield, U.S.A.

MUIR, D.C.F. (1966); J. Physiol., 184,73(P).

MUIR, D.C.F. and DAVIES, C.N. (1967); Ann. occup. Hyg. 10,161.

M^{c}KNIGHT, M.E. and TILLERY, M.I. (1967); Am. ind. Hyg. Ass. J., Sept. - Oct., 498.

NATANSON, G.: Quoted by FUCHS, N.A. (1964); The Mechanics of Aerosols, Pergamon Press, Oxford.

OLSON, D.E.; DART, G.A. and FILLEY, G.F. (1970); J. appl. Physiol., 28,482.

PALMES, E.D. and KAMINER, A.J. (1960); Physiologist, 3,122.

PATTERSON, H.S. and CAWOOD, W. (1936); Trans. Faraday Soc., 32,1084.

PEDLEY, T.J.; SCHROTER, R.C. and SUDLOW, M.F. (1970a); Respir. Physiol., 9,371.

" " " " " " " (1970b); ibid. 9,387.

PHILIPSON, K. (1973); J. Aerosol Sci., 4,51.

PICH, J. (1972); J. Aerosol Sci., 3,351.

POISEUILLE, J.L.M. (1840); Comptes Rendus, 11.

PRANDTL, L. (1952); Essentials of Fluid Dynamics, Blackie and Son Ltd., London and Glasgow (Authorised Translation).

RAABE, O.G. (1970); In Inhalation Carcinogenesis, Proceedings of a Biology Division, Oak Ridge National Laboratory, conference (Oct. 1969).

RAYLEIGH, LORD (1879); Proc. Lond. math. Soc., 10,4.

REYNOLDS, O. (1883); Phil. Trans., Scientific Papers Vol. 2, 51.

ROWE, M. (1970); J. Fluid Mech., 43,771.

SCHERER, P.W. (1972); J. Biomechanics, 5,223.

SCHILLER, L. (1922); Forschungscheft des Ver. Deutsch Ing., 248,16.

SCHILLER, W. (1932); Handbuch der Experimentalphysik Leipzig No. 4. Part 4.

SCHLESINGER, R.B. and LIPPMANN, M. (1972); Am. ind. Hyg. Ass. J., April, 237.

SCHROTER, R.C. (1972); Private Communication.

SCHROTER, R.C. and SUDLOW, M.F. (1969); Respir. Physiol., 7,341.

SCHWENDIMAN, L.C.; POSTMA, A.K. and COLEMAN, L.F. (1964); Hlth. Phys., 10,947.

SEHMEL, G.A. (1967); Am. ind. Hyg. Ass. J., Sept. - Oct., 491.

" " (1970); ibid. Nov. - Dec., 758.

SINCLAIR, D. and LA MER, V.K. (1949); Chem. Rev., 44,245.

STEIN, F.; ESMEN, N. and CORN, M. (1966); Am. ind. Hyg. Ass. J., Sept. - Oct., 428

STÖBER, W. and FLACHSBART, H. (1973); Atmos. environ. 7,737.

STOKES, G.G. (1850); Trans. Cambridge Phil. Soc., 9,8.

STRÖM, L. (1972); Atmos. environ. 6,133.

TASK GROUP ON LUNG DYNAMICS (1966); Hlth. Phys., 12,173.

TIMBRELL, V.; BEVAN, N.E.; DAVIES, A.S. and MUNDAY, D.E. (1970); Nature, Lond., 225 (5227), 97.

WALTON, W.H. and PREWETT, W.C. (1949); Proc. Phys. Soc. B., 62,341.

WATSON, H.H. (1936); Trans. Faraday Soc., 32,1073.

WEIBEL, E.R. (1963); Morphometry of the Human Lung, Springer - Verlag, Berlin.

WEIBEL, E.R. and GOMEZ, D.M. (1962); Science, 137 (3530), 577.

WEST, J.B.; FOWLER, K.T.; HUGH-JONES, P. and O'DONNELL, T.V. (1957); Clin. Sci., 16,549.

WEST, J.B. and HUGH-JONES, P. (1959); J. appl. Physiol., 14,753.

WHITBY, K.T. and LIU, B.Y.H. (1968); Atmos. environ., 2,103.

WHITBY, K.T.; LUNDGREN, D.A. and PETERSON, C.M. (1965); Int. J. Air Wat. Pollut., 9,263.

WHITBY, K.T. and PETERSON, C.M. (1965); Ind. Engng Chem. Fund., 4,66.

APPENDIX

(PUBLISHED PAPERS)

International Journal of Applied Radiation and Isotopes, 1974, Vol. 25, pp. 15–18. Pergamon Press. Printed in Northern Ireland

Use of the Spinning Disk Technique to Produce Monodisperse Microspheres of Human Serum Albumin for Labelling with Radioisotopes

JOHN E. ALDRICH
Department of Medical Physics, Royal Infirmary of Edinburgh, Edinburgh, Scotland
and
J. R. JOHNSTON
Institute of Occupational Medicine, Edinburgh, Scotland

(*Received* 7 *July* 1973)

A commercially available Spinning Disk Aerosol Generator has been used to produce monodisperse microspheres of Human Serum Albumin in the size ranges suitable for lung perfusion and ventilation studies. The technique of generation used is especially useful where a variable range of particle sizes is required for routine experimental investigations; a simple method for denaturing and subsequent radioisotopic labelling of the microspheres is described.

L'EMPLOI DE LA METHODE DU DISQUE TOURNOYANT POUR PRODUIRE DES MICROSPHERES MONODISPERS MONODISPERSES D'ALBUMINE DE SERUM HUMAIN POUR LE MARQUAGE AUX RADIOISOTOPES

On a employé un générateur d'aérosol à disque tournoyant disponible dans le commerce pour produire des microsphères monodisperses d'albumine de sérum humain danses les gammes de grandeur convenables aux études de la perfusion et de la vantilation pulmonaires. La méthode de génération employée est surtout utile lorsqu'une gamme variable de grandeurs des particules est demandée pour des recherches expérimentales de routine; on décrit une méthode simple pour dénaturer les microsphères et ensuite pour les marquer aux radio-isotopes.

ПРИМЕНЕНИЕ МЕТОДА ВРАЩАЮЩЕГОСЬ ДИСКА ДЛЯ ПРОИЗВОДСТВА МОНОДИСПЕРГИРОВАННЫХ МИКРОСФЕР СЫВОРОТОЧНОГО АЛЬБУМИНА ЧЕЛОВЕКА ПРИ МАРКИРОВКЕ РАДИОИЗОТОПАМИ

Применен генератор аэрозолей типа вращающегось диска в промышленном выпуске для производства монодиспергированных микросфер Челевеческого сывороточного альбумина в шесть интервалах по размеру пригодных для перфузии легких, исследований вентиляции. Метод генерирования оказывается особенно полезным при необходимости непостоянного интервала размеров частиц в течении рутинных экспериментальных исследований. При этом описан простой метод денатуризации и последующей радиоизотопической маркировки микросфер.

ANWENDUNG DES SPINSCHEIBENVERFAHRENS AUF DIE HERSTELLUNG MONODISPERSER KÜGELCHEN MENSCHLICHEN SERUMALBUMINS ZUM MARKIEREN MIT RADIOISOTOPEN

Ein auf dem Markt erhältlicher Spinscheiben-Aerosolgenerator wurde dazu verwendet, monodisperse Kügelchen menschlichen Serumalbumins in den für Lungenperfusion und

Correspondence to: John R. Johnston, Physiology Branch, Institute of Occupational Medicine, 8 Roxburgh Place, Edinburgh, EM89SU, Scotland.

Belüftungs-Studien geeigneten Grössenbereichen herzustellen. Die verwendete Herstellungsweise ist besonders nützlich, wo ein wechselnder Bereich von Korngrössen für laufende experimentelle Untersuchungen verlangt wird; eine einfache Methode zur Denaturierung und nachfolgender Radioisotopen-Markierung der Kügelchen wird beschrieben.

1. INTRODUCTION

MICROSPHERES of human serum albumin (H.S.A.) suitable for labelling with radionuclides, e.g. technetium-99*m*, are available commercially for the study of lung perfusion (3*M* albumin microspheres; Sorin TcKS kit). Special studies of pulmonary perfusion and ventilation necessitated the use of radioisotopically labelled microspheres of various sizes not available in kit form. Initially, the method of ZOLLE[1] and PASQUALINI[2] was used, but the many variables inherent in this technique and the wide scatter of particles sizes made the method unsuitable for our purpose. Instead, a monodisperse aerosol of H.S.A. was produced by a commercially available air-driven spinning disk apparatus incorporating automatic satellite removal (Research Engineers Ltd., Orsman Rd, London, U.K.). The aerosol was dried and the resulting particles collected for denaturing and radioisotopic labelling.

The spinning disk principle has received much attention as a technique for producing aerosols of uniform size and in sufficient concentrations for experimental purposes. Ample information regarding the principles involved can be found in the work of the original investigators (WALTON and PREWETT,[3] MAY[4]), and the reader is referred to these papers for a fuller account of the fundamentals of the technique. Basically, however, when a solution is fed on to the centre of a disk, rotating at high speeds, centrifugal and surface tension effects cause the liquid film to be broken up into discrete droplets of size governed by the following equation.[3]

$$d = k/w[\gamma/\rho D]^{1/2} \qquad (1)$$

where

d = droplet dia.
w = disk angular velocity
γ = surface tension of solution
D = disk dia.
ρ = density of solution
k = dimensionless parameter of mean value 4·5 for an air-driven disk.[3,4]

Spraying solutions of known concentration and evaporating the solvent from the resultant droplets produces a dry particle flux. The particle size is related to the droplet size by the equation

$$d_p/d = (C/\rho_p)^{1/3} \qquad (2)$$

where

d_p = particle dia.
C = solution concentration (wt./vol.)
ρ_p = particle density.

At a constant disk angular velocity, equation (1) shows that, with all other variables fixed, the droplet diameter is constant. Variation of the solution concentrations will result in different particle sizes.

This technique has been used with solutions of H.S.A. to produce monodisperse microspheres suitable, after denaturing, for tagging with radionuclides.

2. EXPERIMENTAL

For the production of large diameter microspheres the spinning disk aerosol generator was mounted coaxially at the top of a 0·4 m dia. Perspex cylinder of height 1 m in a manner similar to that described by PHILIPSON[5] and shown in Fig. 1. Our particle size requirements necessitated the production of large droplets of solution, greater than 40 μm, which have, characteristically, large settling velocities. To buoy-up such droplets for drying purposes, in our large diameter chamber, would have required excessive amounts of clean dry air.[6] The experimental arrangement adopted eliminated the need for such an air supply, the droplets being dried as they settled under gravity.

Particles with a diameter greater than 20 μm were required for lung scanning purposes in order to ensure that they were trapped in the lung capillary bed and to avoid liver uptake. To produce such particles a solution of H.S.A. was fed at a controlled rate on to the centre of the 0·026 m dia. disk rotating at a predetermined speed. This resulted

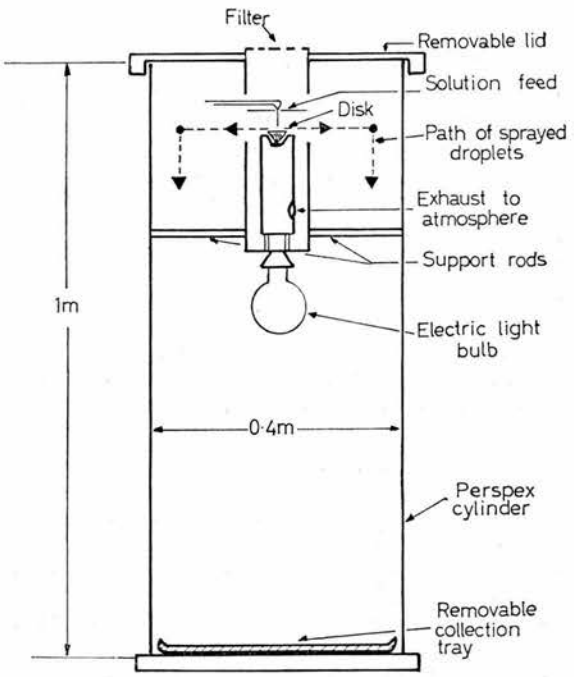

FIG. 1.

in the production of droplets of H.S.A. solution which projected tangentially from the disk edge, a distance proportional to their mass. The maximum size of droplet which could be produced by the apparatus was fixed (approximately) by the radius of the chimney, i.e. droplets having a range greater than this impacted on the walls and were lost: Thus, the largest size of aqueous droplet which could be generated in the apparatus was about 70 μm dia. The droplets produced fell under gravity through the field of a heater (an electric light bulb of 200 W) placed under the base of the generator to enhance the solvent evaporation. To ensure complete wetting of the disk surface during operation, it was ground with carborundum powder on a glass block, before each run. A plate at the base of the chimney was used to collect the dry particles. In a typical experiment, 15 ml of a 10% (wt./vol.) aqueous solution of H.S.A. was injected on to the centre of the disk at a rate of about 0·5 ml min^{-1}. The disk was operated with compressed air, the rotational speed being 36×10^3 rev/min. A resultant mass of about 800 mg of spheres was obtained. Using light microscopy the mean diameter was measured as 18·2 μm with a coefficient of variation of 9·5 per cent. Since the quantities of microspheres required for lung scanning are of the order of 2 mg per patient,[7] it can be seen that one simple experiment produces sufficient material for several hundred patients.

This technique has been used to produce monodisperse microspheres down to about 12 μm dia. by alteration of the disk running speed and/or the solution concentrations. It was found that the apparatus was unsuitable for producing particles less than this size, because of poor uniformity and difficulty in obtaining sufficient material. To obtain these small particles, it was necessary to mount the generator in a separate assembly and use an updraught of air to dry the droplets rather than rely on their gravitational settlement. With the "updraught" technique, there was no difficulty in obtaining particles of the order of 3 or 4 μm (typical coefficient of variation 7 per cent). It was more convenient, however, to collect such particles by aspiration through a filter.

3. DENATURING AND LABELLING OF THE MICROSPHERES

Microspheres of about 20 μm dia. were collected from the plate at the base of the chimney by scraping them into a test-tube with a glass slide. The smaller particles collected on the filters were dislodged by ultrasonication in olive oil.

These microspheres consist of native albumin which will readily dissolve in water. To denature, about 50 mg were thoroughly mixed with 10 ml of olive oil B.P. using a magnetic stirrer. The oil was then slowly heated to 160°C and maintained at this temperature for 20 min. After cooling, the denatured microspheres were washed with ether to remove all traces of oil and sterilised, dry, at 160°C for 1 hr. The resultant spheres dispersed easily and expanded by about 20 per cent of their dry diameter when suspended in water.

Technetium-99*m* and indium-113*m* were used as radioactive labels for the microspheres. In the case of the former, the method of

RHODES[7] was used, technetium being reduced with sodium thiosulphate at low pH to facilitate binding to the albumin. Labelling efficiency using this method was found to be about 80 per cent.

Indium labelling was accomplished using the technique described by ZOLLE[1] for microspheres containing ferric hydroxide. In the present study, the iron was added in the form of ferric chloride (1 ml of 1 % $FeCl_3.6H_2O$). Labelling efficiency greater than 90 per cent was achieved consistently.

4. BIOLOGICAL DISTRIBUTION

To study the localisation of the particles, 0·1 mg of the 18·2 μm mean (dry) diameter particles labelled with Tc-99*m*, were injected intravenously into 40-day old Sprague–Dawley rats. At sacrifice (30 min after injection) the lungs and livers were excised and blood samples taken for assay of the radioactivity. Ninety-five per cent of the radioactivity was located in the lungs, the rest being divided between the liver and the blood.

To date, no experiments have been performed using the smaller microspheres but we hope to demonstrate their potential as a suitable aerosol for inhalation studies in the near future.

5. CONCLUSIONS

Monodisperse microspheres of H.S.A. have been produced routinely by a commercially available spinning disk aerosol generator, and a simple method for the denaturing and labelling of the microspheres is described. The techniques used in this study should be particularly attractive to nuclear medicine laboratories requiring reproducible and readily available supplies of H.S.A. for scintigraphic experiments.

Acknowledgements—The authors are grateful to Dr. D. C. F. MUIR for his helpful criticism of this work and to Miss J. BARBOUR for typing the manuscript.

REFERENCES

1. ZOLLE I., RHODES B. A. and WAGNER H. N., JR. *Int. J. appl. Radiat. Isotopes* **21,** 155 (1970).
2. PASQUALINI R., PLASSIO G. and SOSI S. *J. biol. nucl. Med.* **13,** 80 (1969).
3. WALTON W. H. and PREWETT W. C. *Proc. phys. Soc. B.* **62,** 341 (1949).
4. MAY K. R. *J. appl. Phys.* **20,** 932 (1949).
5. PHILIPSON K. *Aerosol Sci.* **4,** 51 (1973).
6. ELLISON J. McK. *Ann. Occup. Hyg.* **10,** 363 (1967).
7. RHODES B. A., STERN H. S., BUCHANAN B. A., ZOLLE I. and WAGNER H. N., JR. *Radiology* **99,** 613 (1971).

Aerosol Science, 1973, Vol. 4, pp. 269 to 270. Pergamon Press. Printed in Great Britain.

INERTIAL DEPOSITION OF PARTICLES IN THE LUNG

J. R. JOHNSTON and D. C. F. MUIR
Institute of Occupational Medicine, Edinburgh

(*Received* 11 *December* 1972)

Abstract—Initial results on the inertial deposition of aerosol particles in simple bends are reported. Reference to the literature has revealed an error in the interpretation of previous experiments. This has led to incorrect estimates of particle deposition in the human lung. The implications of this error are discussed.

AS PART of an investigation into factors determining the deposition of aerosols in the human respiratory tract, we are engaged in measuring the impaction of particles in bent and bifurcating tube systems.

Initial results with simple 90° bends with axial curvatures in the range 2·5–15 dia. and fluid Reynolds Numbers from 100 to 1000 are in close agreement with experimental values obtained by LANDAHL and HERRMANN (1949) who found that the impaction efficiency was 50 per cent when the quantity ($\rho d^2 V/18\eta D$) had a value of about 0·25, where

- ρ density of the particles
- d particle dia.
- V average velocity of carrier fluid (air)
- η dynamic viscosity of air
- D tube dia.

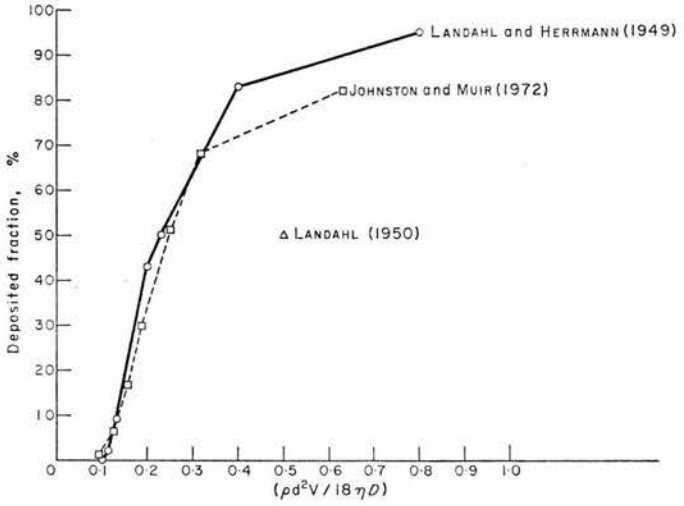

FIG. 1.

However, in a later paper, LANDAHL (1950) stated that a 50 per cent impaction efficiency obtained when the quantity $(\rho d^2 V/18\eta R)$, the Stokes number, had a value of unity, R being the tube radius.

The two statements are clearly incompatible, and it would appear that an error has arisen in the 1950 paper.

The value quoted by LANDAHL (1950) has been used widely in the calculation of aerosol deposition in the respiratory tract (ALTSHULER, 1959; LIPPMANN and ALBERT, 1969; BEECKMANS, 1964; Report for Committee II of the International Commission on Radiological Protection, 1966).

This has led to an underestimate of the efficiency of impaction in the upper airways.

The effect is illustrated in the figure which shows the theoretically calculated results obtained by LANDAHL and HERRMANN (1949) together with results obtained experimentally in our investigations. Also shown, is the value which corresponds to the impaction efficiency quoted by LANDAHL (1950); it is evident that the impaction efficiency should be about 80 and not 50 per cent for this particular value of $(\rho d^2 V/18\eta D)$.

The overall effect of this underestimate on the calculated deposition of inhaled dust in the lung will be assessed when our investigations of impaction in bifurcating tubes is complete However, it is likely that there will be a shift to smaller sizes in the calculated size distribution of particles which are able to penetrate to the alveoli when a non-homogeneous aerosol is inhaled.

Attention is drawn to the problem at this stage in case others are using the data of LANDAHL (1950) to calculate the probable behaviour of aerosol particles in the lung.

REFERENCES

ALTSHULER, B. (1959) *Bull. math. Biophys.* **21,** 257.
BEECKMANS, J. M. (1965) *Can. J. Physiol. Pharmac.* **43,** 157.
LANDAHL, H. D. (1950) *Bull. math. Biophys.* **12,** 43.
LANDAHL, H. D. and HERRMANN, R. G. (1949) *J. Colloid Sci.* **4,** 103.
LIPPMANN, M. and ALBERT, R. E. (1969) *Am. ind. Hyg. Ass. J.* May–June, 257.
TASK GROUP ON LUNG DYNAMICS (1966) *Hlth. Phys.* **12,** 173.